JOURNAL OF SCIENTIFIC PERSPECTIVES

JSP

International Peer-Reviewed and Open Access Electronic Journal

RATING ACADEMY JOURNALS

ratingacademy.com.tr/ojs

Volume / Cilt : 3 Year / Yıl : 2019 Issue / Sayı : 2

E-ISSN : 2587-3008

DOI : 10.26900

ABOUT THE JOURNAL

OWNER

Rating Academy Ar-Ge, Yazılım, Danışmanlık, Yayıncılık, Eğitim ve Organizasyon Ltd. Şti.

Contact

Sarıcaeli Köyü ÇOMÜ Sarıcaeli Yerleşkesi No: 276 D-I, Çanakkale / TÜRKİYE

E-mail: info@ratingacademy.com.tr

Web: http://ratingacademy.com.tr/journals/index.php/jsp

JOURNAL OF SCIENTIFIC PERSPECTIVES JSP

EDITORIAL BOARD

REFEREE BOARD

THE REFEREES IN THIS ISSUE

Prof. Dr. Neşet AYDIN, Çanakkale Onsekiz Mart University, Turkey

Prof. Dr. Ali H. MERİÇLİ, Near East University, Cyprus

Prof. Dr. İ. İrem ÇANKAYA, Hacettepe University, Turkey

Prof. Dr. Hüsniye KAYALAR, Ege University, Turkey

Prof. Dr. Mehmet Zeki SARIKAYA, Düzce University, Turkey

Prof. Dr. Ayşegül ÖKSÜZ, Süleyman Demirel University, Turkey

Prof. Dr. Selehattin YILMAZ, Canakkale Onsekiz Mart University, Turkey

Assoc. Prof. Dr. Tuna AYDIN, Kırıkkale University, Turkey

Assist. Prof. Dr. Müge TARHAN, Uşak University, Turkey

Assoc. Prof. Dr. Uğur CENGİZ, Canakkale Onsekiz Mart University, Turkey

Assoc. Prof. Dr. Burak ÖTERLER, Trakya University, Turkey

Assoc. Prof. Dr. Gülşen SAĞLIKOĞLU Canakkale Onsekiz Mart University, Turkey

Assoc. Prof. Dr. Şefik Baran TARHAN Uşak University, Turkey

Assist. Prof. Dr. Göktuğ GÜNKAYA, Anadolu University, Turkey

Assist. Prof. Dr. Sabah İFTİKHAR, COMSATS University, Pakistan

JOURNAL OF SCIENTIFIC PERSPECTIVES JSP

THE AIM AND SCOPE OF THE JOURNAL

Journal of Scientific Perspectives provides open access to its content, embracing the principle of increasing the global sharing of information on free scientific research. This journal is a material in which academic studies are included and so,it provides a social service for the benefit of institutions and individuals engaged in scientific research as. In this context, it is aimed at providing readers with a common platform to share and improve the quality of recent research advancements in the fields of basic sciences, engineering, natural sciences and health sciences. Thus, It is aimed at promoting research worldwide and publishes basic and advanced research work from the fields above.

The journal accepts only original works of quality which are products of a new solution approach or give a new view of an existing knowledge. In this context, it is open to any kind of constructive, creative and institutionalized knowledge providing that they contribute to universal science and technology. Thus, it is aimed to index the journal with various international indexes.

The study fields covered by the journal are

Basic Sciences and Engineering

- Chemical Engineering
- Computer Engineering and Informatics
- Constructional Engineering
- Environmental Engineering
- Electrical and Electronic Engineering
- Food Engineering
- Geology Engineering
- Industrial Engineering
- Mechanical Engineering
- Mining Engineering
- Physical Engineering
- Textile Engineering
- Other Engineering Fields
- Chemistry
- Physics
- Mathematics
- Statistics
- Materials Sciences (Material and Metallurgy Engineering, Topographical Engineering etc.)
- Space Sciences
- Earth Sciences
- Architecture
- Urban and Regional Planning
- Astronomy and Astrophysics

Health Sciences

- Medical Sciences (Surgery, International Medicine, Basic Medical Sciences)
- Dentistry
- Pharmacology and Pharmaceutics
- Nursing
- Nutrition and Dietary
- Veterinary Medicine

Natural Sciences

- Biology
- Environmental Sciences
- Food Science and Technology
- Animal Husbandary
- Forestry
- Marine, Aquatic Sciences and Fisheries
- Agricultural Science

There are no limits to the fields in which the study will be accepted to the journal. The journal is open to all works aimed at contributing to the national and international developments of the professional organizations and individuals who follow the developments in the field of health, science and engineering and to create a resource in these fields.

PUBLICATION POLICIES

1. *Journal of Scientific Perspectives* has begun publication in July 2017. It is an internationally peer-reviewed and periodical journal published regularly in four issues per year in **January, April, July and October**, in the fields of **basic sciences, engineering, natural sciences** and **health sciences**. All articles submitted for publication are evaluated by the editor in chief, field editor, editorial board and referees.
2. Journal only accepts the studies written in **English.** Original research papers, technical notes, letters to the editor, discussions, case reports and compilations are published in our journal.
3. Only the original scientific researches are included. It is essential that the information created in scientific study needs to be new, suggest new method or give a new dimension to an existing information
4. Journal of Scientific Perspectives is an **open access electronic journal**. All articles published in the journal are assigned the **DOI number**. Researchers worldwide will have full access to all the articles published online and can download them with zero subscription fees. In addition, because of the influence of your research, you will quickly become an Open Access (OA) author, because an OA article has more chances to be used and the plods through the subscription barriers of traditional publishing models.
5. The editor-in-chief and the relevant field editor have the authority not to publish the articles, to make regulations based on the format or to give back to the author for correction that do not comply with the conditions of publication within the knowledge of the editorial board. All studies submitted to *Journal of Scientific Perspectives* are sent to at least **two referees** after the initial review of the editor in chief, relevant field editor and editors related to the study issue with respect to formatting and content. After having positive feedbacks from both of the referees, the manuscripts are published. In case of having one positive and one negative feedback from the referees, the manuscript is sent to **a third referee**. Identities of authors are kept in the posts to be sent to the referees (Double-blind peer review). In addition, the authors are not informed about the referee
6. It is general essential that studies which aren't seemed enough need to be changed in accordance with suggests of referees. Studies which aren't reached intended level or aren't seemed enough in terms of scientific are refused with unexplained reason. The works are published with the condition to be taken in order
7. The referee process is carried out by the **editor in chief.** A study that the chief editor does not find suitable or does not accept is not included in the journal. In this regard, authors can not create a liability for the journal and other boards of the journal.

8. After the field editor has been appointed by the editor in chief, **7 days** are given to him/her for the appointment of the referee. While he/she appoints the referees, he takes the views of the other editors related to the study issue. The studies sent to the referees for evaluation are expected to be answered within **30 days**. In case this is overcome, the editor makes a new referee appointment and withdraws the request from the former referee.
9. Required changes must be made by the author within **15 days** after the decision of "Correction required" given in article acceptance decision.
10. The studies submitted for publication in the journal must have not been published elsewhere or have not been sent another journal to be published. The studies or their summaries which were presented in a conference or published can be accepted if it is indicated in the study. In addition, if the work is supported by an institution or is produced from a dissertation, this should be indicated by a footnote to the title of the work. Those who want to withdraw their publications for publication for some reason must apply to the journal management with a letter. The editorial board assumes that the article owners agree to abide by these terms.
11. All responsibility of the studies belong to the authors. Studies should be prepared in accordance with international scientific ethics rules. Where necessary, a copy of the ethics committee report must be added.
12. The articles submitted to the *Journal of Scientific Perspectives* are sent to the referees after they have been checked with the "iThenticate" plagiarism scanning program to see if they are partially or completely copied (plagiarism) from another study. Regulation is demanded from the author for the articles which are high in the plagiarism result (60% and over). If the required regulation is not made within **60 days**, the study is rejected.
13. Copyright of all published studies belongs to the *Journal of Scientific Perspectives*.
14. **No copyright payment** is made.
15. For the studies accepted for publication in our journal, copyright transfer form signed must be added to the system or mail to
16. No study has differentiation or superiority from another study. Each author and study has the same rights and equality. No privileges are recognized.
17. Studies submitted for publication in our journal must be prepared according to the rules of spelling of journal. Spelling and template are included in are included in the "Author Guidelines" heading
18. Articles submitted for evaluation must not exceed 25 pages after they are prepared according to the specified template. Article summary should not exceed 300 words and minimum 3 and maximum 7 keywords should be written.

ETHICAL GUIDELINES

Journal of Scientific Perspectives (JSP) is committed to meeting and upholding standards of ethical behavior at all stages of the publication process. It strictly follows the general ethical guidelines provided by the Committee on Publication Ethics (COPE), the Open Access Scholarly Publishers Association (OASPA) and Cambridge Journals Ethical Standards and Procedures. Depending on these principles and general publication requirements, editors, peer reviewers, and authors must take the following responsibilities in accordance to professional ethic and norms. The proper and ethical process of publishing is dependent on fulfilling these responsibilities

The Responsibilities of Editor(s)

- The editor in chief and relevant editor(s) should acknowledge receipt of submitted manuscripts to the authors within ten days. The editor in chief and relevant editor(s) have responsibility in order to determine which of the submitted manuscripts could be published.
- Editors should adopt editorial policies that encourage maximum transparency, complete, impartial and honest reporting
- The submitted manuscripts will be controlled by the editor and the associate editor(s) in case of the plagiarism possibility. In this stage, the detected plagiarized manuscripts by the The editor in chief and relevant editor(s) will be rejected by the editor and associate editor(s). No way that the plagiarized manuscripts will be taken in the consideration process.
- The unpublished data and method in the submitted manuscripts should not be exploited/use by anyone in her/his study without the written permission of the author.
- The submitted manuscripts should be evaluated in accordance to the framework of solely intellectual norms in regardless of social, religious, cultural, economical background.
- The submitted manuscripts should not be disclosed no one other than the reviewer, the publisher, the editor assistants and the author(s) of such manuscripts by The editor in chief and relevant editor(s).
- When obtained interest struggle/conflict among the submitted manuscripts and other author(s) and/or institution, such submitted manuscripts should be recuse himself or herself from the review process.
- The final decision concerning the acceptance or rejection of the submitted manuscripts belongs to the editor in chief. This situation will be decided with reference to the originality and significance of the submitted manuscripts.
- The editor in chief should not oblige the authors to cite any articles or papers in the journal as the submitted manuscripts of the authors to be able to accept in the journal.

The Responsibilities of Reviewer(s)

- The reviewers have responsibility to the editor to inform the editor and the associate editors regarding the review process of the submitted manuscript in case the reviewers do not feel enough qualified in order to review the assigned manuscript of if they cannot complete the review process on time.
- The reviewers should complete her/his task in the respect to principle of secrecy. Reviewers should not share or discuss any data regarding the submitted study with no one except the editors.
- The reviewer should not disclose and share any data/content and opinions of the submitted manuscripts and should not use personal interest. Furthermore, the reviewers should not use any data of the unpublished paper.
- The criticism of the reviewers should be based on objective and scientific perspective and also the reviewers should avoid from personal criticism against the author(s). The reviewers are supposed to support her or his opinions by providing clear and tangible proofs.
- If the reviewers detect any similarities between the assigned manuscript and another published articles in the journal or in an another journal, they are supposed to notify the editor about this situation.
- The reviewers should not take any part in evaluation process of the submitted manuscripts with author(s) who have competition, cooperation or other kind of relations or links.
- Reviewers should conduct the work they agree to evaluate on time.

The Responsibilities of the Author(s)

- The author(s) should not send the same study manuscript to more than a/one journal simultaneously.
- The authors should gather the data relating the studies in the framework of principle of ethic. The publisher, the editor and the reviewer could demand the raw data from the author(s) which the study is based on.
- The studies which are sent to the journal should provide details and references/sources in an adequate level. Dishonesty and incorrect statements are unacceptable due to causing unethical principles.
- The submitted manuscripts should be original and the originality of the study should be ensured by the author(s). If others' papers and/or words are used in the context of the submitted manuscript, the reference should be provided in accordance to appropriate style. Also excerpts should be in an appropriate style in accordance to the writing rules of the journal and scientific ethics. The authorities are supposed to refer to other publishments which effect the essence of their submitted studies.
- The authors are supposed to notify a conflict of interest, financial sources and foundations if any of them are supported their studies.
- All the person(s) who contributed to the submitted manuscript in the respect of design, interpretation or implementation should be written on the submitted manuscript. All participations contributed in essence, should be listed respectively. Also apart these persons should be added to the part of "Acknowledgement".
- If the author detects any flaw or error(s) in the context of the submitted manuscript, the author is responsible to urgently notify this situation to the editor or the publisher in behalf of collaboration in order to correct such error(s) or flaw(s).

AUTHOR GUIDELINES

INSTRUCTION FOR AUTHORS

The authors are cordially invited to submit significant new findings of their research work papers in word and pdf formats to the journal office via online submission or e-mail:jsp@ratingacademy.com.tr along with a JSP cover letter. The journal will cover the topics related to the fields of **basic sciences, engineering, natural sciences** and **health sciences.** All articles submitted for publication are evaluated by the editor-in-chief, field editor, editorial board and referees. The original research papers, technical notes, letter to the editor, debates, case presentations and reviews only in *English* are published in the journal.

The editorial board of JSP welcomes original novel contributions and reviews in word format. By submission of a manuscript an author certifies that the work is original and is not being considered simultaneously by other journals. All articles are subjected to critical reviews by referees.

Cover Letter

The cover letter should be prepared and sent to the Editor-in-Chief via e-mail.

Software and Format

- Regular paper should describe new and carefully confirmed findings, and experimental procedures should be given in sufficient detail for others to verify the work. The length of a full paper should be the minimum required to describe and interpret the work clearly. The total length of any manuscript submitted must not exceed **25 pages.**
- Papers should be written in clear, concise language (*English*).
- Manuscripts should be prepared in English using a word processor. MS Word for Windows and .docfiles are preferred. Manuscripts may be prepared with other software provided that the full document (with figures, schemes and tables inserted into the text) is exported to a MS Word format for submission.
- Do not use desktop publishing software such as Aldus PageMaker or Quark XPress. If you have prepared your manuscript with one of these programs, export the text to a word processing format.
- Times New Roman font is preferred. The font size should be 12 PT.
- The first line of the paragraph should be shifted by 1,25 cm from the left margin. Paragraph spacing after a single paragraph (6 nk) should be given.
- Papers should be single spaced with ample margin. The page setup is A4 size.
- The manuscript, which does not show the names of the authors, must include the followings: Title, Abstract, Keywords under the abstract, introduction, main text, conclusion, references and appendix.
- No footer, header or page numbers required.
- Name each file with your last name of the first author.

1. Title of the paper: The title must concise and informative and should not exceed the 60 characters (12-15 words) including spaces (with key words appropriate for retrieval purposes) and provide peer readers with a quick overview of the paper contents. Avoid abbreviations and formulae where possible.

Title of the paper set in the midst, should be written in bold, in Times New Roman 12 font size and 1,5 spaced.

Headings and subheadings must be numbered 2., 2.1., 2.1.1. as etc decimally with bold letters. All headings should be written in bold but only the first letters of the subtitles should be capital. Spacing before and after a heading (6 nk) should be given.

2. Name of the author(s) with titles and the name and address of the institution where the work was done must be given. Provide, also, with the e-mail address of first and/or the corresponding author so that an immediate communication with the editor is possible. But these are not shown on the manuscript. They must be registered to the system while uploading the manuscript and indicated in the cover letter.

3. Abstracts and Key Words: All papers must have an abstract not more than 300 words of clear, informative and giving significant objectives, methodology, results and conclusion in the paper. Between **3** and **6** key words must be provided for the purpose of indexing and information retrieval. Abstract and key words must be written in <u>Times New Roman</u> <u>11 font size</u> and <u>single spaced</u>. It also should be in <u>*italic letters*</u>. Presentation of numerical results should be avoided as far as possible in the abstract.

4. Text: The paper must be divided into sections and subheadings starting preferably with Introduction and ending with Conclusion followed by Acknowledgement.

5. Tables: Tables should be single spaced. The tables should be kept to a minimum and be designed to be as simple as possible. Tables are to be typed single-spaced throughout, including headings and footnotes. Each table should be numbered consecutively in Arabic numerals and supplied with a heading and a legend. The title should be placed at the top. Explanatory information and experimental conditions should be given as a note at the bottom. Explanatory information and experimental conditions should be given as a note at the bottom of the columns. Tables should be self-explanatory without reference to the text. The same data should not be presented in both table and graph form or repeated in the text.

The headlines of the tables must be written in Times New Roman 12 font and with bond letters. References for the tables (figure of graph) must be below the table (figure or graph) with a font size of 11 font.

6. Figure: Illustrations must be numbered consecutively in Arabic numerals. They should be cited in the text as Figure 1, Figure 2, and so on. Begin each legend with a title at the bottom of the illustration and include sufficient description so that the figure is understandable without reading the text of the manuscript. Graphics should be prepared using applications capable of generating high resolution (300 dpi) JPEG before pasting in the Microsoft Word manuscript file.

The headlines of the figures must be written in Times New Roman 12 font and with bond letters. References for the tables (figure of graph) must be below the table (figure or graph) with a font size of 11 font.

7.Citations: All papers cited in the text, tables, and figures must be included in the references and all papers cited the references section should be cited in the text. Authors should monitor references at all phases of manuscript preparation. References in the text should be cited by author and year. Single author: Clark (2004) or (Clark, 2004). Two authors: Gupta and Clark (2015) or (Gupta and Clark, 2012). More than two authors: Gupta *et al*. (2015) or (Gupta *et al*., 2015). In the event that an author cited has had two or more works published during the same year, the reference, both in the text and in the reference list, should be identified by a lower case letter like a and b after the date to distinguish the works.

8.References: References should be listed at the end of the paper in alphabetical order. Articles in preparation or articles submitted for publication, unpublished observations, personal communications, etc. should not be included in the reference list. Journal names are abbreviated according to Biological Abstracts and correctly format the references of your paper. Authors are fully responsible for the accuracy of the references. All the references must be in the following order.

Books:

SURNAME, NAME, Publication Year, *Name of Book*, Publishing, Place of Publication, ISBN.

MERCER, P.A. and SMITH, G., 1993, *Private Viewdata in the UK*, 2

Journals:

SURNAME, NAME, Publication Year, Name of Article, *Name of Journal*, Volume Number and Page Numbers.

EVANS, W.A., 1994, Approaches to Intelligent Information Retrieval, *Information Processing and Management*, 7 (2), 147-168.

Conferences:

SURNAME, NAME, Publication Year, Name of Report, *Name of Conference Bulletin*, Date and Conference Place, Place of Publication: Publishing, Page Numbers

SILVER, K., 1991, Electronic Mail: The New Way to Communicate, *9th International Online Information Meeting*, 3-5 December 1990, London, Oxford: Learned Information, 323-330.

Thesis:

SURNAME,NAME , Publication Year, Name of Thesis, Master's Degree/Doctorate, Name of Institute

AGUTTER, A.J., 1995, The Linguistic Significance of Current British Slang, Thesis (PhD), Edinburgh University.

Maps:

SURNAME, NAME , Publication Year, Title, Scale, Place of Publication: Publishing.

MASON, James, 1832, Map of The Countries Lying Between Spain and India, 1:8.000.000, London: Ordnance Survey.

Web Pages:

SURNAME, NAME, Year, Title [online], (Edition), Place of Publication , Web address: URL

HOLLAND, M., 2002, Guide to Citing Internet Sources [online], Poole, Bournemouth University, http://www.bournemouth.ac.uk/library/using/guide_to_citing_internet_sou rc.html, [Date Accessed: 4 November 2002].

Identification: It is particularly important that the authors get their biological material authentically identified and quote at least once, on its first citation in the paper, the technical name of the species concerned in full preceded by its popular name where possible, e.g. The water bug *Sphaerodema rusticum* (Fabr). Genus and species names should be italic.

Footnotes: Footnotes should be avoided as far as possible. Essential footnotes may, however, be indicated by superscribed reference marks (*, †, ‡,).

Statement of human and animal rights

When reporting experiments on human subjects, authors should indicate whether the procedures followed were in accordance with the ethical standards of the responsible committee on human experimentation (institutional and national) and with the Helsinki Declaration of 1975 (revised in 2000). If doubt exists whether the research was conducted in accordance with the Helsinki Declaration, the authors must explain the rationale for their approach, and demonstrate that the institutional review body explicitly approved the doubtful aspects of the study. When reporting experiments on animals, authors should be asked to indicate whether the institutional and national guide for the care and use of laboratory animals was followed.

Statement of Informed Consent

Patients have a right to privacy that should not be infringed without informed consent. Identifying information, including patients names, initials, or hospital numbers, should not be published in written descriptions, photographs, and pedigrees unless the information is essential for scientific purposes and the patient (or parent or guardian) gives written informed consent for publication. Informed consent for this purpose requires that a patient who is identifiable be shown the manuscript to be published. Authors should identify Individuals who provide writing assistance and disclose the funding source for this assistance.

Identifying details should be omitted if they are not essential. Complete anonymity is difficult to achieve, however, and informed consent should be obtained if there is any doubt. For example, masking the eye region in photographs of patients is inadequate protection of anonymity. If identifying characteristics are altered to protect anonymity, such as in genetic pedigrees, authors should provide assurance that alterations do not distort scientific meaning and editors should so note.

Submission: The manuscript should be submitted preferably by our online manuscript submission centre in the following URL: http://www.ratingacademy.com.tr/jsp/ or as e-mail attachment to the Editorial Office via: info@ratinacademy.com.tr. All contacts shall be by e-mail. All the corresponding authors should have an e-mail id. All submissions will be acknowledged within a short time.

Brief checklist for submission.

1. Have you provided a Cover Letter?
2. Have you provided the informations of the correponding author and the other authors to the system?
3. Have you provided an Abstract of 300 words ?
4. Have you provided Keywords?
5. Are your Tables denoted by Arabic numerals, and are they in order as cited in the text?
6. Are your Figures denoted by Arabic numerals, and are they in order as cited in the text?
7. Are your References cited in the required format of the Journal?
8. Is institutional approval number provided for the mammalian animal used for the experiment?
9. Have you obtained permission and submitted documentation for all Personal Communications cited?

Technical Notes: Technical notes are shorter than research articles and may be used to describe a new methodology or to present results from new techniques or equipment. A technical note should not exceed 20 pages with no more than 5 figures and tables. These rules are valid for debates and case presentations.

Proofs and Reprints: Electronic proofs will be sent (e-mail attachment) to the corresponding author as a PDF file. Corrections should be restricted to typesetting errors. Authors are advised to check their proofs very carefully before return, since inclusion of late corrections cannot be acceptable Corrected proofs are to be returned to the publishers.

Page proofs are considered to be the final version of the manuscript. The Editorial Board reserves the right to make changes like typographical or minor clerical errors if necessary in the research articles. No changes will be made in the manuscript at the proof stage.

Authors will have free electronic access to the full text (PDF) of the article. Authors can freely download the PDF file from which they can print unlimited copies of their articles.

The Editorial Board reserves the right to make changes if necessary mainly to improve the quality of the paper.

The responsibility of the contents rests upon the authors and not upon the publisher.

Authors are requested to prepare the manuscript according to our journal "Instructions for authors" guidelines.

Subscription Rates and Terms: Those who are interested to obtain the electronic copy of the JSP, he/she can download it free of charge.

JOURNAL OF SCIENTIFIC PERSPECTIVES JSP

ABSTRACTING & INDEXING

ProQuest

Google Scholar

Base

Academic Resource Index: ResearchBib

Academic Keys

PKP Index

DIIF

SCIWIN (Scientific World Index)

INTERNATIONAL INSTITUTE OF ORGANIZED RESEARCH (I2OR)

Cosmos Impact Factor

ISRA:Journal-Impact-Factor (JIF)

	Internatıonal Servıces For Impact Factor And Indexıng (ISIFI)
	PAK Academic Search (Pending)
	CrossRef
	DOI
	Scientific Indexing Services
	Scilit
	OALib
	OCLC WorldCat
	Turkish JournalPark
	Scipio
	Scopemed
	Journal Index
	AcademicKeys
	Sparc Indexing

JOURNAL OF SCIENTIFIC PERSPECTIVES JSP

International Peer-Reviewed Journal

E-ISSN: 2587-3008
DOI: 10.26900

Volume: 3 ***Issue:*** 2 ***Year***: 2019

CONTENTS

Basic Sciences and Engineering

Health Sciences

Journal of Scientific Perspectives

Volume 3, Issue 2, Year 2019, pp. 85-98
E - ISSN: 2587-3008
URL: http://ratingacademy.com.tr/ojs/index.php/jsp
DOİ: https://doi.org/10.26900/jsp.3.010
Research Article

THE EFFECT OF COMBINATION OF BORIC ACID AND LITHIUM CARBONATE ON SINTERING AND MICROSTRUCTURE IN SINGLE FIRING WALL TILE

Savaş ELMAS* & İsmail TARHAN**

** Res. Assist., Çanakkale Onsekiz Mart University, Faculty of Fine Arts, Ceramic and Glass Department, Çanakkale, TURKEY, E-mail: savaselmas@comu.edu.tr*
ORCID ID: https://orcid.org/0000-0003-2913-0303

*** Prof. Dr., Çanakkale Onsekiz Mart University, Faculty of Arts and Sciences, Physics,Çanakkale, TURKEY, E-mail: ismailtarhan@comu.edu.tr*
ORCID ID: https://orcid.org/0000-0001-6156-0827

Received: 3 March 2019; Accepted: 14 April 2019

ABSTRACT

The aim of this study was to determine the effect of boric acid and lithium carbonate on microstructure and sintering characteristics of wall tile after firing. Amount of Li2 (CO3) (0.1-0.3-0.6-0.9-1.2-4 wt.%) were added in wall tile corresponding to each constant amount of added of H3BO3 (0.1-0.3-0.6-0.9-1.2-2 wt.%). All samples were fired in 1135 0C 35 minutes in an industrial fast firing kiln. Dry strength, fired strength, water absorption and colorimeter values of all samples were determined after firing. Scanning electron microscope (SEM), x-ray diffraction (XRD) analysis, optical dilatometer measurements were performed in order to determine the microstructure and melting temperature for prescribed purpose (1-2-7-8-11-32-37). Standard (1) and alternative (8) receipe's thermogravimetric and diferantial thermal analyses were performed. 37 (2% H3BO3 + 4% Li2 (CO3) recipe's sintering starting temperature was 984 0C. In the recipe 8 (0.3% H3BO3 + 0.1% Li2(CO3) is an alternative to the standard wall tile, which can be used with higher strength values.

Keywords: *Flux, Sintering, Microstructure, Boric acid, Litium carbonate, Wall tile*

1. INTRODUCTION

Under the conditions of increasing competition with globalization, the price of the product is one of the factors considered as a priority for the customers. Reducing the sintering temperature and improving the microstructure are important issues today. The microstructure affects the physical properties desired from the product. The largest energy consumption in the ceramic industry is in firing. 55% of the thermal energy is used here. The approximate energy consumption in ceramic tile production is 4608 kj / kg. The firing part uses most of the thermal energy at 2556 kj / kg. [1]. It was found that the use of 0.5-2% boric acid added samples as a fast single firing wall tile is suitable [2]. With increasing amount of boric acid, firing shrinkage increases. Quartz, mullite and spherical anorthite crystals were found in the microstructure [2]. The addition of 0.4-0.5% ulexite was found to shorten the grinding time, increase dry strength and reduce the firing temperature [3]. In the porcelain tiles with boric acid addition, the amount of B_2O_3 increased to 0.5-1%, the firing temperature of 15 ^{0}C and 28 ^{0}C was observed respectively [4]. It was observed that the desired results were obtained in the conditions where the addition of lithium oxide to the porcelain body did not exceed 1.5% [5]. The presence of spodumene increases mullitization reaction and gives better physical and chemical properties[6].According to Moreno et al. [4],Yet & Kara [7] and Cigdemir et al. [8] rheological problems caused by boric acid addition in slip can be solved by electrolyte addition. It was determined that the addition of boric acid up to 0.9% did not alter of rheological properties of slip[4]. The presence of spodumene increases mullitization reaction and gives better physical and chemical properties[9].

The aim of this study is to reveal how to effect the usage of both boric acid and lithium carbonate, both of which are active flux, on sintering behaviour and microstructure of wall tile body.

2. EXPERIMENTAL PROCEDURE

The raw materials used in the study were obtained from Etili Seramik A.Ş (Çanakkale). Standard wall tile recipe is prepared according to Table 1. Chemical analysis of the raw materials used in the recipe is shown in Table 2. Amount of $Li_2(CO_3)$ (0.1-0.3-0.6-0.9-1.2-4 wt.%) were added in wall tile corresponding to each constant amount of added of H_3BO_3 (0.1-0.3-0.6-0.9-1.2-2 wt.%). Thus, the formation temperature of liquid phase, microstructure and physical properties of products were investigated. Grinding was carried out in a 2 kilogram alumina ball in laboratory type mill with 40% water added to the mixture and 2-3% on 63 micron sieve. The slip density was adjusted to 1680-1700 g / l. After that, the slip dried at 110 ^{0}C in the dryers then was moistened with 5-6% by hand and shaped by laboratory type press with 270 kg / cm^2 pressure. Dimensions of the samples are 7.5x 13x1 cm. All samples were fired in 1135 ^{0}C 45 min. in continuous industrial roller kiln. The prepared samples consist of 37 different recipes in total and the prescriptions are shown in Tables 3-4-5 and 6. Scanning electron measurements were measured by SEM-JEOL JSM-7100F 20 kv, Au / Pa (80-20%). XRD measurement was performed with PAN Analytic Empeyron Series (10-70 theta, 45 Kv, K alpha). Fired strength test was performed on a 3-point Gabrielli brand strength measuring instrument. In the water absorption test, the samples were first held in boiling water for 2 hours and then in cold water for 3 hours; behind this process, samples are wiped with wet towel [9]. Colour measurement values were measured with Minolta CR 300.

Table 1. Standard wall tile formulation

Raw material	(wt.%)
Calcite	10
Kaolin	25
Feldspar	25
Quartz	40

Table 2. Chemical analysis of raw materials (wt.%)

Raw material	SiO_2	Al_2O_3	Fe_2O_3	CaO	MgO	Na_2O	K_2O	TiO_2	L.I
Kaolin	77.36	14.76	0.83	0.54	0.27	3.49	6.06	0.28	1.26
Quartz	99.13	0.35	0.025	0.02	0.02	0.27	0.01	-	0.17
Calcite	0.83	0.31	0.11	54.9	0.69	0.07	0.01	0.01	43.02
Feldspar	69.53	18.25	0.10	0.70	0.15	10.10	0.28	0.29	0.35

L.I: Loss of ignition

Table 3. Prepared wall tiles formulations (wt.%)

	1(std)	**2**	**3**	**4**	**5**	**6**	**7**	**8**	**9**
Calcite	10	10	10	10	10	10	10	10	10
Kaolin	25	25	25	25	25	25	25	25	25
Feldspar	25	25	25	25	25	25	25	25	25
Quartz	40	40	40	40	40	40	40	40	40
H_3BO_3	0	0.1	0.1	0.1	0.1	0.1	0.1	0.3	0.3
$Li_2(CO_3)$	0	0.1	0.3	0.6	1.2	2	4	0.1	0.3

Std:Standard

Table 4. Prepared wall tiles formulations (wt.%)

	10	**11**	**12**	**13**	**14**	**15**	**16**	**17**	**18**
Calcite	10	10	10	10	10	10	10	10	10
Kaolen	25	25	25	25	25	25	25	25	25
Feldspat	25	25	25	25	25	25	25	25	25
Quartz	40	40	40	40	40	40	40	40	40
H_3BO_3	0.3	0.3	0.3	0.3	0.6	0.6	0.6	0.6	0.6
$Li_2(CO_3)$	0.6	1.2	2	4	0.1	0.3	0.6	1.2	2

Table 5. Prepared wall tiles formulations (wt.%)

	19	**20**	**21**	**22**	**23**	**24**	**25**	**26**	**27**
Calcite	10	10	10	10	10	10	10	10	10
Kaolin	25	25	25	25	25	25	25	25	25
Feldspar	25	25	25	25	25	25	25	25	25
Quartz	40	40	40	40	40	40	40	40	40
H_3BO_3	0.6	0.9	0.9	0.9	0.9	0.9	0.9	1.2	1.2
$Li_2(CO_3)$	4	0.1	0.3	0.6	1.2	2	4	0.1	0.3

Table 6. Prepared wall tiles formulations (wt.%)

	28	**29**	**30**	**31**	**32**	**33**	**34**	**35**	**36**	**37**
Calcite	10	10	10	10	10	10	10	10	10	10
Kaolin	25	25	25	25	25	25	25	25	25	25
Feldspar	25	25	25	25	25	25	25	25	25	25
Quartz	40	40	40	40	40	40	40	40	40	40
H_3BO_3	1.2	1.2	1.2	1.2	2	2	2	2	2	2
$Li_2(CO_3)$	0.6	1.2	2	4	0.1	0.3	0.6	1.2	2	4

3. RESULTS AND DISCUSSION

3.1. Optical Properties

The physical appearances of the fired samples are as shown in Figure 1. The colour of the fired product changes with adding together of H_3BO_3 - $Li_2(CO_3)$ that effectively effect on sintering. The chromatic coordinate measurement values of the prepared recipes are given in Table 7. In groups containing 0.1-0.3-0.6-0.9 wt.% H_3BO_3, the L value decreases to 1.2 wt.% and body's colour is obtained dark. In these H_3BO_3 groups the L value is increased in the addition of 2 and 4 wt.% of $Li_2(CO_3)$. The L value decreases until the addition of 0.6 wt.% of

$Li_2(CO_3)$ in the group containing 1.2 and 2 wt.% of H_3BO_3. In the presence of 0.1-0.3-0.6-0.9 wt.% H_3BO_3 the same type reaction take places in the presence of up to 1.2 wt.% $Li_2(CO_3)$ and then changes the reaction in the incremental additions. This also shows that H_3BO_3 and Li_2 (CO_3) affect the melting characteristics of each other's presence. According to Vilches's study on the subject can be explained by the increased vitrification and thus seen clearly effects of chromophore oxides [10]. 2% H_3BO_3 + 4% $Li_2(CO_3)$ doped as 37 sample is formed by the high amount of low viscosity liquid phase deformation is observed.

Figure 1. Physical appearance of prepared wall tiles

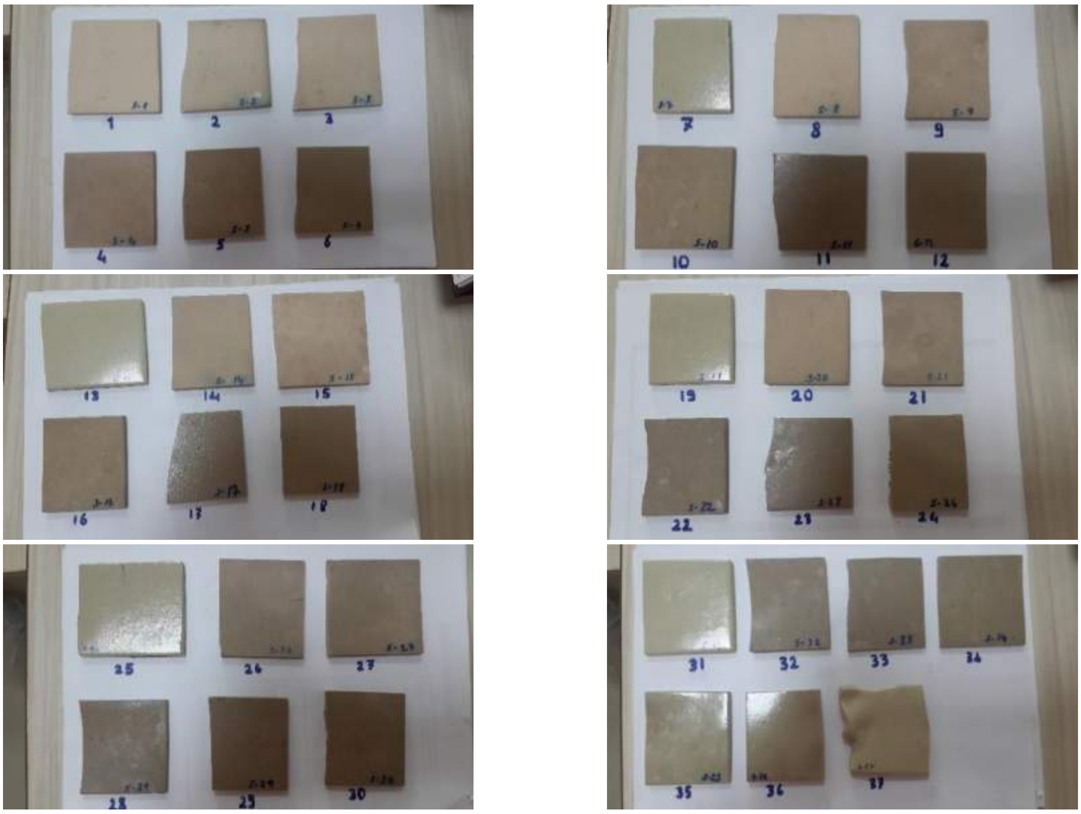

Table 7. Colorimetrer degree of prepared wall tiles

no	L	a	b	no	L	a	b	no	L	a	B
1	79.67	4.73	15.56	**14**	66.38	5.11	16.17	**27**	58.91	3.62	13.3
2	75.15	3.64	14.02	**15**	71.2	4.78	17.23	**28**	53.65	3.9	13.24
3	76.1	5.1	14.2	**16**	62	4.5	16.4	**29**	55.7	3.7	14.8
4	61.95	6.21	14.26	**17**	59.11	3.11	14.26	**30**	56.29	3.76	14.92
5	60.3	3.3	15.3	**18**	59.3	3.11	14.26	**31**	69.8	0.9	14.2
6	60.64	3.32	15.41	**19**	70.49	0.93	14.98	**32**	56.91	3.1	12.69
7	74.25	0.56	13.61	**20**	71.66	4.26	14.51	**33**	56.53	2.7	12.32
8	74.89	5.09	15.87	**21**	64.01	4.17	15.21	**34**	57.9	2.49	13.14
9	63.49	4.48	15.46	**22**	58.27	4.12	13.74	**35**	65.08	1.12	13.2
10	61.67	4.52	16.46	**23**	55.38	3.9	14.12	**36**	64.23	2.17	13.99
11	54.68	3.69	14.45	**24**	61.52	2.62	15.16	**37**	74.14	0.09	14.02
12	58.93	2.95	14.39	**25**	69.33	0.67	13.81				
13	73.78	0.13	13.72	**26**	61.13	3.3	12.6				

3.2. Physical Properties

With the addition of lithium carbonate up to 2%, strength increases are observed in the samples with 0.1-0.3-0.6 and 1.2% H_3BO_3 followed by a reduced strength value. The water absorption value decreases in all trials with increasing $Li_2(CO_3)$. This shows that sintering increases and porosity decreases. No 8 as 0.3 wt.% H_3BO_3 + 0.1 wt.% $Li_2(CO_3)$ doped trial shows very close water absorption and firing shrinkage with standard wall tiles. The water absorption in the wall tile was 23.62% and the firing shrinkage was 0.69% while in 0.3% H_3BO_3 + 0.1% Li_2 (CO_3) added sample as number 8, these values were respectively 19.49% and 1%. In contrast the fired strength of the standard wall tile was 184.94 kgf / cm^2 and the strength value of this recipe was increased to 334.97 kgf/cm^2. Except for 2% H_3BO_3 doped prescription all other H_3BO_3 additive recipes show a reduction in the firing shrinkage value of Li_2 (CO_3) up to 1.2%. The water absorption value reaches zero by 1.2% $Li_2(CO_3)$ in all boric acid samples except 0.1% H_3BO_3. In the group containing 0.1% H_3BO_3. the water absorption value reaches to zero with the addition of 2% $Li_2(CO_3)$. In a study by Cengiz and Kara [2], water absorption and firing shrinkage in the addition of 2% H_3BO_3 to the wall tile were found to be 17.2%and 1.4% respectively. Added 0.1% Li_2 (CO_3) + 2% H_3BO_3 body's water absorption and fired shrinkage's values were found as 6.5% and 8.38% respectively. The decrease in the water absorption value and the increase in the fired shrinkage indicate that an active sintering mechanism has taken place.

Figure 2 a According to quantity of $Li_2(CO_3)$ in 0.1 wt. % added H_3BO_3 sample's fired flexural strength-water absorption graphic.
b According to quantity of $Li_2(CO_3)$ in 0.3 wt.% added H_3BO_3 sample's fired strength-water absorption graphic

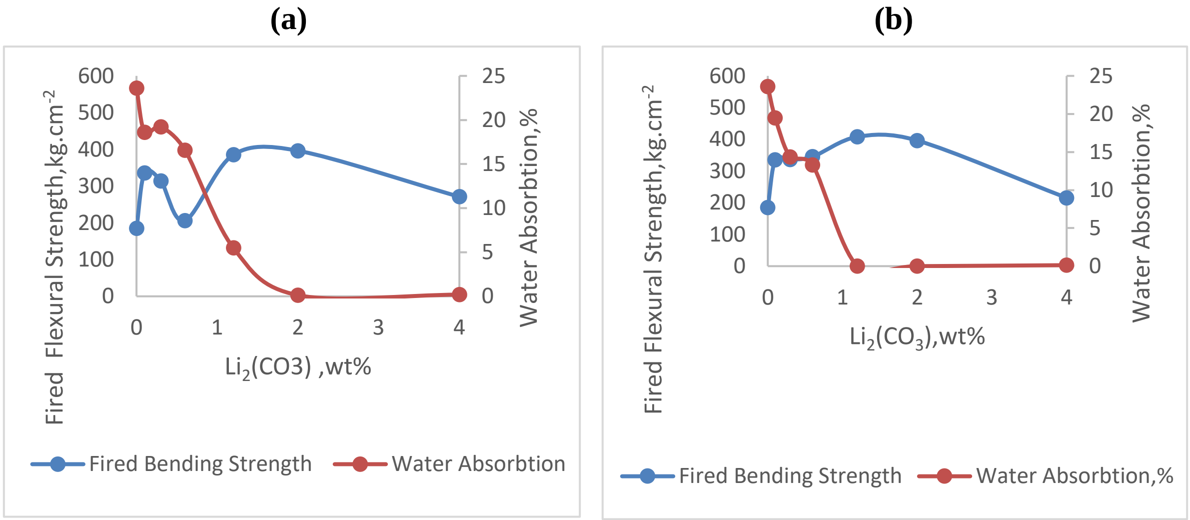

(All figure's first degrees are standard samples without H_3BO_3 and $Li_2(CO_3)$)

Figure 3 a According to quantity of $Li_2(CO_3)$ in 0.6 wt.% added H_3BO_3 sample's fired flexural strength-water absorption graphic
b According to quantity of $Li_2(CO_3)$ in 0.9 wt.% added H_3BO_3 sample's fired flexural strength-water absorption graphic

(a)

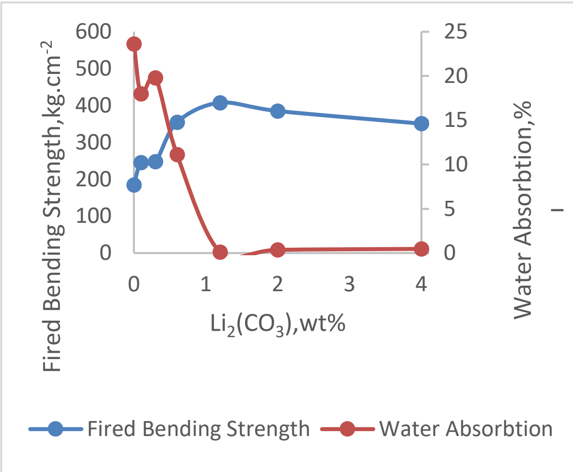

(b)

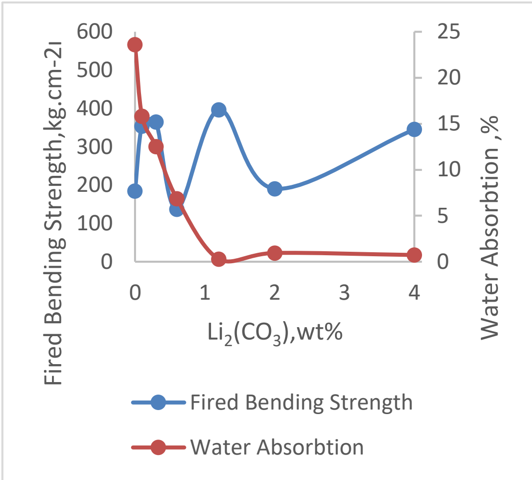

(All figure's first degrees are standard samples without H_3BO_3 and $Li_2(CO_3)$)

Figure 4 a According to quantity of $Li_2(CO_3)$ in 1.2 wt.% added H_3BO_3 sample's fired flexural strength-water absorption graphic
b According to quantity of $Li_2(CO_3)$ in 2 wt.% added H_3BO_3 sample's fired flexural strength-water absorption graphic

(a)

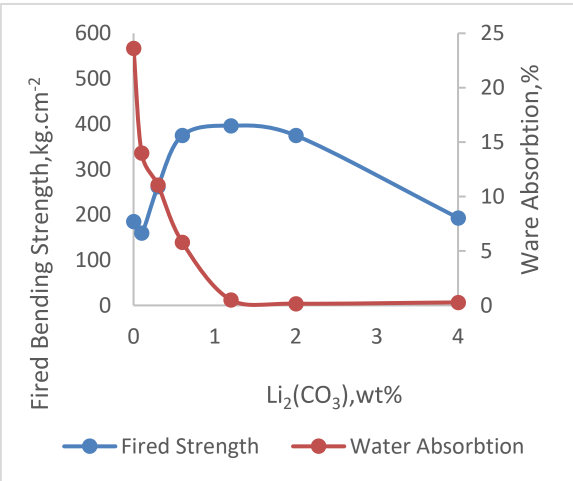

(b)

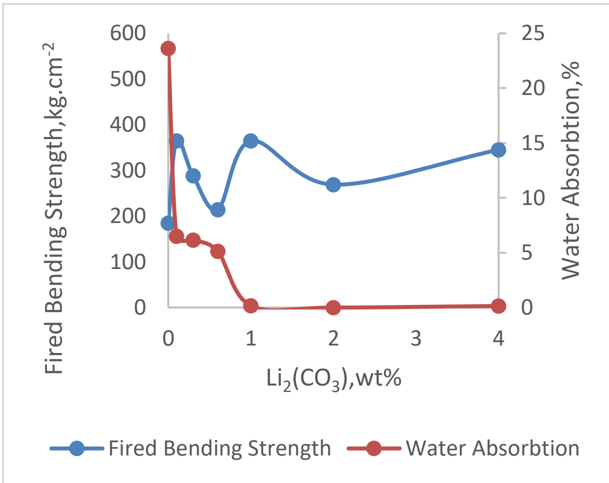

(All figure's first degrees are standard samples without H_3BO_3 and $Li_2(CO_3)$)

Figure 5. a.b.c.d.e.f respectively 0.1-0.3-0.6-0.9-1.2 ve 2 wt.% H_3BO_3 contain wall tile sample's fired shirinkage-wt.% $Li_2(CO_3)$ graphics.

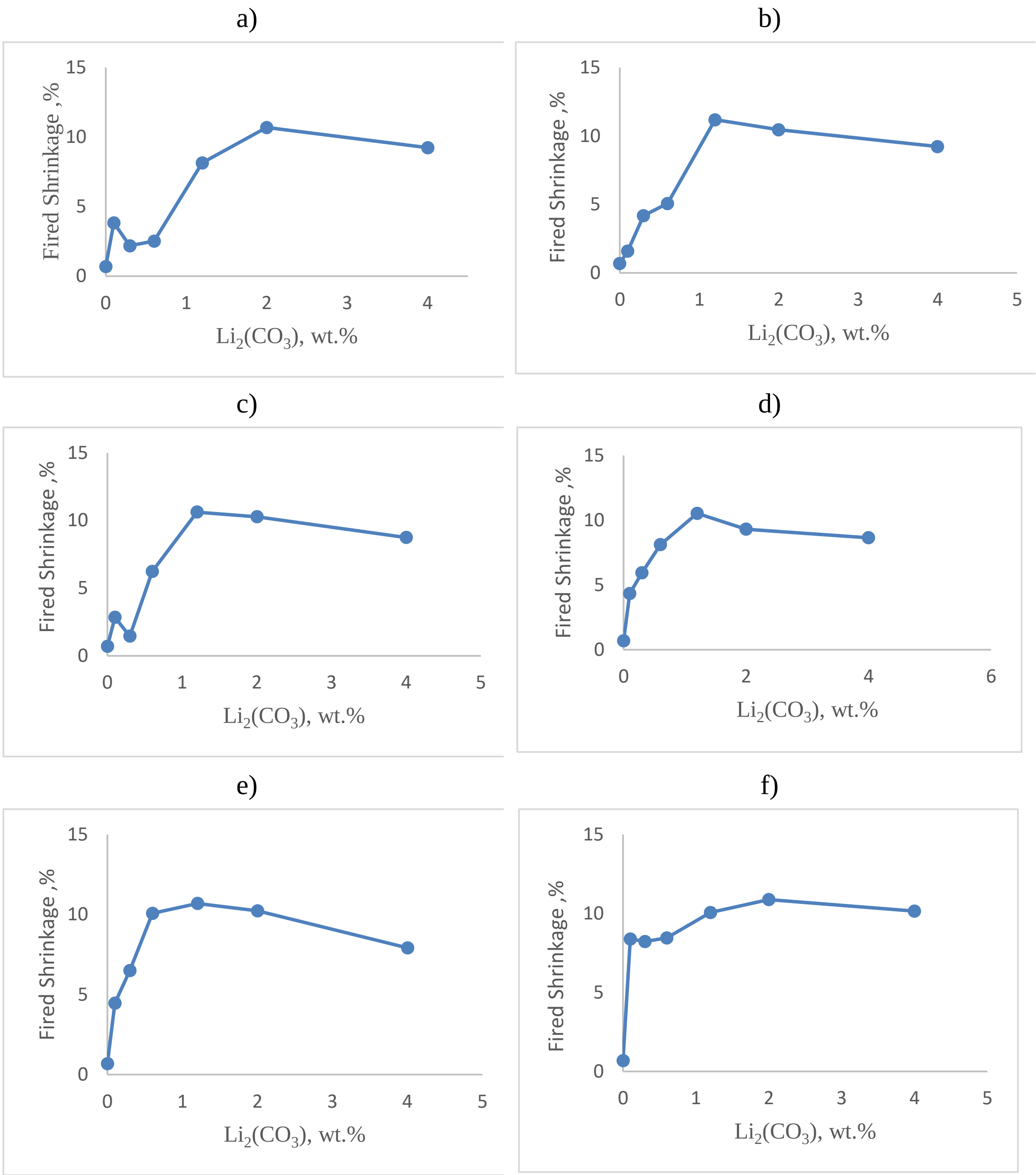

3.3. Rheological Behaviour

The viscosity of the standard sample measured with fordcup is 29 seconds, while the alternate body number 8's (0.3% H_3BO_3 + 0.1% $Li_2(CO_3$ added) is 36 seconds. According to Moreno [4], the addition of up to 0.9% of H_3BO_3 does not alter the rheological properties.

3.4. Microstructral Analysis

The secondary electron images of the standard body and H_3BO_3-$Li_2(CO_3)$ doped wall tile bodies obtained from the fractured surfaces of the bodies are shown in Figure 6. It is observed that the glassy phase is formed by the increasing amount of boric acid and lithium carbonate and hence the sintering takes place rapidly. Particularly number 7, 11, 32 and 37 added 0.1% H_3BO_3 + 4% $Li_2(CO_3)$, 3%H_3BO_3+1.2% $Li_2(CO_3)$, 2 % H_3BO_3 + 0.1 % $Li_2(CO_3)$, 2%H_3BO_3 + 4% $Li_2(CO_3)$ respectively have high percentage of glassy phase are seen in the experiment. The number of seven while the size of the pores with increasing value of 0.1% H_3BO_3 + 4% Li_2 (CO_3) increased and there was a wide por size distribution. The number of 11 pore's, which is added 0.3% H_3BO_3 + 1.2% Li_2 (CO_3), were reduced and narrow por size distribution is observed. With the addition of 2% H_3BO_3 + 0.1% Li_2 (CO_3) supplemented with the same boric acid amount as 37 and 2% H_3BO_3 + 4% Li_2 (CO_3) addition, the pores are increased in size with increasing Li_2 (CO_3). The maximum strength of 0.3% H_3BO_3 + 2% Li_2 (CO_3) added 11 is believed to result in eutectic and high viscosity and low viscosity glassy phase. SEM images of the experiment with 0.1% H_3BO_3 + 0.1% Li_2 (CO_3) which is an alternative wall tile prescription of 8 are similar with the standard wall tiles. 0.1wt.% H_3BO_3 + 4 wt.% Li_2 (CO_3) addition prescription is the recipe with the minimum amount of H_3BO_3 and the sintering is provided because of the presence of 4% Li_2 (CO_3). While this recipe shows a wide pore size distribution, the pore size distribution in the no 11 sample 0.3 wt.% H_3BO_3 + 1.2 wt.% Li_2 (CO_3) added sample narrowed and the small pores are generally dispersed in the glassy structure. 32 no sample, which is added 2wt. % H_3BO_3 + 0.1 wt.% Li_2 (CO_3) trial shows medium and small pores with narrow pore size distribution and no 37 sample 2% H_3BO_3 + 4% $Li_2(CO_3)$ added trial in the experiment large and small 2 size pore. According to Iqbal & Lee [11], the decrease in the size of the pores and the increase in the size of the glassy structure can be attributed to the easier integration of the pores by decreasing the viscosity. No 7 although the amount of boric acid with 0.1 wt.% H_3BO_3 + 4 wt.% Li_2 (CO_3) is low, the presence of lithium carbonate decreases the initial temperature of the liquid phase required for sintering with boric acid. increases the amount and decreases the viscosity of the glassy structure. According to Eplerr [12], the Li_2O-SiO_2-Al_2O_3 triple system constitutes approximately 15% Li_2O-79% SiO_2-8% Al_2O_3 eutectic below 1000 ^{0}C[13]. It is thought that boric acid is involved in eutectic formation and this effect is effective in reducing the temperature and decreasing the viscosity of the glassy phase.

Figure 6 a 1 no sample (standart wall tiles)
b 2 no sample (H_3BO_3 0.1 wt.% + $Li_2(CO_3)$ 0.1 wt.%
c 7 no sample (H_3BO_3 0.1 wt.% + $Li_2(CO_3)$ 4 wt.%)
d 8 no sample (H_3BO_3 0.3 wt.% + $Li_2(CO_3)$ 0.1 wt.%(replacing wall tiles)
e 11no sample (H_3BO_3 0.3 wt.% + $Li_2(CO_3)$ 1.2 wt.%) (Max.strength)
f 32 no sample (H_3BO_3 2 wt.% + $Li_2(CO_3)$ 0.1 wt.%
g 37 no sample (H_3BO_3 2 wt.% + $Li_2(CO_3)$ 4 wt.%) sample's SEM photographs

(a) 1 no sample

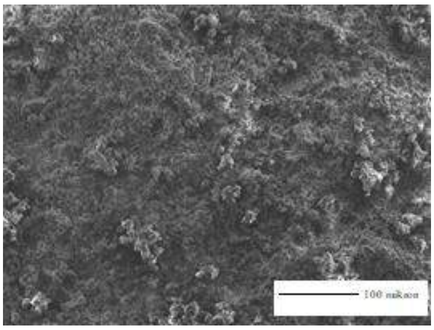

b) 2 no sample

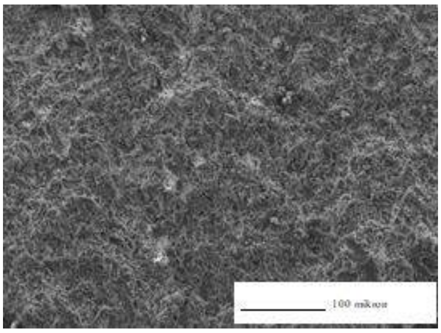

(c) 7 no sample

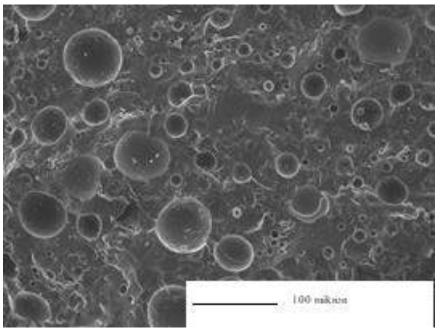

(d) 8 no sample

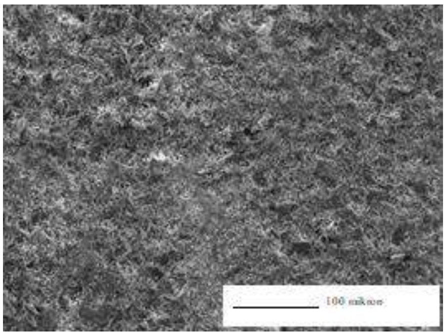

(e) 11 no sample

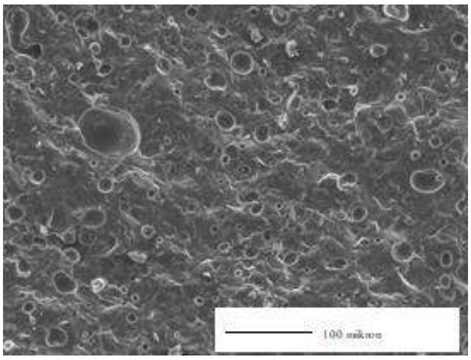

(f) 32 no sample

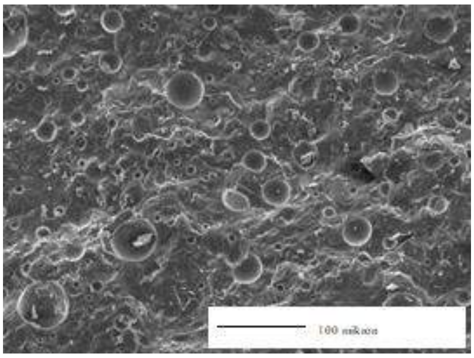

(g) 37 no sample

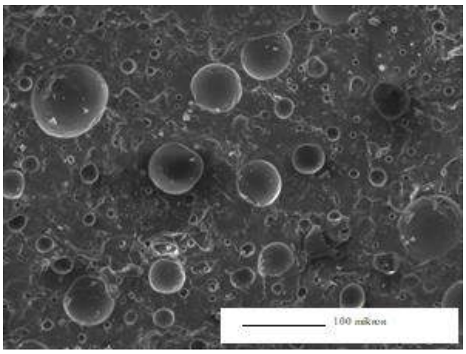

3.5. Phase Analysis

The crystalline phases in the samples of the wall tiles are given in Figure 7. Kurama et al. [14], as shown in the study on the subject, as a result of the system's low firing temperature and short firing time is available free quartz. In addition, plagioclases and low quantity of mullites phases were detected. In no 7 (added H_3BO_3 0.1 wt.% Li_2 (CO_3) 4 wt.%) and no 37 (added H_3BO_3 2 wt.% + Li_2 (CO_3) 4 wt.%) samples mullite formation occur due to low viscosity of glassy phase. According to Low et all. [15], the use of spodumene provides better physical and mechanical properties to ceramics. Prescription 1-2 and 8 no samples show mullite peaks. In experiment 37 (H_3BO_3 2 wt.% + Li_2 (CO_3) 4 wt.%) quartz content is low; the reason for this is that the viscosity of the liquid phase formed is low and thus its activity is high. No 2 as 0.1 wt.% H_3BO_3+ Li_2 (CO_3) 0.1 wt.% added and no 8 as 0.3 wt.% H_3BO_3+ 0.1 wt.% Li_2 (CO_3) added, despite of the same amount of $Li_2(CO_3)$, the quartz dissolution in glassy phase decreased with increasing H_3BO_3 no 8 as H_3BO_3 0.3 wt.% H_3BO_3+ 0.1 wt.% Li_2 (CO_3) added recipe is close to the XRD graphics of the standard wall tile and from the strength measurements that no 8 sample has a better strength value.

Figure 7. Fired wall tiles sample's XRD patterns (Q: Quartz. M: Mullite. P: Plagioaclase.)

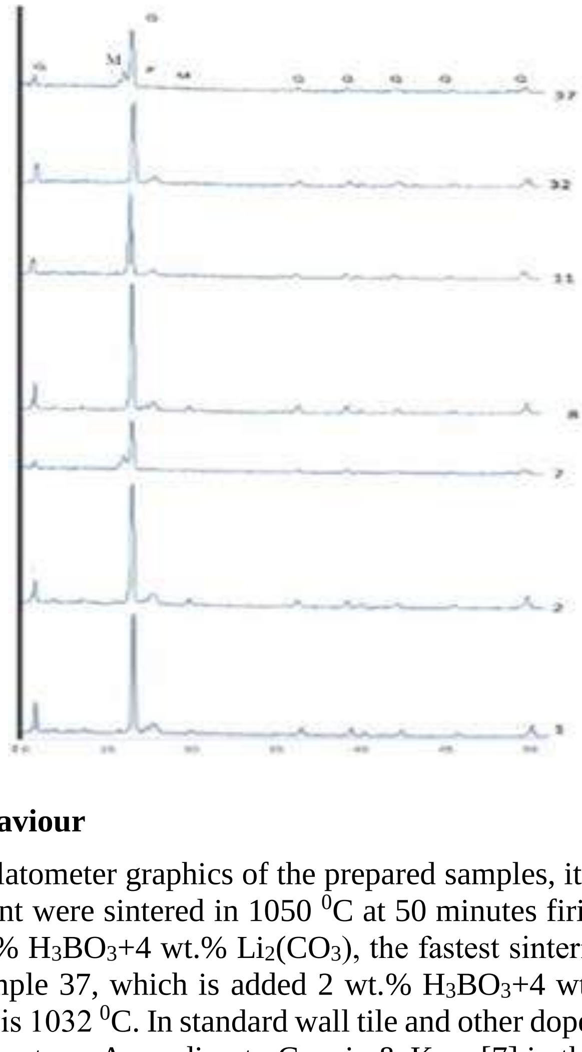

3.6. Firing Behaviour

In the optical dilatometer graphics of the prepared samples, it was observed that only 7 and 37 of the experiment were sintered in 1050 ^{0}C at 50 minutes firing time. In no 7 sample, which is added 0.1 wt.% H_3BO_3+4 wt.% $Li_2(CO_3)$, the fastest sintering's temperature is 1038 ^{0}C. Whereas in the sample 37, which is added 2 wt.% H_3BO_3+4 wt. % $Li_2(CO_3)$, the fastest sintering's temperature is 1032 ^{0}C. In standard wall tile and other doped samples, sintering does not appear in this temperature. According to Cengiz & Kara [7] in the standard wall tile body, the temperature, which sintering is the fastest is 1148^{0}C, which the other name is flex point. Whereas added 1% H_3BO_3 body's fastest sintering's temperature is 1142 ^{0}C. Figure 7 shows the optical dilatometer graphics of the selected experiments.

Figure 8 a) 1-2-7-8-11-32-37 no sample's dilatometric curves
b) 7 no sample 0.1 wt.% H_3BO_3 + 4 wt.% $Li_2(CO_3)$ added wall tile's dilatometric curve
c) 37 no sample 2 wt.% H_3BO_3 + 4 wt.% $Li_2(CO_3)$ added wall tile's dilatometric curve

a)

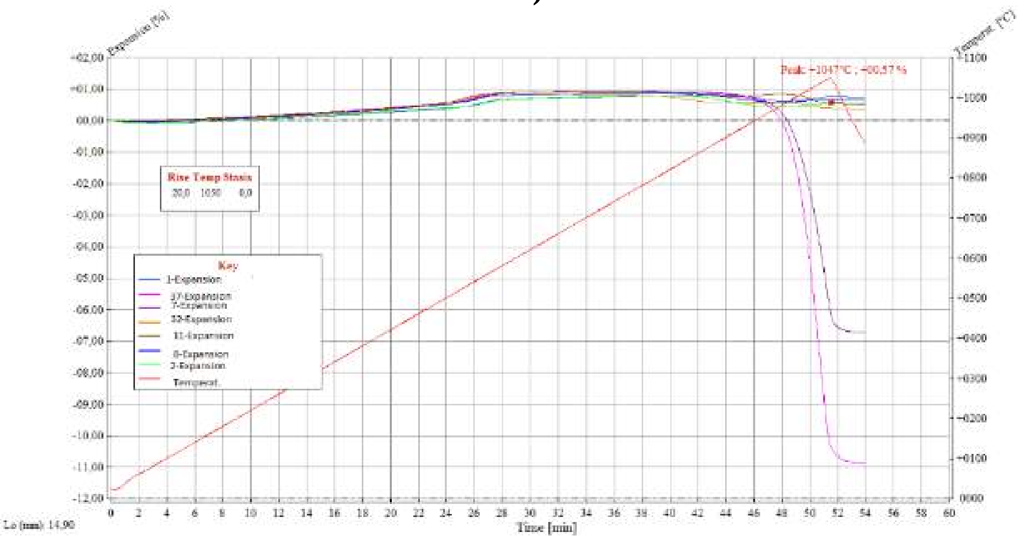

b)

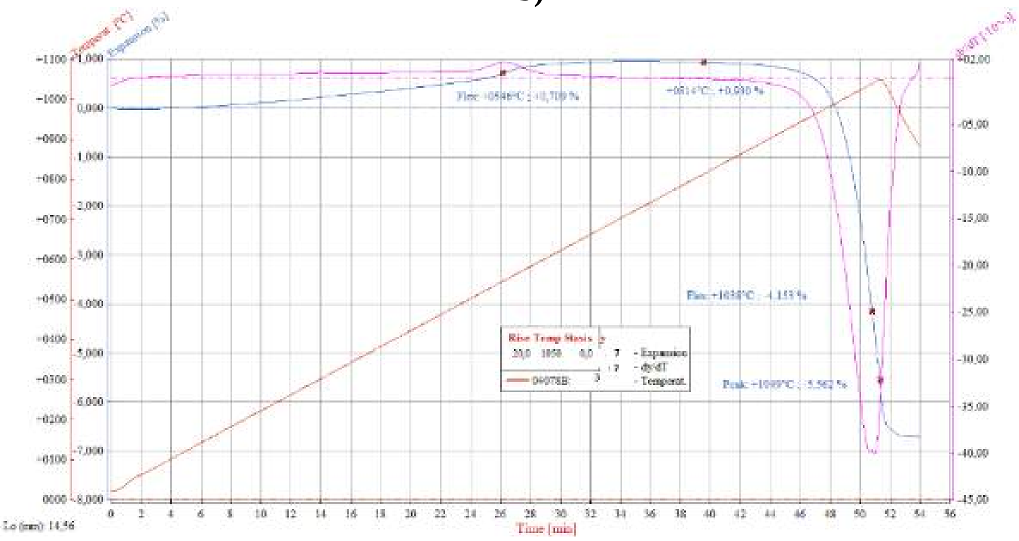

(c)

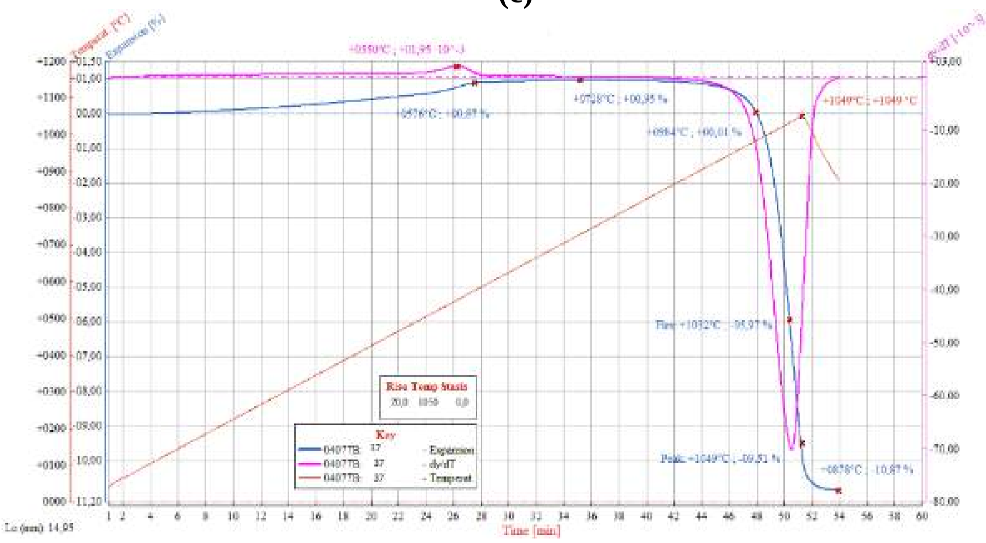

Thermogravimetric and differential thermal analysis of standard and alternative masse 8 are given in figures 9-10-11 and 12. The characteristic endothermic peaks of the standard and the number 8 were 59.8,518.3, 577 and 773 ^{0}C and 60.8, 521.9, 576 and 772.5 ^{0}C, respectively. The first peak, second, third and fourth peaks show the temperature of the water absorbed physically, the temperature of formation of the metakaolin, the quartz alpha beta conversion and the decay temperature of $CaCO_3$, respectively. An exothermic peak was observed in the standard sample at 997.6 °C, whereas in the 8. prescription it was observed at 995.3 °C and more severe. It is thought that the increase in strength is caused by anorthite mineral formation [16]. Since the thermogravimetry curve of the alternative mass is below the standard mass, the formation of metakaolin and the decomposition of $CaCO_3$ in the alternative mass show that the reaction is efective . When the DTG graph is seen, the temperature at which the formation temperature of metakaolan is most rapid is 508.8 ^{0}C and the temperature is 506 ^{0}C in standard mass. The temperature at which the calcite is decomposed most rapidly is 766.7 and 767.4 0C in the alternative receipe and the standard. The mass loss resulting from the calcite decomposition of the standard mass appears to be 4.60 % while the alternative mass is 4.60%. This shows that the body reacts with a small amount of the Ca element in the calcite which decomposes. The starting and ending temperature of decomposition of calcite in both bodies did not change.

Figure 9. Thermogravimetric analysis of standart receipe

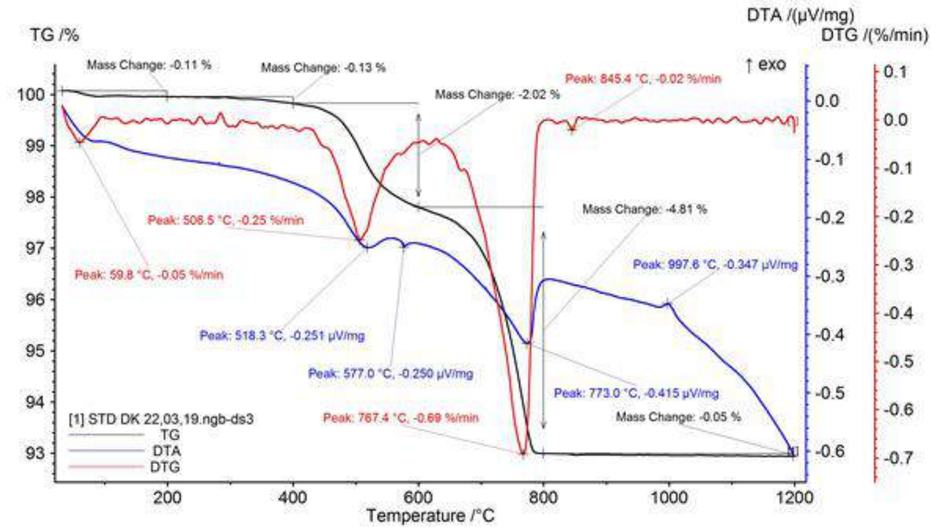

Figure10 Thermogravitmeric analysis of alternative receipe (8 no receipe)

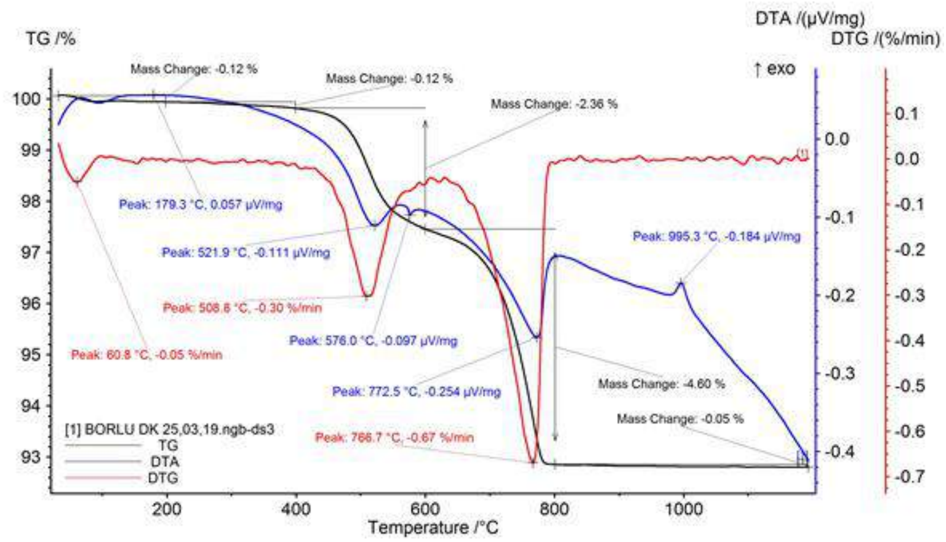

Figure 11. Thermogravimetric and differantial thermogravimetric analysis of both of the standard and alternative receipe.

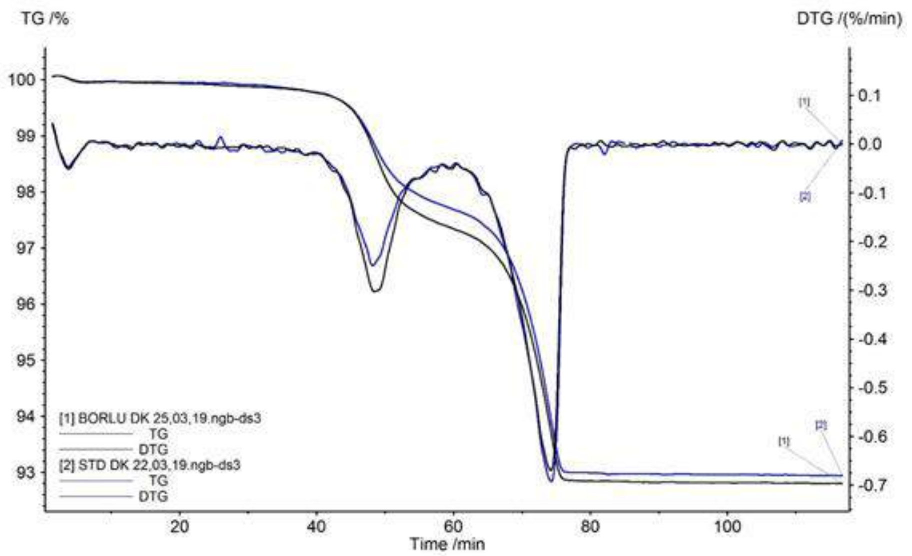

Figure 12. Differantial thermal analyses of both of standard anf alternative receipe

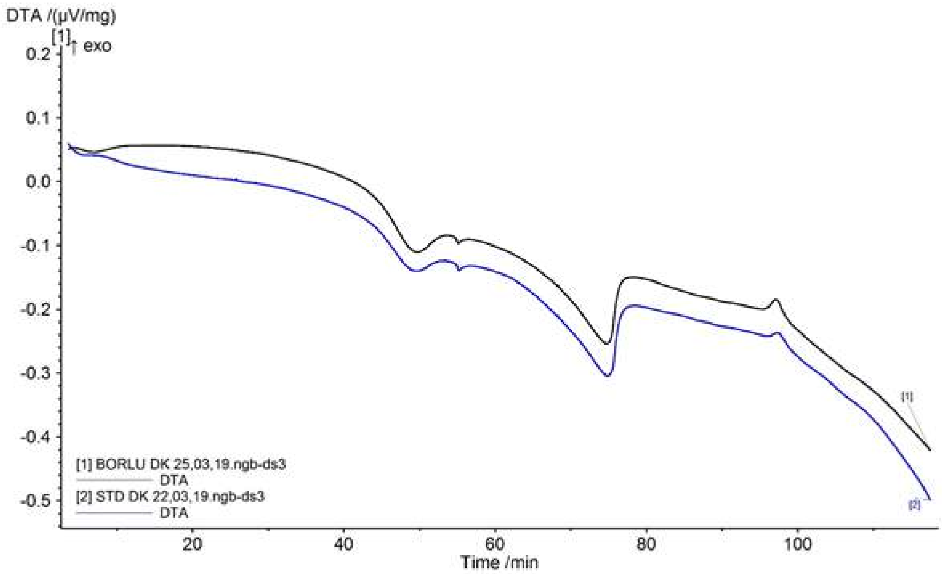

4. CONCLUSIONS

The combined use of H_3BO_3 and $Li_2(CO_3)$ allows an active liquid phase sintering than the individual adding. The combined use of the active flux increases the mullitization reactions and gives better physical and chemical characteristics. The decomposition of $CaCO_3$ does not change with the added flux. 0.3wt.% H_3BO_3 + 0.1 wt% Li_2 (CO_3) doped wall tile test showed similar water absorption and firing value with standard wall tile. The samples contain this added ratio show the fired strength is 334.97 kgf/cm^2 whereas the standard wall tile's strength is 184.94 kgf/cm^2.

REFERENCES

[1] MEZQUITA, A., BOIX, J., MONFORT, E., MALLOL G, 2014, Energy Saving In Ceramic Tile Kilns: Cooling Gas Heat Recovery, *Aplied Termal Engineering*. 65. 101-110.

[2] CENGİZ, Ö., KARA, A., Tek Pişim Duvar Karosu Bünyelerinde Borik Asit İlavesinin Sinterleme Davranışına Etkileri, *Afyon Kocatepe Üniversitesi Fen Bilimleri Dergisi*, Özel Sayı, 29-35

[3] SOMANY, S., TRIVEDI, G.G., SRIDHAR, T., GOEL, A., MOHANTY, D., PITCHUMANI, B., 2014, *Increase In Vitrified Tile Production By The Use of Borate Flux*, Qualicer. Spain.

[4] MORENO A., GARCİA -TEN J., BOU E., GOZALBO A., 2000., *Using Boron As an Auxiliary Flux in Porcelain Tile Compocitions*, 77-91. Qualicer. Spain.

[5] TULYAGANOV, D.U., AGATHOPOULOS, S., FERNANDES, H.R., FERREIRA, J.M.F., 2005, Influence of Lithium Oxide as Auxiliary Flux on The Properties of Triaxial Porcelain Bodies. *Journal of the European Ceramic Society*, 26. 1131-1139.

[6] LOW.M., MATHEWS T., GARROD, T., ZHOU, T.,1997, Processing of spodumene-modified mullite ceramics, *Journal of Materials Science*, 32. 3807-3812

[7] YET, G., KARA, A. ,2007, Bor ve Türevlerinin Yer Karosu Çamur Reolojisi ve Sinterleme Davranışları Üzerine Etkileri. IV.Uluslararası Katılımlı Seramik, Cam, Emaye, Sır ve Boya Semineri, 505-520.

[8] ÇİĞDEMİR, G., KARA, A., KARA, F. ,2005, Porselen Karo Bünyelerine Borik Asit İlavesinin Etkileri.I. Ulusal Bor Çalıştayı, 19-24.

[9] TS EN 14411/Grup BIII. Su Emmesi E>10% olan Kuru Preslenmiş Seramik Karolar, 2006.

[10] VILCHES, E.S., 2002, Technical Considerations on Porcelain Tile Products and Their Manufacturing Process, Volume 1. 57-83. Qualicer. Spain.

[11] IQBAL Y., LEE W.E., 2000, Microstructural Evolution in Triaxial Porcelain, *J.Am. Ceram.Soc.* 83[12]. 3121-27.

[12] EPPLER, R.A. ,1963, Glass Formation and Recrystallization in The Lithium Metasilicate Region of The System Li_2O-Al_2O_3-SiO_2, *Journal of the American Ceramic Society*. 46(2):100.

[13] CARUS, L.A., BRAGANÇA, S.R. ,2013, Investigation of Spodumene-bearing Rock as a Flux for Bone China Production, *Material Research* 16(6). 1398-1404.

[14] KURAMA. S., KARA A., KURAMA H., 2007, Investigationnof Borax Waste Behaviour in The Wall Tile Production, *Journal of European Ceramic Society*. 27. 1715-1720.

[15] LOW, I. MATHEWS, E. GARROD, T., ZHOU, D., PHILIPS, D.N. and PILLAI, X.M., Processing of Spodumen-Modified Mullite Ceramics.,1997, *J.Mater Sci.* 32. 3817-3812.

[16] SIDNEI, J.G,S, JOSE N.F.,2003, Sintering Behavior of Porous Wall Tile Bodies During Fast Single-Firing Process. *Materials Resarch*, 8,197-200

Journal of Scientific Perspectives

Volume **3,** Issue **2,** Year **2019**, pp. **99-110**
E - ISSN: **2587-3008**
URL: http://ratingacademy.com.tr/ojs/index.php/jsp
DOİ: https://doi.org/10.26900/jsp.3.011
Research Article

pH-RESPONSIVE CARBOXYMETHYL CELLULOSE CONJUGATED SUPERPARAMAGNETIC IRON OXIDE NANOCARRIERS

Tülin GÜRKAN POLAT * & Seda DEMİREL TOPEL **

** Dr., Akdeniz University, Faculty of Engineering, Material Science and Engineering, 07058, Antalya, TURKEY, E-mail: tulingurkan@gmail.com*
ORCID ID: https://orcid.org/0000-0002-6545-0518

*** Assist. Prof. Dr., Antalya Bilim University, Faculty of Engineering, Material Science and Nanotechnology Engineering, Antalya, TURKEY, Corresponding author*
E-mail: seda.demireltopel@antalya.edu.tr
ORCID ID: https://orcid.org/0000-0002-0567-5627
(The authors are equally contributed.)

Received: 27 January 2019; Accepted: 12 March 2019

ABSTRACT

In the present study, polyethyleneimine (PEI) coated superparamagnetic iron oxide nanoparticles (SPIONs) having the size of 15 nm in diameter with high magnetic saturation (60 emu/g) have been prepared by co-precipitation method. The synthesized PEI-Fe3O4 nanoparticles have been fully characterized by transmission electron microscope (TEM), dynamic light scattering (DLS), Fourier transform infrared (FTIR) spectroscopy, X-ray photoelectron spectroscopy (XPS) and X-ray diffraction (XRD) techniques. The free amine groups on the PEI-Fe3O4 surface has been covalently functionalized with carboxymethyl cellulose (CMC) by the catalysis of N,N'-Dicyclohexylcarbodiimide (DCC) and N, N'-Dimethylpyridin-4-amine (DMAP) coupling to produce CMC-Fe3O4 nanocarriers. The prepared CMC-Fe3O4 nanocarriers have been loaded with a well-known anti-tumor drug doxorubicin (Dox) and investigated its loading and releasing profiles from the nanocarrier. The CMC acted as an excellent nanocarrier for Dox with a loading efficiency ≈ 86%. The drug releasing profile has been studied at different pH values (3.5; 5.5; and 7.4). When the pH of the release medium (phosphate buffer solution) was changed from 7.4 to 5.5 or 3.6, the drug release has been increased which indicates that the drug releasing is pH dependent.

Keywords: *Superparamagnetic iron oxide, carboxymethyl cellulose, doxorubicin, pH, drug release*

1. INTRODUCTION

Nanotechnology has been become a fast growing research field in worldwide. The reason of its fast growing dramatically is that the nanotechnology has the potential to profoundly *improve* the *quality* of our health and our lives. Nanostructured materials (nanoparticles, nanotubes, nanowires, thin films, nanocomposites) exhibit new physical, chemical and biological properties relative to bulk materials [1]. Due to the large surface area/volume ratio of the nano-sized materials, they can easily functionalize with ligands or coating agents. As a result of this property, the new nanomaterial can gain new properties which can be applied in many industries such as electric&electronics, biomedical, medical, food, agriculture, textile and cosmetics [2].

Nanomaterials can be classified into four categories: (i) carbon based, (ii) inorganic based, (iii) organic based, and (iv) composite based nanomaterials [3]. Magnetic iron oxide nanoparticles (IONPs) are in the class of inorganic nanomaterial and generally used in lithium ion batteries, supercapacitors, catalysis, releasing therapeutic agents, labelling the cells and separation of biochemical products [4]. Due to their low cytotoxicity and superparamagnetic properties (Fe_3O_4 and γ-Fe_2O_3), they can also be used as magnetic resonance imaging (MRI) and thermal therapy agent in the biomedical field [5].

IONPs composed of different magnetic properties and chemical ingredients. The main compounds of iron oxides are hematite (α-Fe_2O_3), magnetite (Fe_3O_4) and maghemite (γ-Fe_2O_3). Each of these three iron oxides has unique biochemical, magnetic, catalytic, and other properties which provide suitability for specific technical and biomedical applications. Even magnetite (Fe_3O_4) and maghemite (γ-Fe_2O_3) have the same physical properties, maghemite has less magnetic than the magnetite [4].

In order to synthesize these IONPs, a variety of synthetic methods such as co-precipitation, thermal decomposition, hydrothermal and solvothermal syntheses, sol-gel synthesis, microemulsion, ultrasound irradiation and biological synthesis can be carried out [6]. The bare magnetic nanoparticles have the problems about aggregation and surface oxidation which limits their therapeutic usage. Therefore, they need to be surface engineered in order to improve on their dispersibility, stability, and biocompatibility. For this reason, the surface of IONPs should be further functionalized with silica or polymeric coatings such as polyethylene glycol-PEG, dextran, polyethyleneimine-PEI, polyacrylic acid and/or chitosan depending on the biomedical applications [7]. As a result of the surface modification with these polymeric materials, the agglomeration can be inhibited and the superparamagnetic properties can be protected due to high surface energies of IONPs. In addition, the surface modification also offers the functional groups for further functionalization by anchoring drug molecules, antibodies or peptides.

IONPs can also be modified with a pH responsive polymer in order to apply to a pH dependent drug delivery systems [8]. The microenvironment of the tumor tissue has low pH values (5.8) and even lower at endosomes (pH 5.0-6.0) and lysosomes (pH 4.0-5.0) which emphasize the importance of pH parameter on cancer [9]. In recent years, many pH-responsive IONPs have been developed. Among these studies, IONPs have been coated with imidazole modified PEG-polypeptide (mPEG-poly(L-asparagine) [10], bovine serum albumin [11], alginate [12],

β-cyclodextrin [13], poly (N-isopropylacrylamide) [14], polyethyleneglycol (PEG) [15] and hydroxyapatite [16] to obtain core-shell iron oxide structures. These core-shell structures have been loaded with an anti-tumour drug, doxorubicin and investigated their pH dependent releasing profiles. According to the studies mentioned above, the drug delivery in acidic buffer media (pH 5.5) is higher than that of physiological medium pH 7.4. The advantage of using iron oxide nanoparticles is that they can be directed through the cancer side via the guide of external magnetic field. By the carrying of these nanoparticles to the targeted cancer side, Dox delivers through the surface of magnetic nanocarrier due to the acidity of the microenvironment of the cancer tissue.

In the current study, PEI has been coated to the surface of Fe_3O_4 nanoparticles *in situ* and further functionalized with CMC by using DCC/DMAP coupling to produce CMC-Fe_3O_4 nanocarriers (Fig.1). For the surface functionalization, a cellulose based coating agent has been chosen due to its sustainability, biodegradability and biosafety. Additionally, cellulose has a well-documented history of successful use in U.S. Food and Drug Administration approved drugs/products [17].

Figure-1. The binding of carboxymethyl cellulose (CMC) to the PEI coated Fe_3O_4 nanoparticles covalently.

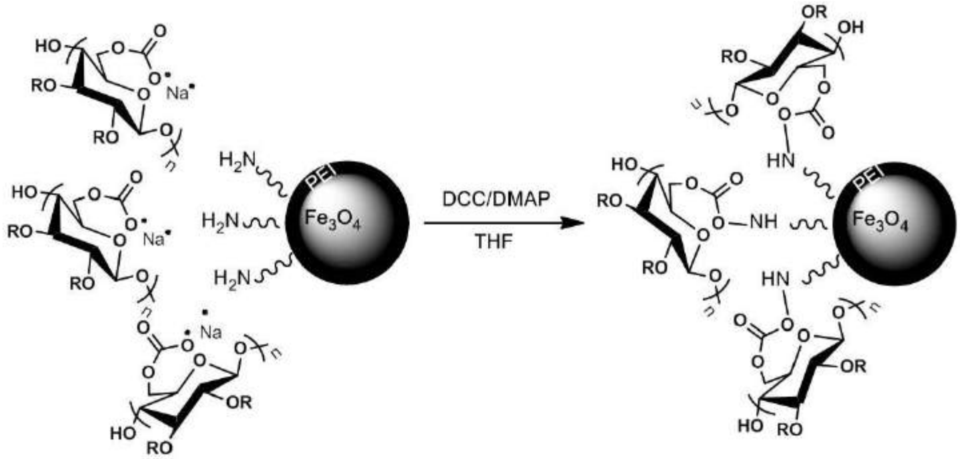

In some recent studies, CMC nanoparticles has been mixed with zein [18], graphene oxide [19] or resin [20] to produce CMC based nanocomposites as pH-responsive drug delivery nanocarriers. With the light of these studies, among many polymeric nanocarrier systems, cellulose based nanocarriers are seem to be ideal candidates for drug loading and pH-dependent drug delivery.

There is also a few study based on CMC based IONPs for pH-responsive drug delivery applications. Lang and co-workers prepared 5-Fluorouracil, an anti-cancer drug, loaded CMC-IONPs nanocarriers and investigated their drug release profiles at different pH values (5.5 and 7.4) [21]. In the preparation method of these nanocarriers, firstly CMC has been prepared as nanoparticles, then IONPs have been synthesized, and the synthesized IONPs were embedded to CMC nanoparticles. The drug loading efficiency was 89% and more than 85% of the encapsulated drug was released in a period of 60 h. in pH 5.5 buffer, whereas 74% of the drug was released in pH 7.4 buffer. The saturation magnetization was found as $8x10^{-5}$ Wb m/kg for CMC-IONPs.

Movagharnezhad and co-workers prepared a core-shell CMC-magnetic nanoparticles (MNP) by the covalent bonding of hexamethylenediamine modified CMC with hexamethylenediisocyanate grafted MNP [22]. The prepared CMC-MNP has been loaded with Dox molecules with ≈57.5% drug loading efficiency. The drug release studies showed that at pH 5.0, 65% of Dox was released within 5 hours, whereas only 50% of the Dox was released at pH 7.4 within this time interval.

In another study, Kanagarajan and co-workers developed CMC-$MnFe_2O_4$ magnetic nanocarriers for an anticancer hydrophobic drug, curcumin [23]. The preparation technique of these nanocarriers includes firstly the synthesis of magnetic $MnFe_2O_4$ nanoparticles, then coating with CMC and then with glutaraldehyde for crosslinking the polymer matrix. The resultant nanocarrier has ≈40% drug loading efficiency and pH-dependent drug release studies show that 46% of the drug has been released from the nanocarrier at pH 5.5 during 120 h, whereas 42% of the drug has been released at pH 7.4 during 120 h. The saturation magnetization of the CMC-$MnFe_2O_4$ nanoparticles were also found to be 36.1 emu/g.

The originality of our study is the covalently functionalization of CMC polymer having carboxylic acid functional group with PEI-Fe_3O_4 nanoparticles having the free amine group on the surface. As a result, the resultant nanocarriers provides a higher saturation magnetization (58 emu/g) compared to the related to the studies mentioned above. Additionally, in literature, after the introduction of CMC to the IONPs, the saturation magnetization has been decreased significantly [21-23], whereas in our study, the saturation magnetization was slightly decreased after CMC functionalization.

2. MATERIALS AND METHODS

2.1. Materials

Raw materials used during the synthesis, including iron(III) chloride hexahydrate ($FeCl_3 \cdot 6H_2O$), iron(II) chloride hexahydrate ($FeCl_2 \cdot 4H_2O$), polyethylenimine (PEI), carboxymethyl cellulose (CMC), *N,N′*-dicyclohexylcarbodiimide (DCC), 4-dimethylaminopyridine (DMAP), sodium hydroxide (NaOH), dimethyl sulfoxide (DMSO) were purchased from Sigma-Aldrich with minimum purity of 99%. Ammonium hydroxide (NH_4OH) with 25% purity was purchased from Merck. Doxorubicin HCl salt used as model drug was purchased from Toronto Research Chemicals. Dialysis tubing, 12,000 Da MWCO, 25 mm flat-width, from Sigma-Aldrich was used for drug loading studies. Deionized water and anhydrous ethanol were used in the experiments and purification processes.

2.2. Methods

2.2.1. Synthesis of PEI coated superparamagnetic Fe_3O_4 nanoparticles

$FeCl_3.6H_2O$ (2.36 g, 8.73 mmol) and $FeCl_2.4H_2O$ (0.86 g, 4.32 mmol) were transferred into three-necked flask and 40 mL of deionized water including PEI solution (2g/50 mL). The resulting solution was stirred and heated to 80°C under nitrogen atmosphere. Subsequently, NH_4OH (5 mL, 25%) was added into the flask and stirred for further one hour. After one hour, the reaction mixture was cooled to room temperature and the obtained Fe_3O_4 nanoparticles were separated from the mixture by means of a magnet. After washing three times with deionized water and ethanol, the nanoparticles were filtered and dried in a vacuum oven at 40°C [24].

2.2.2. Synthesis of CMC-Fe_3O_4 by covalent bonding of PEI-Fe_3O_4 with CMC

PEI coated Fe_3O_4 nanoparticles (20 mg) were dispersed in DMSO (15 mL). DMAP (10 mg) and DCC (10 mg) were added to the nanoparticle solution and stirred under nitrogen atmosphere for 10 minutes. Then, CMC (200 mg) was added into the above reaction mixture and stirred at room temperature overnight. The resulting CMC-Fe_3O_4 NP's were collected by centrifugation at 7500 rpm, washed 3 times with THF (50 mL), then washed twice with ethanol (50 mL). Finally, the CMC-Fe_3O_4 nanoparticles were dried in a vacuum oven at 40°C.

2.2.3. Preparation of Dox loaded CMC-Fe_3O_4 nanoparticles

For drug loading studies, doxorubicin (Dox), an anticancer drug, was selected as a model drug. To prepare the drug loaded CMC-Fe_3O_4 NPs, doxorubicin HCl (2.5 mg, 4.6 µmol) was dissolved in deionized water (20 mL). After adding CMC-Fe_3O_4 nanoparticles (150 mg) into this solution, the solution was transferred to a dialysis tube (MWCO: 12000 g/mol, diameter: 25 mm) and placed in the beaker containing deionized water (500 mL). It was kept at room temperature under stirring at 200 rpm for 24 hours for loading of the drug into the CMC-Fe_3O_4 nanoparticles. At the end of this period, the drug loaded nanoparticles were separated from the loading medium by centrifugation (7500 rpm). Drug concentrations loaded to CMC-Fe_3O_4

nanoparticles were determined by using Perkin Elmer, Lambda 650 UV-Visible spectrophotometer. The loading efficiency (LE%) and loading capacity (LC%) of Dox into the NPs were calculated using Equations (1) and (2), respectively.

$$\mathrm{LE\%} = \frac{\text{Total amount of Dox (mg)} - \text{The amount of Dox released from dialysis membrane (mg)}}{\text{Total amount of Dox (mg)}} \mathrm{x}100 \qquad \text{Eq-(1)}$$

$$\mathrm{LC\%} = \frac{\text{Total amount of Dox (mg)} - \text{The amount of Dox released from dialysis membrane (mg)}}{\text{The weight of NPs (mg)}} \mathrm{x}100 \qquad \text{Eq-(2)}$$

2.2.4. Dox release from CMC-Fe_3O_4 NPs

Dox release from nanoparticles was analyzed using a UV-Visible spectrophotometer (Perkin Elmer, Lambda 650). The calibration curve was constructed by analysing five different concentrations of Dox standard solutions in the concentration range of 5-50 ppm. Absorption spectra of Dox was measured in the range of 200-800 nm wavelength and the wavelength of maximum absorption of Dox was determined as 480 nm. The calibration curve was constructed by analysing five different concentrations of Dox standard solutions in the concentration range of 5-50 ppm. Molar absorptivity coefficient (ε) was calculated by using Lambert-Beer equation given in Equation (3) (Skoog et al. 1998).

$$A = \mathrm{l.\varepsilon.C} \qquad \text{Eq-(3)}$$

Here, A is the absorbance of the solution; I is the length of the cuvette and C is the concentration of the solution. Quartz cuvettes with 1 cm light path were used in the measurements.

Drug releases were performed with a dialysis method at three different *pH values.* For this purpose, Dox-loaded CMC-Fe_3O_4 NPs were divided into three equal parts by weighing. 2 mL of three different phosphate buffer solution (PBS) (pH = 3.5; pH = 5.5 and pH = 7.4) were added and each of the solutions were transferred into the dialysis membrane. Dialysis membranes were placed into the bottles containing 50 mL of buffer solution at three different pHs (3.5; 5.5 and 7.4) and allowed to stir at room temperature at a stirring rate of 200 rpm. At certain time intervals (2, 4, 6, 8, 24, 48, 72, 96, 120 and 144 hours), 1 mL solution was withdrawn from each release medium for analysis and after the measurement it was put back into the medium.

2.2.5. Characterization

The synthesized PEI-Fe_3O_4 and CMC-Fe_3O_4 nanoparticles were characterized by various techniques. Transmission electron microscopy (TEM) (ZEISS, LEO 906E) and dynamic light scattering (DLS) (Malvern, Nano ZS) analyses were performed to identify the surface morphology, particle size and particle size distributions of PEI-Fe_3O_4 and CMC-Fe_3O_4 in aqueous solutions. The Fourier transform infrared spectroscopy (FTIR) spectra were collected on a PerkinElmer L160000R FTIR spectrometer in order to confirm the functional groups of the polymers attached on the surface of Fe_3O_4 nanoparticles. Amount of polymer coating on the *Fe_3O_4 surface* was determined by using a Perkin Elmer, Pyris Series STA-8000 thermogravimetric analyzer (TGA) with a heating ramp of 10°C/min from 30 to 800°C under nitrogen purge (20 mL/min). The *in situ* functionalization of PEI to the Fe_3O_4 nanoparticles was further proved by X-ray photoelectron spectroscopy (XPS) (Thermo Scientific, K-Alpha-monochromated). Magnetic properties of the synthesized magnetic nanoparticles were measured with vibrating sample magnetometer (VSM), (Cryogenic Limited PPMS). UV-Visible spectrophotometer (Perkin Elmer, Lambda 650) was used for drug release experiments.

3. RESULTS AND DISCUSSION

3.1 Characterization studies of PEI-Fe_3O_4 and CMC-Fe_3O_4 nanocarriers

The surface morphology and particles sizes of both synthesized PEI-Fe_3O_4 and CMC-Fe_3O_4 nanoparticles have been determined by TEM and DLS techniques. The dilute solutions of the samples were dropped onto the carbon coated TEM grid and dried at room temperature for TEM measurements. According to the TEM measurements, PEI coated Fe_3O_4 nanoparticles have the size of 15 ± 5 nm in diameter with spherical shape (Fig 2A, 2D). After functionalization with CMC polymer, the sizes of the Fe_3O_4 nanoparticles have not been changed dramatically (Fig 2B), but their dispersibility in aqueous solution increased significantly. Electron diffraction pattern also indicates that the synthesized nanoparticles have highly crystalline structure. In Fig.2E, it can be clearly seen that the CMC-Fe_3O_4 nanoparticles are well dispersed in aqueous solution and did not precipitate over a week. When a magnet placed to one side of the bottle, CMC-Fe_3O_4 nanoparticles were collected in 40 seconds leading to a clear solution (Fig 2F).

Figure-2. TEM images of PEI-Fe_3O_4 nanoparticles (**A**),
CMC-Fe_3O_4 nanoparticles (**B**),
Electron diffraction pattern (**C**),
DLS of CMC-Fe_3O_4 nanoparticles in aqueous solution (1mg/mL) (**D**),
The well dispersed CMC-Fe3O4 nanoparticles in H2O (**E**),
with a neodymium magnet (**F**).

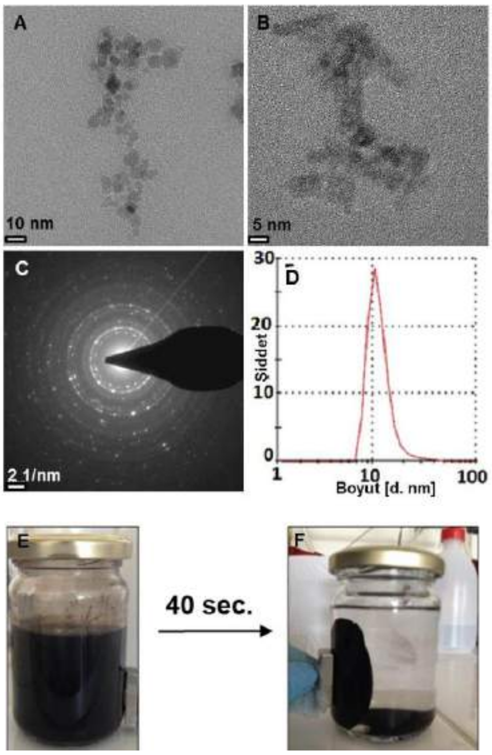

The crystal phase of the all synthesized nanoparticles have been determined by XRD measurements. Both the nanoparticles, as depicted in Fig. 3, bare Fe_3O_4, PEI-Fe_3O_4 and CMC-Fe_3O_4 nanoparticles have been exhibited strong diffraction peaks indexed as (111), (220), (311), (440), (422), (511), (440) and (533). These peaks were coherent with the reference of JCPDS card no-79-0417 and indicated that IONPs are in cubic phase. On the other hand, it should be noted that the peak positions did not changed after the functionalization with CMC polymer, which indicated that the crystallinity of the IONPs was not affected by the polymer modification process.

$$D = \frac{0.9\,\lambda}{\beta.\cos\theta} \qquad \text{Eq-(4)}$$

The size of the nanoparticles can also be calculated from the Debye-Scherrer's equation given in Eq-4, where D is the mean crystallite size, β is full width of half maximum intensity, θ is the Bragg's angle in degrees, and λ is the X-ray wavelength. The peak (311) at 2θ = 35.6° was used for the calculation because of its well resolution. The size of the PEI-Fe_3O_4 and CMC-Fe_3O_4 nanoparticles were calculated to be 19.8 nm and 25.04 nm, respectively which are coherent with the TEM data.

Figure-3. XRD spectra of bare Fe_3O_4, PEI-Fe_3O_4 and CMC-Fe_3O_4 nanoparticles

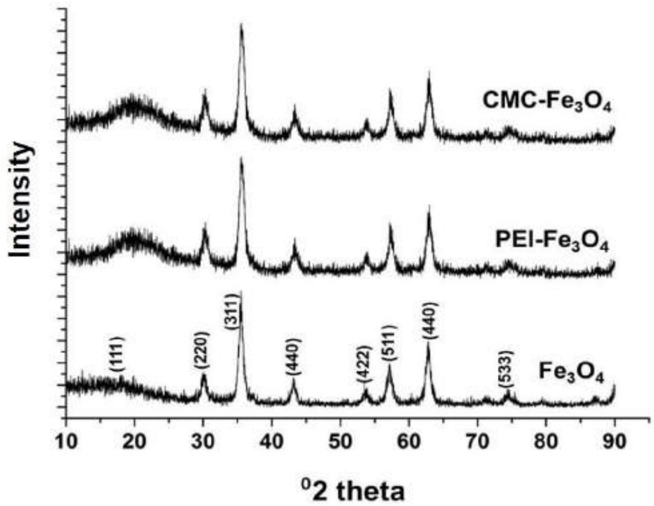

The existence of functional groups of PEI and CMC on the Fe_3O_4 nanoparticles have been proved with FTIR analysis (Fig. 4). In the FTIR spectrum of bare Fe_3O_4, the peaks at 3345 cm^{-1} and 1623 cm^{-1} represent the stretching of hydroxyl groups (–OH) and/or bending vibrations of adsorbed water molecules, respectively. In addition, the peak at 548 cm^{-1} is the characteristic absorption band of Fe-O stretching vibrations. By the modification of Fe_3O_4 with PEI, the peak 2837 cm^{-1} have been appeared due to the C-H stretching vibrations of the aliphatic chains. Additionally, N-H stretching, C-N stretching vibrations belonging to free amine groups (-NH_2) in the PEI were appeared at 3351cm^{-1}, 1617 cm^{-1} and 1320 cm^{-1}, respectively. Due to the modification with PEI, the stretching peak of Fe-O was shifted to 561 cm^{-1}. After the covalently bonding between PEI and CMC polymers, amide functional group (-NHCO-) has been formed which can be seen at 3325 cm^{-1} as stretching of N-H, 1623 cm^{-1} as stretching of carbonyl group (Amide-I band, C=O), 1571 cm^{-1} as the stretching of N-H (Amide-II band, N-H) and 1313 cm^{-1} as the stretching vibration of C-N (Amide-III band, C-N) [25]. These are the essential absorption bands of amide which was also proved that the CMC has been covalently bonded to the surface of PEI-Fe_3O_4.

Figure-4. FTIR spectra of the bare Fe_3O_4, PEI-Fe_3O_4 and CMC-Fe_3O_4 nanoparticles

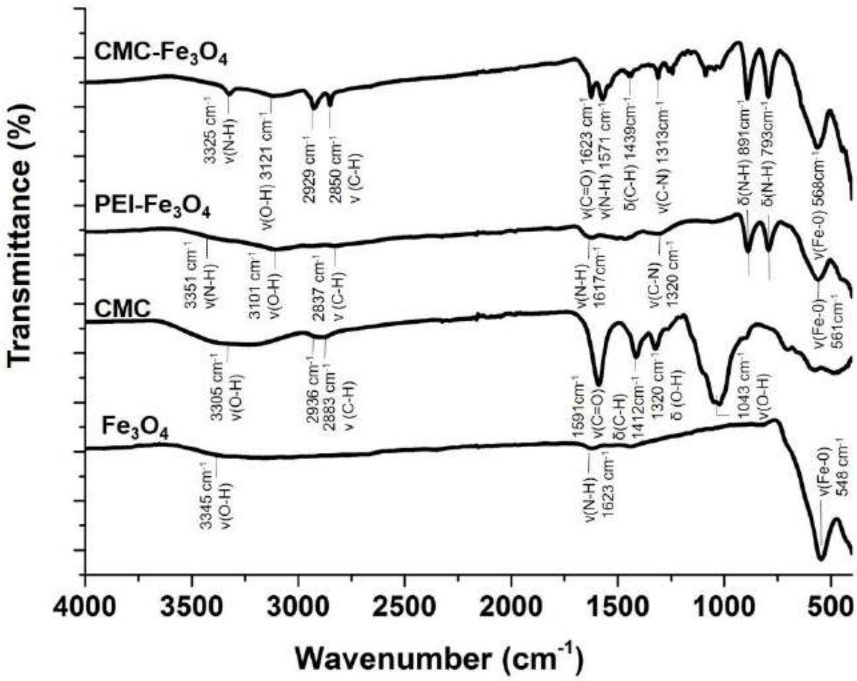

In addition, XPS spectrum confirms the existence of PEI on the magnetic nanoparticle surface Fig. 5A. The peak at 402 eV corresponds to N 1s which proves that the magnetic Fe_3O_4 nanoparticles coated with PEI (Fig. 5C). The peaks correspond to the binding energies at ~711 eV and ~725 eV are related to Fe 2p3/2 and Fe 2p1/2, respectively [26]. Also, the binding energy at 531 eV is attributed to O1s indicating O-Fe in magnetic phase (Fig. 5B).

Figure-5: XPS spectra of the PEI-Fe_3O_4 nanoparticles coated on a silicon wafer (**A**), binding energies of Fe 2p orbital at PEI-Fe_3O_4 nanoparticles (**B**), binding energy of N 1s orbital at PEI-Fe_3O_4 nanoparticles (**C**)

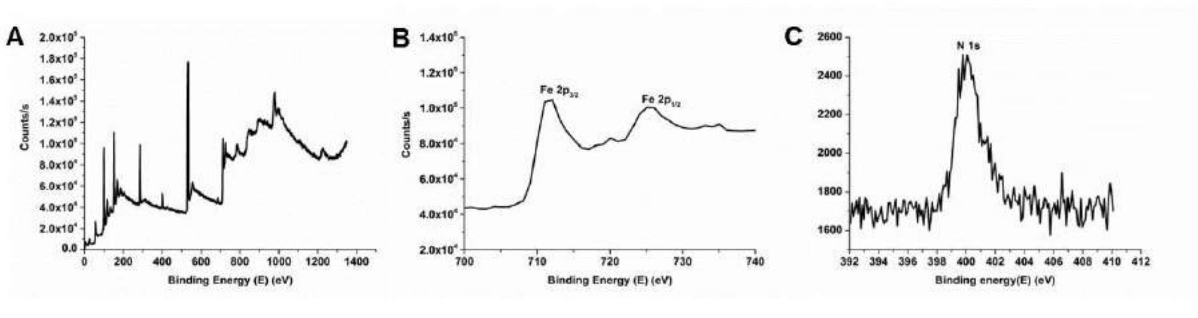

In order to determine the mass percentages of the PEI and CMC polymers on the Fe_3O_4 nanoparticles, thermal gravimetric analysis (TGA) has been carried out (Fig. 6). All samples were heated from 25ºC to 800 ºC at a heating rate of 5 ºC/min. under nitrogen atmosphere. First of all, for all samples there are 2.5 % weight loss due to the removal of residual moisture owing to the adsorbed water molecules. On the other hand, for PEI and CMC polymers, there are 14 % and 15 % weight loss in total, respectively due to the decomposition of the organic polymers. Also, the Fe_3O_4 nanoparticles were thermally stable up to 800°C which indicated the presence of Fe_3O_4 nanoparticles. The TGA results confirmed that the modification with CMC polymer has been done successfully.

Figure-6. TGA curves of bare Fe_3O_4, PEI-Fe_3O_4 and CMC-Fe_3O_4

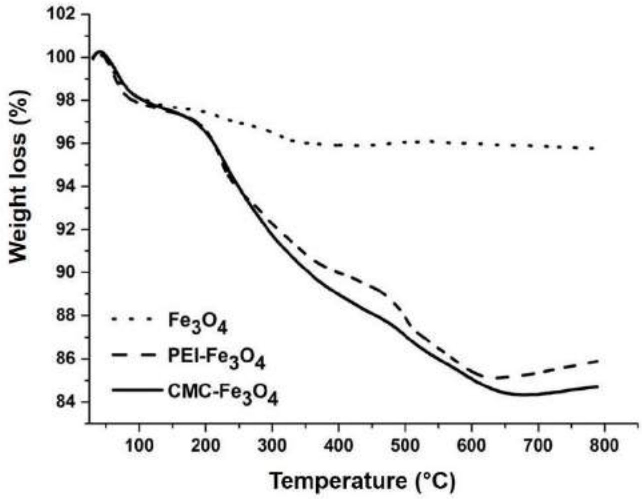

A vibrating sample magnetometer (VSM) was used to study the magnetic properties of *in situ* synthesized PEI-Fe_3O_4 and CMC-Fe_3O_4 nanoparticles. The saturation magnetizations (Ms) were obtained 60 and 58 emu/g for PEI-Fe_3O_4 and CMC-Fe_3O_4 nanoparticles, respectively (Fig. 7). In addition, there was no hysteresis loop in the magnetization curve, demonstrated that the IONPs are superparamagnetic. It should be noted that, the saturation magnetization of IONPs was slightly decreased after the modification with CMC, which means that synthesized CMC-Fe_3O_4 nanocarriers were still superparamagnetic which makes them also a good candidate for T1 contrast agent for MRI.

Figure-7. VSM of PEI-Fe_3O_4 and CMC-Fe_3O_4 nanoparticles

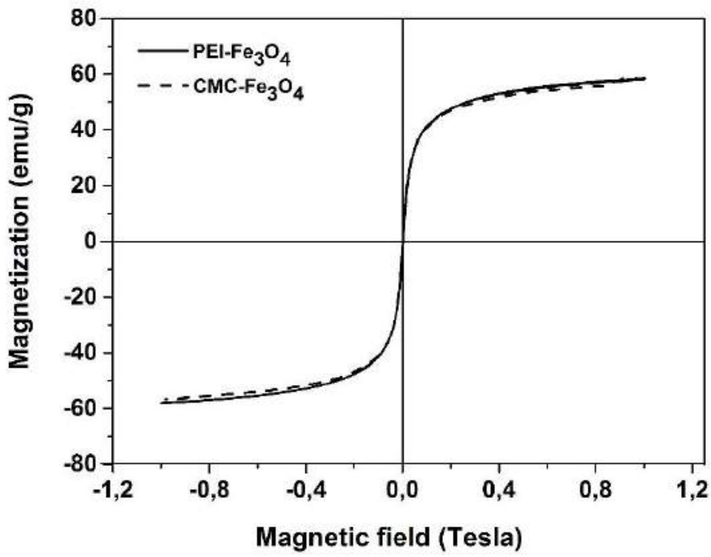

3.2 Drug loading efficiency and in vitro drug release studies

After the preparation of CMC-Fe_3O_4 nanocarriers, Dox molecules have been loaded via adsorption in buffer solution and studied their Dox releasing profiles in phosphate buffer solution (PBS) having different pH values (3.6, 5.5 and 7.4) [23]. The working principle of our system can be explained as follow: due to the chemical structure of CMC, it is interacted with Dox molecules via hydrogen bonds at neutral pH. With the decreasing of pH, CMC is protonated and the interaction between Dox and CMC becomes weak, and then Dox molecules become free from the CMC polymer (Fig. 8).

Figure-8. The interaction mechanism between CMC-Fe_3O_4 nanocarrier and Dox molecule and releasing of Dox depending on pH

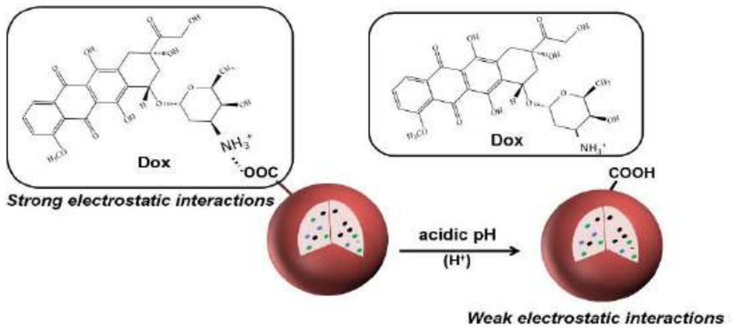

According to the adsorption studies of Dox molecules onto the CMC-Fe_3O_4 nanocarriers, the Dox loading efficiency and drug loading capacity has been calculated as 86.2% and 1.44%, respectively. On the other hand, *in vitro* drug release from Dox loaded CMC-Fe_3O_4 nanocarriers at three different pH values were done as shown in Fig. 9. At physiological pH 7.4, 3.24% drug released was observed for 144 h, which increased to 6.30% at pH 5.5 and 11.8% at pH 3.6 for 144 h (Fig. 9).

Figure-9. Drug release profiles of CMC-Fe_3O_4 nanocarriers at pH 3.6, 5.5 and 7.4

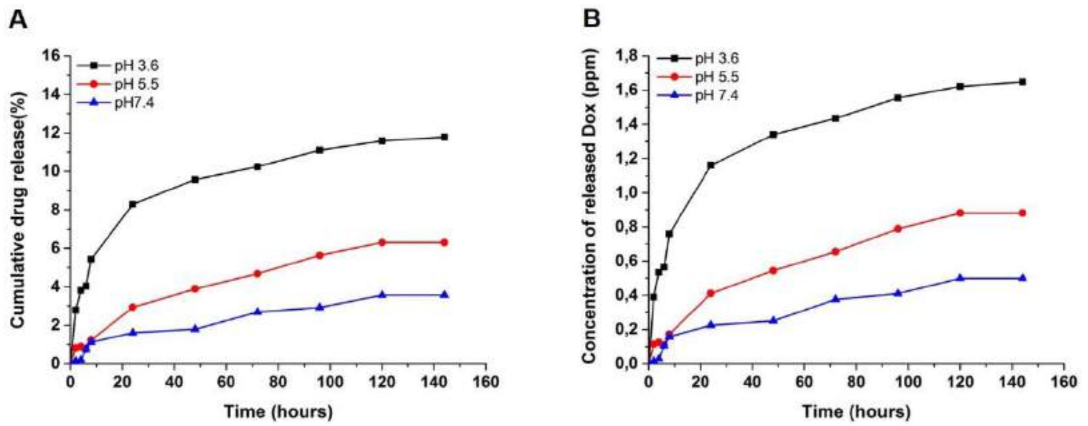

4. CONCLUSION

In this study, superparamagnetic CMC-Fe_3O_4 nanoparticles have been developed as a drug-delivery carrier. The resultant Dox loaded CMC-Fe_3O_4 nanocarriers were approximately 15 nm in diameter with a spherical shape and high encapsulation efficiency. *In vitro* studies of the drug release pattern showed a sustained release of Dox over a period of 144 hours at acidic, mild acidic and neutral conditions where the pHs 3.6, 5.5 and 7.4, respectively. Among these different pH values, the CMC-Fe_3O_4 nanocarriers exhibited higher Dox release profile at acidic medium (pH 3.6). On the other hand, due to the superparamagnetic property of the nanocarriers, they can be used as T1 contrast agent for MRI. As a result, dual function CMC-Fe_3O_4 nanocarriers with combined characteristics of MRI and controlled drug delivery could be of high clinical significance in the treatment of cancer.

Acknowledgments

This work was funded by TUBITAK-1002 (Project no. 116Z164) and the authors are grateful to Prof. Meltem Asilturk for her support and laboratory facilities.

REFERENCES

[1] KAUR G., SINGH T., KUMAR A. 2012, Nanotechnology: A review, *Int J. Edu. & Appl. Sci.* 2, 50-54.

[2] BHATTACHARYYA, D., SINGH, S., SATNALIKA, N., KHANDELWAL, A., JEON, S.H., 2009, Nanotechnology, Big things from a tiny world: a review. *Int. J. Service, Sci and Tech*. 2, 29-39.

[3] JEEVANANDAM, J., BARHOUM, A., CHAN, Y.S., DUFRESNE, A., 2018, Danquah M.K. Review on nnaoparticles and nanostructured materials: history, sources, toxicity and regulations. *Beilstein J. Nanotech*. 9, 1050-1074.

[4] VALLABANI, N.V.S., SINGH, S. 2018, Recent advances and future prospects of iron oxide nanoparticles in biomedicine and diagnostics. *3 Biotech*. 8, 279-302.

[5] STEPHEN, Z.R., KIEVIT, F.M., ZHANG, M. 2011, Magnetite nanoparticles for medical MR imaging. *Mater. Today*. 14, 330-338.

[6] ANSARI, M.O., AHMAD, F., PARVEEN, N., AHMAD, S., JAMEEL, S., SHADAB, G.G.H.A., 2017, Iron oxide nanoparticle-synthesis, surface modification, applications and toxicity: a review. *Materials Focus*, 6, 1-11.

[7] ZHU N., JI, H., YU P., NIU, J., FAROOQ, M.U., AKRAM, M.W. UDEGO, I.O., LI, H., NIU, X. 2018, Surface modification of magnetic iron oxide nanoparticles. *Nanomaterials*. 8, 810-837.

[8] NEDAL, A.S. H. M. and THABIT, N.Y. 2018, *Stimuli responsive polymeric nanocarriers for drug delivery applications*. Woodhead publishing; Elsevier, Chapter.2.

[9] KATO, Y. OZAWA, S., MIYAMOTO, C., MAEHATA, Y., SUZUKI, A,. MAEDA, T., BABA, Y., 2013, Acidic extracellular microenviroment and cancer. *Cancer Cell. Int.* 13, 89-98.

[10] YU, S. WU, G. GU, X. WANG, J. WANG, Y., GAO, H., MA, J. 2013, Magnetic and pH-sensitive nanoparticles for antitumor delivery. *Coll. and Surf. B: Biointer*. 103, 15-22.

[11] SEMKINA, A., ABAKUMOV, M., GRINENKO, N., ABAKUMOV, A., SKORIKOV, A., MIRONOVA, E., DAVYDOVA, G., MAJOUGA, A.G. NUKOLOVA, N., KABANOV, A., CHEKJONIN, V., 2015, Core-shell-corona doxorubicin loaded superparamagnetic Fe3O4 nanoparticles for cancer theranostics. *Coll. and Surf. B: Biointer*. 136, 1073-1080.

[12] PENG N., WU B., WANG, L, HE, W., AI, Z., ZHANG, X., WANG, Y., FAN, L., YE, Q. 2016, High drug loading and pH-responsive targeted nanocarriers from alginate-modified SPIONs for anti-tumor chemotherapy. *Biomater. Sci.* 4, 1802-1813.

[13] DAS, M., SOLANKI, A., JOSHI, A., DEVKAR, R., SESHADRI, S., THAKORE, S. 2019, β-cyclodextrin based dual-responsive multifunctional nanotheranostics for cancer cell targeting and dual drug delivery. *Carbohydrate Polym.* 206, 694-705.

[14] POORGHOLY, N., MASSOUMI, B., GHORBANI, M., JAYMAND, M., HAMISHEHKAR, H. 2018, Intelligent anticancer drug delivery performances of two poly(N-isopropylacrylamide)-based magnetite nanohydrogels. *Drug Dev. and Indust. Pharm.* 44, 1254-1261.

[15] DUTTA, B., SHETAKE, N.G., GAWALI, S.L., BARICK, B.K., BARICK, K.C., BABU, P.D., PRİYADARSİNİ K.I., HASSAN P.A. 2018, PEF mediated shape-selective

synthesis of cubic Fe_3O_4 nanoparticles for cancer therapeutics. *J. Alloys and Comp.* 737, 347-355.

[16] AVAL, N.A., ISLAMIAN, J.P., HATAMIAN, M., AEABFIROUZJAEI, M., JAVADPOUR J., RASHIDI, M.R. 2016, Doxorubucin loaded large-pore mesoporous hydroxyapatite coated superparamagnetic Fe_3O_4 nanoparticles for cancer treatment. *Int. J. Pharm*. 509, 159-167.

[17] JORFI, M., FOSTER, E.J., 2015, Recent advances in nanocellulose for biomedical applications. *J. Appl. Polym. Sci.* 132, 41719-4138.

[18] LIANG, H., HUANG, Q., ZHOU, B., HE, L., LIN, L., AN, Y., Lİ, Y., LİU, S., CHEN, Y., Lİ, B. 2015, Self-assembled sein-sodium carboxymethyl cellulose nanoparticles as an effective drug carrier and transporter. *J. Mater. Chem.* 3, 3243-3252.

[19] RASOULZADEH, M., NAMAZI, H. Carboxymethyl cellulose/graphene oxide bio-nanocomposite hydrogel beads as anticancer drug carrier agent. 2017, *Carbohyd. Poly.* 168, 320-326.

[20] SINGH, V., JOSHI, S., MALVIYA, T. 2018, Carboxymethyl cellulose-rosin gum hybrid nanoparticles: An efficient drug carrier. *Int. J. Bio. Macromol*. 112, 390-398.

[21] SIVAKUMAR, B., ASWATHY, R.G., NAGAOKA, Y., SUZUKI, M., FUKUDA, T., YOSHIDA, Y., MAEKAWA, T., SAKTHIKUMAR D.N. 2013, Multifunctional carboxymethylcelluose based magnetic nanovectors as a theragnostic system for folate receptor targeted chemotherapy, imaging and hyperthermia against cancer. *Langmuir*. 29, 3453-3466.

[22] MOVAGHARNEZHAD, N., MOGHADAM, P.N. 2017, Hecamethylene diamine/ carboxymethyl cellulose grated on magnetic nanoparticles for controlled drug delivery. *Polym. Bull.* 74, 4645-4658.

[23] KANAGARAJAN, S.V. and THİYAGARAJAN D. 2019, Carboxymethyl cellulose-functionalised magnetic nanocarriers for pH responsive delivery of curcuminin cancer therapy. *Mater. Res. Express*, 6, 016105-11.

[24] DEMİREL TOPEL, S., TOPEL, O., BOSTANCİOGLU, R.B., KOPARAL, A. T. 2015, Synthesis and characterization of Bodipy functionalzed magnetic iron oxide nanoparticles for potential bioimaging applications. *Coll. and Surf. B: Biointer.* 128, 245-253.

[25] DEMİREL TOPEL, S., TURGUT CİN, G., AKKAYA, E.U. 2014, Near IR excitation of heavy atom free Bodipy photosensitizers through the intermediacy of upconverting nanoparticles. *Chem. Commun*. 50, 8896-8899.

[26] LU W., LİNG, M., HUANG, P., LI, C., YAN, B. 2014, Facile synthesis and characterization of PEI coated Fe_3O_4 superparamagnetic nanoparticles for cancer cell separation. *Mol. Med. Rep.* 9 ,1080-1084.

Journal of Scientific Perspectives
Volume 3, Issue 2, Year 2019, pp. 111-118
E - ISSN: 2587-3008
URL: http://ratingacademy.com.tr/ojs/index.php/jsp
DOİ: https://doi.org/10.26900/jsp.3.012
Research Article

DETERMINATION OF SOME MACRO ELEMENT CONCENTRATIONS AND CHLOROPHYLL-A DISTRIBUTION IN A SHALLOW LAKE WETLAND (GÖKÇEADA SALT LAKE LAGOON, ÇANAKKALE/TURKEY)

Herdem ASLAN* & Onur GÖNÜLAL*

** Prof.Dr., Çanakkale Onsekiz Mart University, Faculty of Arts and Science, Department of Biology, Çanakkale, TURKEY, E-mail: asherdem@comu.edu.tr*
ORCID ID: https://orcid.org/0000-0002-0872-2919

*** Assoc. Prof. Dr., Istanbul University, Department of Gökçeada Marine Research, Faculty of Fisheries, Istanbul, TURKEY, E-mail: ogonulal@istanbul.edu.tr*
ORCID ID: https://orcid.org/0000-0002-5559-3953

Received: 8 February 2019; Accepted: 2 April 2019

ABSTRACT

In this study, the macro element concentrations and chlorophyll-a distribution in the Gökçeada Salt Lake Lagoon which is in the category of Shallow Lake Wetland in Gökçeada (Canakkale) were evaluated. For this purpose, some macro elements (Nitrite, Nitrate, Sulfate, Phosphate, Calcium, Magnesium, Potassium, and Phosphorus) and chlorophyll-a levels as well as water temperature and dissolved oxygen values were measured in 2016 as seasonally (January, May, August, November) from three stations. During the autumn season, nitrite, nitrate, phosphate and sulfate values measured as 5.65 ppm; 16.9 ppm; 77 ppm; and 8547 ppm, respectively. As a result, the macro element concentrations deposited in the sediment and the chlorophyll-a amounts of the lake was signed to the ecological conditions are very suitable for the development of eutrophication. In the end of the study, some suggestions were done to protect the ecosystem balance.

Keywords: *Gökçeada, Salt Lagoon, Macro element, eutrophication*

1. INTRODUCTION

Wetlands encompass many different and productive resources worldwide like supply water and food, flood control, microclimate stabilization, wave breaking, and aquaculture due to their hydrodynamic structure meanwhile ensuring to preserve the biodiversity of the region as well (Ceran, 2006; Erdem, 2013). The ecological balance in wetlands is provided by existing harmony between physicochemical and biological properties with the surrounding environmental conditions, thus these ecosystems maintain their function through protection of this balance (Camur-Elipek, et al., 2017).

The coastal lagoons, which are considered as wetlands, also exhibit a special hydrological structure by forming a transition zone between fresh and salt water because they are very close to the marine areas and they have perfect hydrodynamic perspective and very sensitive structures (Camur-Elipek and Kirgiz, 2011; Erdem, 2013). However, the pollution, carefree agricultural and tourism activities, which accelerate with the increase in human population, lead to deterioration of natural balance especially in coastal lagoons. Human activities have become a major environmental concern to affect these sensitive areas (Çamur-Elipek and Kirgiz, 2011). This problem may lead to a change in the dynamics of living organisms in the wetland and may cause the deterioration of the entire ecosystem and the food chain (Çamur-Elipek, et. al., 2010).

High concentrations of nitrogen and phosphorus elements play an important role in the pollution caused by nutrients in aquatic ecosystems (Alkan et al., 2013). These elements, which are necessary for the biochemical cycle, are usually incorporated into the water by anthropogenic activities and their excessive amounts lead to eutrophication which causes serious environmental problems in the aquatic ecosystem (Luo et al., 2011; Alkan et al., 2013). Eutrophication is the major factor on oxygen deficiency due to algal explosion, fish deaths and biodiversity decline (Alkan et al., 2013).

The importance of coastal lagoons in terms of ecological equilibrium with rich biodiversity structure has started to attract attention in Turkey (Dugan, 1991; Sıvacı et al., 2008; Demir, 2008; Turan, 2001). However, each wetland ecosystem has its own physicochemical and biological properties due to autochtonic and allochonic factors like as climatic and topographic conditions of the its geography. Therefore, each wetland ecosystem should be evaluated separately.

The effects of environmental factors on wetlands can lead to changes in some physicochemical properties in the water and due to these changes; it reached a visible level of ecosystem degradation. Increased water temperature, especially due to global climate change and low water level, may have an effect on dissolved oxygen values, while an increase in chlorophyll-*a* amounts may lead to a decrease in light permeability in water and thus decrease in oxygen produced by photosynthesis (Kökmen et. al., 2007; Arslan et al., 2018a). Decreased oxygen content may prevent the bacteria that decompose organic matter in the sediment and restore the ecosystem. Another factor that may lead to a similar situation can be found in the increase of excess phytoplankton due to the accumulation of macro and microelements in water, especially due to anthropogenic factors, therefore it would cause eutrophication in the shallow lake wetlands (Çamur-Elipek, et. al., 2010).

Some substances (nitrogen (N), phosphorus (P), potassium (K), calcium (Ca), magnesium (Mg), sulfur (S) and their derivatives (such as ammonium (NH_4), nitrite (NO_2), nitrate (NO_3), sulfate (SO_4) and phosphate (PO_4)) which are called macro elements are introduced into aquatic ecosystems in many ways, thus they can lead to excessive increasing of phytoplankton.

Previously, in the report published by the Ministry of Forestry and Water Affairs in 2012, analyses of the physical and biological data, and water quality as well as the socio-economic evaluation of Gökçeada Salt Lake Lagoon was conducted (Anonymous, 2012). Also, Bassler-Veit et al. (2013) measured some of the environmental variables (temperature, pH and salinity) in the lake. However, the concentrations of macro elements in the wetland and their possible effects on the ecosystem have not been evaluated yet.

The purpose of this study, some macro element concentrations (Nitrite nitrogen, Nitrate nitrogen, Sulfate, Phosphate, Calcium, Magnesium, Potassium, and Sulfur) and chlorophyll-*a*,dissolved oxygen and water temperature analyses were carried out in Gökçeada Salt Lake

Lagoon, which is in the status of National Impact Status. The current levels belong to the nutrients and chlorophyll-*a* of the wetland area and the eutrophication situation that may occur in the area were examined and suggestions were made in terms of sustainable use in the wetland.

2. MATERIAL AND METHODS

Gökçeada Island (in Canakkale) which is the largest island in Turkey, located in the North of the Aegean Sea. Salt Lake Lagoon, located in the south-east of the island, is a coastal lagoon with a maximum depth of 2 meters in an area of approximately 2 km2 (Fig. 1). The National Wetland Committee (NWC) declared Gökçeada Salt Lake as "Wetland of National Importance" in December 2018. Although Gökçeada Salt Lake hosts many species, especially the Flamingo population, the lake is exposed on tourism activities and the effects of the surrounding areas especially in the summer months (Aslan et al., 2018).

In this study, some macro element concentrations, chlorophyll-*a*, water temperature and dissolved oxygen levels were investigated in Gökçeada Salt Lake Lagoon. While sampling was made for some variables (Calcium, Magnesium, Potassium, Phosphorus, water temperature, dissolved oxygen and chlorophyll-*a* levels) in 2016 from 3 stations selected from the lake, at the January, May, August and November, the other parameters (Nitrite (NO_2^-N), Nitrate (NO_3^- N), Sulfate (SO_4^-) and Phosphate (PO_4^{-3}) values) could be measured in a single season at the sampling stations (Fig. 1).

Fig. 1. Location of Gökçeada Salt Lake Lagoon and Sampling Stations (adapted from Google.Earth)

For this purpose, water temperature (^{0}C) and dissolved oxygen (mg/L) values were measured with the YSI556 model multiprobe system device during field studies. Water samples were taken by Ruttner water sampler device and sediment samples were taken by Ekman grab (15x15 cm^2)and the materials were transferred to the laboratories in ÇOBILTUM (Çanakkale Onsekiz Mart University, Science and Technology Research Center) and TUTAGEM (Trakya University, Tecnhnology and Research Center) to analyze macro-element concentrations (Nitrite, Nitrate, Phosphate, Sulfate, Calcium, Magnesium, Sulfur, Potassium). The macro element analyses were made by Ion Chromatography device (IC-MS: Metrohm Ion Chromatography System) and Inductively Paired Plasma Mass Spectrometer device (ICP-MS: Agilent Technologies 7700 XX ICP-MS System) and using EPA 200.8 method (EPA, 1994; Uçar, 2011). The analysis was performed in three replicates for each sample and the mean values of the results calculated according to the calibration curve were taken. In addition, chlorophyll-*a* determinations were carried out using classical spectrophotometric methods (Egemen ve Sunlu, 1999).

3. RESULTS AND DISCUSSION

As a result of the analyzes performed in the samples taken from the stations in the Gökçeada Salt Lake Lagoon, the magnesium ratios ranged from 373 ppm to 5998 ppm and had an average value of 3048 ppm; calcium levels vary between 749 ppm and 18740 ppm and have an average of 9489 ppm; the amount of potassium is between 204 ppm and 4508 ppm and has an average value of 1527 ppm; Phosphorus levels were found to be between 172 ppm and 783 ppm and had an average of 366 ppm (Fig. 2). During the autumn season when the agricultural fertilization periods ended, nitrite, nitrate, phosphate and sulfate values measured as 5.65 ppm; 16.9 ppm; 77 ppm; and 8547 ppm, respectively (Fig. 2). Especially the phosphorus and Nitrogen-N concentrations in the sediment directly affect the quality of water (Perak et al., 2016). Thus, nutrients will lead increasing the primer productivity in an aquatic ecosystem, relatively. The chlorophyll-*a*concentrations which increasing by the macro elements may indicate the environmental conditions are suitable for eutrophication development in the ecosystem.

Fig. 2. Macroelement Concentrations Measured in Gökçeada Salt lake Lagoon (ppm)

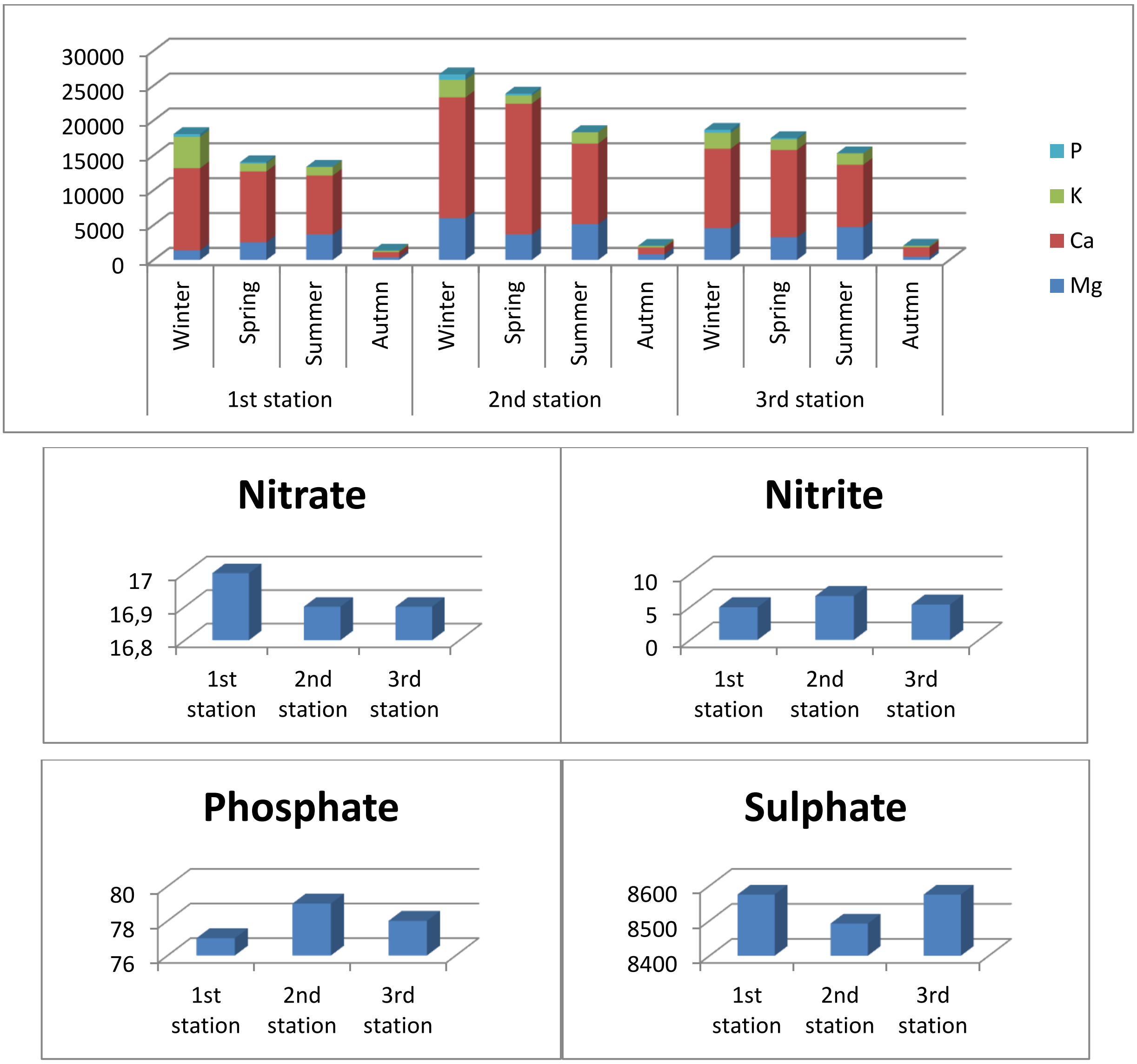

Although macro elements are very important for primer productivity and other organisms in water, they may bioaccumulated by the food web and they may turn into toxic substances. Nitrogen, vital for the metabolic functions of photosynthetic organisms, is an important macro element in the formation of proteins, hormones, chlorophyll, vitamins and enzymes in living organisms. Although the process of demineralization in ecosystems is the main natural source of nitrogen, it is highly effective in transporting nitrogen to aquatic ecosystems in agricultural activities. Photosynthetic organisms may take the nitrogen transported to the aquatic ecosystem with superficial flow waters in the form of Nitrate nitrogen (NO_3^-N) and Ammonium nitrogen (NH_4^+-N) (Chapman and Reis 1999). However, most of the aquatic photosynthetic organisms cannot readily use ammonium nitrogen and can be used after nitrification by converting the nitrate into nitrogen form.

Phosphorus is one of the most basic macro elements necessary for metabolic activities of photosynthetic organisms. Phosphorus and its derivatives, which can enter into aquatic ecosystems, especially in agricultural activities in different ways (such as the use of detergents), act as a catalyst that initiates metabolic reactions in photosynthetic organisms and also encourages the use of nitrogen in the use of nitrogen.

The presence of high levels of macro elements (especially Nitrogen and its derivatives) in aquatic ecosystems leads to an increase in primary productivity. This is the first step the process (called eutrophication) of changing the physical, physiological and biological characteristics of water and the change in the ecosystem structure is inevitable. Phosphate is also an important eutrophication compound and may lead to phytoplankton growth and an increase in chlorophyll-a ratio. Especially high nitrite concentrations and agricultural activities are important factors limiting the life of aquatic organisms (Kökmen et al., 2007; Çamur-Elipek, et al., 2010). In addition, high amounts of nutrients in water are reported to have negative effects on organ development of organisms (Arslan et al., 2018b).

In this study, chlorophyll-*a* amounts were found to vary between 0.56 ppm and 14.56 ppm and have an average of 4.01 ppm (Fig. 3). The chlorophyll values that begin to rise in the winter reaches the highest value in the spring. The determined chlorophyll-*a* values were observed to exceed the recommended eutrophication limit value (0.008 ppm) for the natural conservation area (Anonymous, 2004).

Fig. 3. Seasonal Distribution of Chlorophyll-*a* Concentrations in Gökçeada Salt Lake Lagoon (ppm)

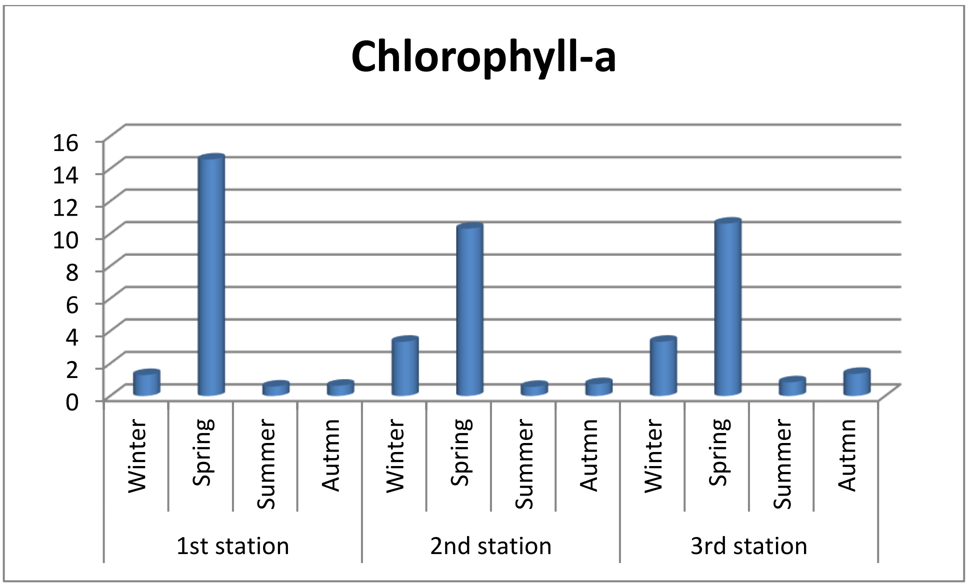

Dissolved oxygen and water temperature values were observed to be inversely related to each other as indicated in the literature (Fig. 4). Since the amount of dissolved oxygen affects the self-cleaning capacity of water, the low concentration, especially in the spring period, triggers eutrophication (Tokatlı et al., 2014; Çiçek et al., 2017). In particular, it is thought that increased primary productivity factors due to temperature increase may cause high chlorophyll-*a* amounts in spring season.

Fig. 4. Comparison of Seasonal Variation of Temperature and Dissolved Oxygen in Gökçeada Salt Lake Lagoon

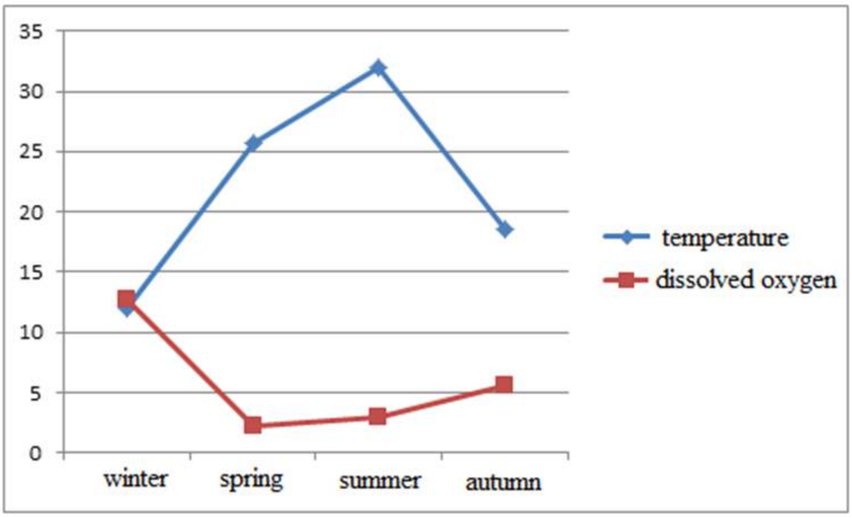

As a result, it has been determined that Gökçeada Salt Lake Lagoon, which is in the protection status for biological diversity, has a high Chlorophyll-*a* concentration during the spring season and it is thought to have developed as a result of the increase in primary productivity. This situation indicates that this area, which hosts many living things and is used for recreational purposes, is about to lose its ecological balance due to eutrophication. In order to prevent this situation, it is necessary to determine the pollutant loads that have a negative impact on the lake and to take necessary measures, and to monitor the water quality of the lake by eliminating the wastes from the settlement area or agricultural wastes. Further investigation should be devoted to monitoring of species and their relationships, in order to predict impact of natural or human induced stress conditions.

Acknowledgements

This study was supported by ÇOMÜ-BAP project (FHD-2016-882) and some results were obtained from the report of TÜBİTAK project (115Y457).

LITERATURES

ALKAN, A., SERDAR, S., FİDAN, D., AKBAŞ, U., ZENGİN, B., KILIÇ, M. B., 2013, Physico-Chemical Characteristics and Nutrient Levels of the Eastern Black Sea Rivers, *Turkish Journal of Fisheries and Aquatic Sciences,* 13: 847-859

ANONYMOUS, 2004, Su Kirliliği Kontrol Yönetmeliği (SKKY), Resmi Gazete Tarihi: 31.12.*2004* Resmi Gazete Sayısı: 25687.

ANONYMOUS, 2012, Gökçeada Lagünü Sulak Alan Alt Havzası Biyolojik Çeşitlilik Araştırması, T.C. Orman ve Su İşleri Bakanlığı Doğa Koruma ve Milli Parklar Genel Müdürlüğü Hassas Alanlar Dairesi Başkanlığı.

ARSLAN, N., ULUKÜTÜK, S., MERCAN, D., 2018a, Assessment of water quality in three sub-basins of Susurluk River (Northwest Anatolia) according to invertebrates and biotic indices, *Biological Diversity and Conservation*, 11(3): 1-8.

ARSLAN, N., MERCAN, D., AKKAN KÖKÇÜ, C., ARSLAN, T., 2018b, Antenna and mouthpart defect in Chironomus (Camptochironomus) tentans larvae (Chironomidae) and their relevance with habitat characteristics, Biological Diversity and Conservation, 11(3): 180-189.

ASLAN, H., GÖNÜLAL, O., CAN YİLMAZ, E., ÇAMUR ELİPEK, B., BAYTUT, Ö., TOSUNOĞLU, M., KARABACAK, E., KURT, Y., 2018, Species diversity in lentic, lotic, marine and terrestrial biotopes of Gökçeada Salt Lake Wetland (Çanakkale, Turkey). *Fresenius Environmental Bulletin,* 27:2853-2867

BASSLER-VEIT, B., BARUT, İ.F., MERİÇ, E., AVŞAR, N., NAZİK, A., KAPAN-YEŞİLYURT, S., YILDIZ, A., 2013, Distribution of microclima, meifauna and macrofauna assemblages in the hypersaline environment of Northeastern Aegean Sea coast, *Journal of coastal Research,* 29 (4): 883-898.

CERAN, Y, 2006, Sulak Alanların Akılcı Kullanımı, Çevre ve İnsan Dergisi, Sayı:66, Çevre ve Orman Bakanlığı Yayını, pp 16-20.

CHAPMAN, J. L., REİS, M. J., 1999, Ecology, principles and applications, Cambridge University Pres, 330 p.

ÇAMUR-ELİPEK, B., ARSLAN, N., KIRGIZ, T., ÖTERLER, B., GÜHER, H., ÖZKAN, N. 2010. Analysis of Benthic Macroinvertebrates in Relation to Environmental Variables of Lake Gala (Edirne/Turkey), *Turkish Journal of Fisheries and Aquatic Sciences,* 10(2): 235-243

ÇAMUR-ELİPEK, B., KIRGIZ, T., 2011. The Evalution of Some Limnological Features of the Lagoon Lakes in European Part of Turkey, edited by Frank Columbus in the book “Lagoons: Biology, Management and Environmental Impact.” at Nova Science Publishers, Inc. 400 Oser Avenue, Suite 1600 Hauppauge, NY 11788, USA.

ÇAMUR-ELİPEK, B., GÜHER, H., OTERLER, B., TAS-DİVRİK, M., ALTINOLUK-MİMİROĞLU, P., 2017. Determining of Water Quality by Using Multivariate Analysis Techniques In A Drinking/Using Water Reservoir In Turkey, *Fresenius Environmental Bulletin* 26(8): 5007-5017.

ÇİÇEK, A., UYSAL, E., KÖSE, E., TOKATLI, C., 2017, Eskişehir’de Yer Alan Bazı Sulama Göletlerinin Su Kalitesinin Değerlendirilmesi, *Nevşehir Bilim ve Teknoloji Dergisi* Cilt 6 (ICOCEE 2017 Özel Sayı) 440-446.

DEMİR, A., 2008, Akyatan Lagününde Tuzluluk ve Bazı Kirlilik Düzeylerinin Saptanarak Coğrafi Bilgi Sistemi Destekli Dağılımlarının Belirlenmesi (Yüksek Lisans Tezi). Çukurova Üniversitesi Fen Bilimleri Enstitüsü, Citing Internet Sources: https://tez.yok.gov.tr/UlusalTezMerkezi/

DUGAN, P. J., 1991, Wetlands, regional planning and the developmentf assistance community, *Landscape and Urban Planning*, 20(1): 211-214.

EGEMEN, Ö., SUNLU, U., 1999. Su Kalitesi, Ege Üniversitesi yayınları

EPA 1994, Creed, J. T., Brockhoff, C. A., Martin, T. D. Method 2008, Determination of Trace Elements in Waters and Wastes by Inductively Coupled Plasma - Mass Spectrometry, Revision 5.4; Environmental Monitoring Systems Laboratory Office of Research and Development, U.S. Environmental Protection Agency, Cincinnati, Ohio. Citing Internet Sources: https://www.epa.gov/homeland-security-research/epa-method-2008-determination-trace-elements-waters-and-wastes

ERDEM, O., 2013, Sulak alanların işlev ve değerleri. Bölüm 2, Sulak alanlar (eds. Dr. B. T. Meriç, S. Çağırankaya), Orman ve Su İşleri Bakanlığı, Doğa Koruma ve Milli Parklar Genel Müdürlüğü,

GÜLER, Ç., 1997, Su Kalitesi. Çevre Sağlığı Kaynak Dizisi, 43, s. 95. Citing Internet Sources: https://sbu.saglik.gov.tr/Ekutuphane/kitaplar/css43.pdf

LUO, G., BU, F., XU, X., CAO, J., SHU, W, 2011, Seasonal variations of dissolved inorganic nutrients transported to the linjiang bay of the three gorges reservoir, China. *Environmental Monitoring and Assessment*, 173: 55- 64

KÖKMEN, S., ARSLAN, N., FILIK, C., YILMAZ, V., 2007, Zoobenthos of Lake Uluabat, a Ramsar Site in Turkey, and Their Relationship with Environmental Variables, *Clean* 35 (3): 266 – 274.

UÇAR, B., 2011, İyon Kromatografi Kullanarak Çeşitli Örneklerde Perklorat Analizi (Musluk Suyu, Havuz Suyu, Yüzey Suyu, Süt) (Yüksek Lisans Tezi). İstanbul Teknik Üniversitesi Citing Internet Sources: https://tez.yok.gov.tr/UlusalTezMerkezi/

PERAK, S. H., TALİB, A., YUSOFF, M. A., HASAN, Z. A., ISMAIL, W. R., ABUSTAN, M. S., 2016, Nutrient Concentration Distribution in Sediment and Overlying Water at Bukit Merah Reservoir, *MATEC Web of Conferences*, 47, 005004.

SIVACI, E.R., YARDIM, Ö., GÖNÜLOL, A., BAT, L., GÜMÜŞ, F. 2008. Sarıkum (Sinop-Türkiye) Lagününün Bentik Algleri, *J. of Fisheries Sciences*, 2(4): 592-600.

TOKATLI, C., KÖSE, E., ÇİÇEK, A., 2014, Assessment of the Effects of Large Borate Deposits on Surface Water Quality by Multi Statistical Approaches: A Case Study of the Seydisuyu Stream (Turkey), *Polish Journal of Environmental Studies*, 23 (5): 1741-1751.

TURAN, L., 2001, Türkiye'nin Ornitolojik Konumu ve Sulak Alanlar, Hacettepe Üniversitesi Eğitim Fakültesi, 72-178.

RATING ACADEMY

JSP

Journal of Scientific Perspectives

Volume **3,** Issue **2,** Year **2019**, pp. **119-132**
E - ISSN: **2587-3008**
URL: http://ratingacademy.com.tr/ojs/index.php/jsp
DOİ: https://doi.org/10.26900/jsp.3.013
Research Article

RSM METHOD AND OPTIMIZATION OF HARD COATED SOFT SUGAR PROCESS PARAMETERS

Özge EYYÜPOĞLU* & Mehmet Ali MARANGOZ ** & Suat Bora YEŞİLTEPE**

** Durukan Confectionery R&D Centre, Turkey, E-mail: ozge.eyyupoglu@durukan.com.tr*
ORCID ID: https://orcid.org/0000-0002-6982-6404

***Durukan Confectionery R&D Centre, Ankara, Turkey,*
E-mail: mehmetali.marangoz@durukan.com.tr
ORCID ID: https://orcid.org/0000-0002-6209-3172

**** Durukan Confectionery R&D Centre, Ankara, Turkey, E-mail: bora.yesiltepe@durukan.com.tr*
ORCID ID: https://orcid.org/0000-0002-6177-091X

Received: 26 December 2018; Accepted: 7 March 2019

ABSTRACT

Nowadays, the textural characteristics of foods affect the consumers' enjoyment about them. Providing ideal textural properties, especially in multi stage food production processes, is a complex and sensitive work that must be carried out with high precision. Hard sugar coated chewy product, "Chewy Drage" is highly preferred by the confectionery consumers all over the world. In this work, the changes in the physical behaviors of "Chewy Drage" with the changes in textural and process parameters was studied. Each process parameter was separately optimized and the relationship between those physical properties was elaborated.

Keywords: *Chewy Dragee, Candy Manufacturing, Texture*

1. INTRODUCTION

Texture of a product covers the structural and mechanical properties. Therefore, understanding the mechanical characteristics of a food product is crucial to understand the textural characteristics and measurement techniques of that product.

Texture defining methods are categorized by 3 methods; those are basic, experimental and imitative ones. Basic force/deformation methods are developed according to the engineering bases of the material and are used to measure the known mechanical characteristics of the food. Experimental methods are used successfully to evaluate these mechanical characteristics and to compare the values obtained from the results of the sensory evaluation of the food. Imitative methods are obtained from the simulations of food chewing. There is no single texturing method that can be successfully used for all food products. Thus, determination of the food quality depends on the right method to be chosen. (1-9)

Confectionery making technology; particularly obtaining a special textural structure is significantly based on the art and science of sugar processing, which are the principal components of the confectionery manufacturing. The most significant factor to obtain the desired quality in confectionery is the control of the crystallization of candy mass and the adjustment of the sugar-water ratio.

In this study, the optimization of production process of “Chewy Dragee” product by using RSM method; and its textural and rheological characterizations were amongst the research topics.

2. METHOD

2.1. Formulation Determination Studies

In this study, 2 different chewy recipes, with and without gelatin, were tested. The recipes were as shown in the Table 1. and Table 2. in terms of their componenets. The effects of formulation changes on product core structure in the process step scale were examined in the production tests.

Table-1: Prescription 1

Sugar	Recipe 1
Glucose Syrup	
Gelatin	
Sorbitol	
Oil	
Lecithin	
Maltodextrin	
Dextrine	
Modified Starch	
Gms	

Table-2: Prescription 2

Sugar	Recipe 2
Glucose Syrup	
Sorbitol	
Oil	
Lecithin	
Maltodextrin	
Dextrine	
Modified Starch	
Gms	

2.2. Process Tests

2.2.1. Experimental Design Formation (RSM Work)

RSM (Response Surface Methodology), is a significant tool used for optimization, high performance operations and product acceptance studies. This optimization method is a statistical technique. The parameters that influence the process are called independent variables and the responses that influences the process are called dependent variables.

In order to achieve the best optimization conditions, it has been determined in which parameter ranges (lower, middle, and upper values) the work should be done (9).

Experiments based on the independent variables f(x) (-1, 0, 1) reveal first degree polynomial equations in response to the dependent variable (y). These equations composed for each process steps helped to optimize the process. The equations that mathematically express the effects of the independent variable on the dependent variable provided both mathematical and experimental observations.

The values expressed as -1, 0, 1 were the lower, upper and middle values of the independent variable in the process step. In this study, 13 testing sets were formed according to these independent variables. Dependent variables were also determined in the end product. These are consistency, viscosity, humidity and color (L, a, b) values.

For each dependent variable, a polynomial equation was formed by the help of RSM technique. Thanks to this equation, it was possible to determine how the change in the process parameters affects to the dependent variable.

2.2.2. Cooking Tests

13 testing sets below allowed us to determine the effect of temperature and vacuum variables on the product consistency, product behavior, viscosity, humidity and color properties in optimal values.

Table-3 Cooking Tests Table

Cooking Tests										
					Texture			Color		
Test No:	Temperature	Vacuum	Temperature (°C)	Vacuum (-Bar)	Consistency (ForcexTime)	Viscosity Index (ForcexTime)	Humidity (%)	L*	a*	b*
1	-1	-1	110	0,3	7815,12	1671,01	6,91	62,34	0,45	10,13
2	1	-1	130	0,3	9291,58	2263,73	6,44	63,50	0,47	10,50
3	-1	1	110	0,7	9514,54	2125,45	6,41	62,83	0,48	10,80
4	1	1	130	0,7	11034,51	3027,16	6,05	63,70	0,49	10,90
5	-1	0	110	0,5	8745,90	1974,02	6,74	62,90	0,46	10,53
6	1	0	130	0,5	9983,63	2265,74	6,28	63,01	0,47	10,44
7	0	-1	120	0,3	8528,86	1759,09	6,61	62,59	0,46	10,62
8	0	1	120	0,7	10234,23	3297,13	6,41	63,97	0,49	10,70
9	0	0	120	0,5	9472,41	2080,37	6,48	62,88	0,46	10,38
10	0	0	120	0,5	9473,30	2050,43	6,51	62,90	0,46	10,38
11	0	0	120	0,5	9459,53	2018,73	6,48	62,85	0,46	10,40
12	0	0	120	0,5	9452,71	2060,65	6,50	62,80	0,46	10,37
13	0	0	120	0,5	9482,60	2067,54	6,49	62,81	0,45	10,39

*The L **value** for each scale therefore indicates the level of light or dark, the a **value** redness or greenness, and the b **value** yellowness or blueness. All three **values** are required to completely describe an object's **color**. *Retrieved from https://www.hunterlab.com on 27.2.2019*

2.2.3. Rapid Cooling Tests

The rapid cooling step is required for continuous production processes. 13 tests were performed and the mass obtained after cooking was kept at 80-100 C on the cooling stages. Then, the viscosity index and consistency parameters of the mass obtained were measured.

Table-4. Rapid Cooling Tests Table

Rapid Cooling Tests						
Test No.	**Temperature**	**Time**	**Temperature(°C)**	**Time (mins.)**	**Consistency (ForcexTime)**	**Viscosity Index (ForcexTime)**
1	-1	-1	80	5	14325,85	4096,60
2	1	-1	100	5	12149,25	5101,66
3	-1	1	80	10	14685,12	3917,77
4	1	1	100	10	12614,63	4316,72
5	-1	0	80	7,5	14412,90	4718,36
6	1	0	100	7,5	12590,71	4254,53
7	0	-1	90	5	13423,73	4105,61
8	0	1	90	10	13129,20	4971,47
9	0	0	90	7,5	13285,19	4481,95
10	0	0	90	7,5	13387,62	4410,18
11	0	0	90	7,5	13215,38	4414,63
12	0	0	90	7,5	13242,63	4492,23
13	0	0	90	7,5	13399,74	4406,81

2.2.4. Crystallization Tests

This set of experiments allowed us to see the change of sugar amount and time versus texture and color.

Table-5. Crystallization Tests Table

Crystallization Tests								
					Texture	**Color**		
Crystallization	**Amount of Sugar**	**Time**	**Amount of Sugar (%)**	**Time (mins.)**	**Strength(g)**	**L***	**a***	**b***
1	-1	-1	0,50	10	1698,74	81,21	0,50	10,08
2	1	-1	10,00	10	1510,44	81,95	0,51	10,10
3	-1	1	0,50	30	1490,40	80,33	0,49	10,03
4	1	1	10,00	30	1302,30	79,10	0,53	10,39
5	-1	0	0,50	20	1604,59	84,30	0,55	10,52
6	1	0	10,00	20	1403,21	80,15	0,47	10,13
7	0	-1	5,25	10	1515,55	82,99	0,48	10,15
8	0	1	5,25	30	1350,03	81,43	0,49	10,33
9	0	0	5,25	20	1453,85	83,25	0,50	10,29
10	0	0	5,25	20	1452,25	83,78	0,51	10,32
11	0	0	5,25	20	1490,91	83,90	0,51	10,30
12	0	0	5,25	20	1450,10	83,56	0,53	10,25
13	0	0	5,25	20	1482,44	83,45	0,52	10,15

*The L **value** for each scale therefore indicates the level of light or dark, the a **value** redness or greenness, and the b **value** yellowness or blueness. All three **values** are required to completely describe an object's **color**. *Retrieved from https://www.hunterlab.com on 27.2.2019*

2.2.5. Drum Cooling Tests

The effect of temperature and time on the texture was tested and the results were shown on Table 6.

Table-6. Drum Cooling Tests Table

Cooling Tests					
Tests No:	**Temperature**	**Time**	**Temperature (°C)**	**Time (sec.)**	**Texture (g)**
1	-1	-1	25,0	270	5891,15
2	1	-1	50,0	270	6015,54
3	-1	1	25,0	350	5713,9
4	1	1	50,0	350	5489,65
5	-1	0	25,0	310	6218,32
6	1	0	50,0	310	5849,64
7	0	-1	37,5	270	5987,61
8	0	1	37,5	350	6701,41
9	0	0	37,5	310	6065,22
10	0	0	37,5	310	6293,57
11	0	0	37,5	310	6436,78
12	0	0	37,5	310	6524,25
13	0	0	37,5	310	6604,09

2.2.6. Pre-coating Tests

The effect of coating and time variables on the texture properties was tested and shown on Table-7.

Table-7. Pre-Coating Tests Table

Pre-Coating Tests					
Tests No:	**Amount of Coating**	**Time**	**Amount of Coating (%)**	**Time(mins.)**	**Texture(g)**
1	-1	-1	15,0	25	5317,41
2	1	-1	30,0	25	5325,51
3	-1	1	15,0	35	5916,54
4	1	1	30,0	35	5108,93
5	-1	0	15,0	30	5890,14
6	1	0	30,0	30	5610,25
7	0	-1	22,5	25	5789,54
8	0	1	22,5	35	5503,25
9	0	0	22,5	30	5747,17
10	0	0	22,5	30	5967,94
11	0	0	22,5	30	5924,50
12	0	0	22,5	30	6100,18
13	0	0	22,5	30	6019.75

2.2.7. Aging -Recrystallization Tests

At this stage of the process, it was aimed to reach the suitable form by keeping product for a length of time in certain temperature and humidity range.

Table-8. Aging - Recrystallization Tests

Humidity, temperature

Re-Crystallization Tests							
Tests No:	**Re-crystallization Room Humidity**	**Time**	**Temperature**	**Re-crystallization Room Humidity (%)**	**Time(mins)**	**Temperature(°C)**	**Texture Strength(g)**
1	-1	-1	-1	20	12	15,0	6002,66
2	1	-1	-1	50	12	15,0	4976,55
3	-1	1	-1	20	72	15,0	4704,34
4	1	1	-1	50	72	15,0	5009,03
5	-1	-1	1	20	12	30,0	5157,45
6	1	-1	1	50	12	30,0	4494,15
7	-1	1	1	20	72	30,0	4510,92
8	1	1	1	50	72	30,0	3591,45
9	-1	0	0	20	42	22,5	4597,25
10	1	0	0	50	42	22,5	4103,64
11	0	-1	0	35	12	22,5	4319,44
12	0	1	0	35	72	22,5	4013,43
13	0	0	-1	35	42	15,0	4625,50
14	0	0	1	35	42	30,0	3983,13
15	0	0	0	35	42	22,5	4152,52
16	0	0	0	35	42	22,5	4045,65
17	0	0	0	35	42	22,5	4231,10
18	0	0	0	35	42	22,5	4310,15
19	0	0	0	35	42	22,5	4215,47
20	0	0	0	35	42	22,5	4421,20

2.2.8. Hard Coating Tests

In addition to protecting the physical form of the pre-coated product, the hard coating also contributes to the aroma, color and texture properties of the product. The hard coating stage is one of the critical points for stable values of the product.

With the composed 13 testing sets, the effects of the coating thickness and temperature variables on the humidity, texture and color properties of the product were tried to be determined at this stage of the process.

Table-9. Hard Coating Tests

Hard Coating									
Test No	**Amount of Coating**	**Tempe rature**	**Amount of Coating (%)**	**Temperature (°C)**	**Strength (g)**	**Humidit y (%)**	**L**	**a**	**b**
1	-1	-1	15	18	4275,34	3	84,7	7,66	86,4
2	1	-1	30	18	4679,43	3,1	80	9,98	89,7
3	-1	1	15	24	4289,42	2,9	78,9	11,7	91,2
4	1	1	30	24	46,80,33	3	77,4	13,7	95,3
5	-1	0	15	21	4374,11	3,2	82	8,95	86
6	1	0	30	21	4784,88	3,3	78,3	12,9	94,8
7	0	-1	22,5	18	4694,5	3,7	84	8,81	86,3
8	0	-1	22,5	24	4473,6	3,3	79,1	13,7	92,2
9	0	0	22,5	21	4502,35	3,6	80,9	9,05	86,6
10	0	0	22,5	21	4421,24	3,5	80,8	12,8	91,6
11	0	0	22,5	21	4614,75	3,5	81,6	12,3	91,4
12	0	0	22,5	21	4215,87	3,4	80,9	11,7	90,2
13	0	0	22,5	21	4743,66	3,5	80,9	9,18	88,2

*The L **value** for each scale therefore indicates the level of light or dark, the a **value** redness or greenness, and the b **value** yellowness or blueness. All three **values** are required to completely describe an object's **color**. *Retrieved from* *https://www.hunterlab.com* *on 27.2.2019***.**

3. RESULTS & DISCUSSIONS

3.1. The Results Obtained

3.1.1. RSM Results after Cooking

Consistency Value;

The formula describing the effects of temperature and vacuum variables on consistency value is shown below.

Consistency (Force x Time) = 9422,2 + 705,7 x **Temperature + 858,0** x **Vacuum + 10,9** x **Temperature** x **Vacuum**

According to the formula obtained, it was observed that the product consistency was changing in directly proportional to the temperature and vacuum. It was seen that both variables were 95% above the effect value.

Viscosity Index Value;

The formula describing the effects of temperature and vacuum variables on viscosity is shown below.

Viscosity (Force x **Time) = 2204,7 + 298** x **Temperature + 459** x **Vacuum + 77** x **Temperature** x **Vacuum**

According to the formula obtained, it was observed that the product viscosity changed in directly proportional with the temperature and vacuum. It was seen that both variables were 95% above the effect value.

Humidity;

The formula describing the effects of temperature and vacuum variables on humidity of the product.

Humidity (%) = 6,4854 - 0,2150 x **Temperature - 0,1817** x **Vacuum + 0,0275** x **Temperature** x **Vacuum**

According to the formula obtained, it was observed that the viscosity of the product changed inversely proportional with temperature and vacuum. It was observed that both variables were 95% above the effect value.

Color Value (L,a,b);

The formula describing the effects of temperature and vacuum variables on product color (L);

L = 63,0062 + 0,357 x **Temperature + 0,345** x **Vacuum - 0,072** x **Temperature** x **Vacuum**

According to the formula obtained, it was observed that the product color (L) value changed in directly proportional with temperature and vacuum. It was observed that both variables were 95% above the effect value.

The formula describing the effects of temperature and vacuum variables on product color (a);

a = 0,46615 + 0,00667 x **Temperature + 0,01333** x **Vacuum - 0,00250** x **Temperature** x **Vacuum**

"a" value was observed to change in directly proportional with the temperature value in cooking parameters. However, this value can be ignored. Temperature does not have much effect on "a" value of the product. It was seen that vacuum value is a more effective factor than the temperature and is also a variable directly proportional to "a" value.

The vacuum variable of the test affects on a value 95% above and temperature variable has shown far below this ratio.

The formula describing the effects of temperature and vacuum variables on product color (b)

b = 10,5031 + 0,0633 x **Temperature + 0,1917** x **Vacuum - 0,0675** x **Temperature** x **Vacuum**

"b" value was observed to change in directly proportional with the temperature value in cooking parameters. However, this value can be ignored. Temperature does not have much effect on "b" value of the product. It was seen that vacuum value is more effective than the temperature and is also a variable directly proportional to "b" value.

The vacuum variable of the test affects on b value was 95% above and temperature variable has shown far below this ratio.

Consistency Value;

The formula describing the effects of temperature and time variables on product consistency

Consistency (Force x Time) = 13310,0 - 1011,5 x Temperature (°C) + 88,4 x Time (mins.) + 182 * Temperature(°C)xTemperature (°C) – 43xTime (mins.)xTime (mins.) + 26,5*Temperature (°C)xTime (mins.)

According to the formula obtained, it was observed that the product consistency value changed inversely proportional with the temperature and changed in direct proportional with the time. It was observed that both variables were 95% above the effect value on the consistency value.

It was observed that the temperature value of the test affects on consistence above 95% value and the time is less effective on consistency.

Viscosity Value;

The formula describing the effects of temperature and time variables on product viscosity

Viscosity (Force x Time) = 4472 + 157 x Temperature (°C) – 16 x Time (mins.) – 64 x Temperature (°C) x Temperature (°C) - 12 Time (min) x Time (min) – 152 x Temperature (°C) x Time (min)

It has been observed that the viscosity values changed in directly proportional with the temperature value in the cooking parameters. However, this value can be ignored on the viscosity value so there is no critical effect value. It has been observed that the time is less effective factor than the temperature and it is changed inversely proportional to the viscosity value.

It has been observed that the effect of temperature value of the test on viscosity value is 70% and the time is less effective (10%) on the viscosity value.

3.1.2. RSM Results after Crystallization

Texture Value;

The formula describing the effects of the amount of the sugar and time on the product texture:

Texture (g) = 1461,81 - 96,30 x Amount of Sugar - 97,00 x Time (min) + 52,3 x Amount of Sugar x Amount of Sugar - 18,8 x Time (min) x Time (min) + 0,05 x Amount of Sugar x Time (min)

According to the formula obtained, it has been observed that the texture value of the product changed inversely proportional to the amount of the sugar and time. It was observed that both variables were 95% above the effect value on the consistency value.

Color Value (L, a, b);

The formula describing the effects of sugar amount and time variables on product color (L);

L = 83,616 - 0,773 Amount of Sugar - 0,882 Time(mins.) - 1,459 Amount of SugarxAmount of Sugar1,474 Time (mins.) x Time(mins.) - 0,493 Amount of Sugar x Time(mins.)

According to the formula obtained, it was observed that the product color (L) value changed inversely proportional to the amount of sugar and time. It was observed that both variables were above 95% of the effect value.

The formula describing the effects of sugar amount and time variables on product color (a);

a = 0,5103 - 0,0050 x Amount of Sugar + 0,0033 x Time (min) + 0,0088 x Amount of Sugar x Amount of Sugar - 0,0162 x Time (min) x Time (min) + 0,0075 x Amount of Sugar x Time (min)

It has been observed that the color value (a) changed inversely proportional to the amount of the sugar and time in the crystallization parameters. However, the effect of the variable on the process can be ignored. It was observed that the time is a variable in direct proportion with “a” value and

b = 10,2831 – 0,0017 x **Amount of Sugar + 0,0700** x **Time** x **(min) - 0,0109** x **Amount of Sugar** x **Amount of Sugar - 0,0959** x **Time (min)** x **Time (min) + 0,0850** x **Amount of Sugar** x **Time (min)**

It has been observed that the b value changed inversely proportional with the amount of sugar in crystallization parameters. However, the effects of the variable on the process can be ignored. It was observed that the time is a variable in direct proportion with b value and the effect of this value is less on process product.

3.1.3. RSM Results after Drum Type Cooling

Texture Value;

The formula describing the effects of temperature and time variables on product textural value;

Texture (g) = 6138 – 78 x **Temperature (°C) + 2** x **Time (sec) – 87** x **Temperature (°C)** x **Time (sec)**

It has been observed that the textural value changed inversely proportional with the temperature of the cooling parameters. The time is directly proportional to the hardness value. However, the effect of the two variables on the process can be ignored.

It has been observed that both variables (temperature and time) have minimum level effect on the product.

3.1.4. RSM Results after Pre-Coating

Texture Value;

The formula describing the effects of coating quantity and time variables on product textural value;

Texture (g) = 5955,7 - 179,9 x **Coating Quantity (%) + 16,0** x **Time (min) - 215,0** x **Coating Quantity (%)** x **Coating Quantity (%) - 318,8** x **Time (min)** x **Time (min) - 203,9** x **Coating Quantity (%)** x **Time (min)**

It has been observed that the texture value changed inversely proportional with the coating quantity in the pre-coating parameters. The time is directly proportional with the hardness value. The effect of the coating quantity on the process is less. The effects of the time on the hardness value can be ignored.

3.1.5. RSM Results after Re-crystallization

Texture Value;

The formula describing the effects of humidity, temperature and time variables on product textural value;

Texture (g) = 4473,3 – 280 x **Re-crystallization Room Humidity (%) – 312** x **Time (min) – 358** x **Temperature (°C) + 134** x **Re-crystallization Room Humidity (%)xTime (min) – 108** x **Re-crystallization Room Humidity (%)** x **Time (°C) – 35** x **Time (min)** x **Temperature (°C)**

It has been observed that the textural value changed inversely proportional with the humidity, time and temperature in the re-crystallization parameters.

3.1.6. RSM Results of Hard Coating

Texture Value;

The formula describing the effects of coating quantity and temperature variables on product textural value:

Texture (g) = 4519,2 + 201,0 x **Coating quantity (%) - 34,3** x **Temperature (°C) - 3,3** x **Coating Quantity (%)** x **Temperature (°C)**

It has been observed that the texture value changed in directly proportional with the coating quantity at the hard coating stage. Coating quantity is shown to be a significant parameter in the hard coating. The changes that can be occurred in the quantity affect the hardness value significantly.

It has been observed that the temperature and thehardness value are nversely proportional. However, it has been proved that these changes do not significantly effect on the system.

Humidity:

The formula describing the effects of coating quantity and temperature variables on product humidity value;

Humidity (%) = 3,3077 + 0,050 x **Coating quantity (%) - 0,100** x **Temperature (°C) + 0,000** x **Coating Quantity (%)** x **Temperature(°C)**

It has been observed that the humidity changed in direct proportional to the coating quantity in the parameters at the hard coating stage. However, it was observed that the humidity in the product did not undergo unusual change with the coating.

It was determined that the temperature changed inversely proportional with the humidity. However, these changes do not have significant effect on the product humidity mathematically.

In summary, it has been observed that the process applied in the hard coating does not lead to a significant change in the amount of normal water in the previous stages.

Color Value (L,a,b);

The formula describing the effects of coating quantity and temperature variables on the product color (L) value;

L = 80,726 - 1,648 x **Coating quantity (%) - 2,212** x **Temperature (°C) + 0,817** x **Coating quantity (%)** x **Temperature (°C)**

It has been observed that the L value changed inversely proportional to the coating quantity and temperature in the parameters at the stage of hard coating. It has been observed when the coating quantity increases the color tone of the product becomes darker (decreases L value) in this process.

The formula describing the effects of coating quantity and temperature variables on the product color value (a)

a = 10,943 + 1,382 x **Coating quantity (%) + 2,090** x **Temperature (°C) - 0,075** x **Coating quantity (%)** x **Temperature (°C)**

It has been observed that a value changed in direct proportional to the parameters at the stage of hard coating. It has been observed when the coating quantity increases the closeness of red in the color tone of the product increases in this process. It has been observed that the coating quantity is an effective variable on the product value.

The formula describing the effects of coating quantity and temperature variables on product color value (b)

b = 89,992 + 2,672 x **Coating quantity (%) + 2,712** x **Temperature (°C) + 0,203** x **Coating quantity (%)** x **Temperature (°C)**

It has been determined that b value changed in direct proportional to the coating quantity in the parameters at the stage of hard coating. It has been observed when the coating quantity increases the closeness of yellow in the color tone of the product increases (increase of b value) in this process. It has been observed that the coating quantity is an effective variable on the product.

4. RESULTS & DISCUSSIONS

The process conditions of the hard coated chewy candy product were studied by using RSM Techniques. The results of the trial sets showed great similarities and gave very close values with the process parameters.

The relevant structure was obtained wth the parameters for cooking temperature of 120 °C and the vacuum degree of (-) 0.5 bar. The product structure did not seem to present major changes according to the results of the rapid cooling trials. The effect of the temperature on the process seemed significant in the trials. 90 °C was a relevant temperature value.

According to the results obtained in the crystallization tests, the changes in the amount of the sugar and process time cause significant changes on the process. Texture and color spectrum parameters of the product were optimized with 5.25% sugar ratio for 20 minutes.

The cooling trials showed that the changes in the temperature and time values do not make any significant changes in the product structure.

Pre-coating trials showed that the changes in the time values do not make any significant changes on the product structure.

According to the results obtained in the re-crystallization tests, it has been observed that the changes in the humidity, time and temperature values make significant changes on the product structure. Considering the products taken as a reference, it has been decided that the products are kept at 22.5 degrees for 42 hours at 35% relative humidity. At 20% relative humidity, the product gets dry and becomes hard. At 50% relative humidity, the product becomes extremely soft.

According to the results obtained in the hard coating tests, coating quantity and temperature have influence on the many specifications of the product. The closest production parameters that we have reached the hardness value of the hard coating layer of the reference product are 15% coating quantity and 18 degrees.

REFERENCES

[1] BAEK *et al.* (1999). Sensory perception is related to the rate of change of volatile concentration in-nose during eating of model gels. *Chemical Senses*, 24, 155-160.

[2] BAINES and MORRIS (1987). Flavour/taste perception in thickened systems: The effect of guar gum above and below c*. Food Hydrocolloids, 1, 197-205.

[3] CLARK (2002). Influence of hydrocolloids on flavour release and sensoryinstrumental correlations. In Phillips and Williams (Eds.), *Gums and stabilisers for the food industry* 11 (pp. 217-224). Cambridge: Royal Society of Chemistry.

[4] FUNAMI (2011). Next target for food hydrocolloid studies: Texture design of foods using hydrocolloid technology. *Food Hydrocolloids*, 25, 1904-1914.

[5] FUNAMI (2016). The formulation design of elderly special diets. *Journal of Texture Studies*, 47, 313-322.

[6] KOÇ and ERTEKİN (2008). Yanit yüzey yöntemi ve gida işleme uygulamalari (Response surface methodology and food processing procedures)

[7] MORRIS, E. R. (1993). Rheological and organoleptic properties of food hydrocolloids. In Nishinari and Doi (Eds.), *Food hydrocolloids, structures, properties, and functions* (pp. 201e210). New York: Plenum Press.

[8] WEEL *et al.* (2002). Flavor release and perception of flavored whey protein gels: Perception is determined by texture rather than by release. *Journal of Agricultural and Food Chemistry*, 50, 5149-5155.

[9] http://forum.gidagundemi.com/gidalarin-teksturel-ozellikleri-t27124.html

Journal of Scientific Perspectives

Volume 3, Issue 2, Year 2019, pp. 133-140
E - ISSN: 2587-3008
URL: http://ratingacademy.com.tr/ojs/index.php/jsp
DOİ: https://doi.org/10.26900/jsp.3.014
Research Article

USING FIRED WALL TILE'S SCRAPS IN FLOOR TILE BODY

Savaş ELMAS*

** Res. Assist., Çanakkale Onsekiz Mart University, Faculty of Fine Arts, Ceramic and Glass Department, Çanakkale, TURKEY, E-mail: savaselmas@comu.edu.tr*
ORCID ID: https://orcid.org/0000-0003-2913-0303

Received: 3 March 2019; Accepted: 29 April 2019

ABSTRACT

The effect of the addition of the fired wall tile's scraps in floor tile body was studied. The fired wall tile's scraps were added to floor tile body according to 1.96-5.66-10.71-17.85 wt. % ratios. The sintering behavior of the floor tile was evaluated by measuring the water absorption, fired shrinkage, dry shrinkage and fired strength. In addition, microstructure and phase analysis were investigated by scanning electron microscopy (SEM), energy dispersive x-ray (EDX) and x-ray analysis (XRD). Firing was carried out at 1189 0C for 40 min. in industrial type continuous kiln. It is seen that the addition of 5.66 wt. % of the wall tile's scrap to the floor tile increases the fired strength value. In the XRD analysis, anorthite phase was observed which shows fired strength and chemical resistance.

Keywords: *Fired scraps wall tiles, Floor tiles, Environment savings, Cost of product*

1. INTRODUCTION

The use of waste in ceramic structures is important due to the protection of the existing raw material, the prevention of the harmful effects to the environment by evaluating the waste material and the price advantage according to the material it will take instead. According to Karamanov and al. [1], with using fired porcelain scraps at 15 wt. % in hard porcelain body, quartz dissolution increase that increase liquid phase content, was determined. The effects of firing at 1300-1350 ^{0}C, improved sintering and mechanical characteristics were determined. In an analysis of Nodeh [2], firing temperature and linear expansion decreased as a result of adding the bone chine porcelain waste to the hard porcelain body. On the other hand, the glassy phase, probability of deformation and total shrinkage increased. The addition of 6 wt.% bone porcelain doubled the fired mechanical strength at 1340 ^{0}C. In a study of Torres at al. [3] the granite fired scraps were added to the porcelain body, it was observed that the additions had no effect on density, shrinkage and plasticity. This study revealed that the recipe containing 25wt.% granite cutting waste additions imparted superior properties (water absorption 0.07%, bending strength > 50MPa) to the porcelain tile structure. Juinora et al. [4] points out that fritted waste and soda lime glass using in glazed and unglazed porcelain tiles, water absorption value has decreased and stain retention resistance has increased. In a study conducted by Martini at al.[5], a high percentage (43.62%) of glass waste-granite-scraps of sanitaryware waste was added to sanitary ware. It was observed that there was no rheological problem. According to a study by Luz[6], the addition of 5% glass replace feldspar to the porcelain body provides standard porcelain values. In another study by Matteuci at al[7] , soda-lime glass was added to the porcelain body up to 10%. It was observed that firing shrinkage and closed porosity increased. Open porosity and bulk density decreased. The use of 0-5% was found to be appropriate.

The aim of this study is to reduce the cost by using re-use of wall tile's scraps in floor tiles also to reduce environmental wastes.

2. EXPERIMENTAL PROCEDURE

The raw materials were prepared from Etili Seramik A.Ş (Çanakkale). Analysis of raw materials are given in Table 1. The samples are ground to degree of 1.55% > 63 microns with alumina ball media in 2 kg laboratory type mills according to composition of Table 2. The density of slurry was measured 1650gr / l. After drying at 110 ^{0}C for 1 day in dryers, granules were moistened with 5-6 % and pressed by laboratory presses with 350kg / cm^2 pressure in size 7x210x100 mm. They were fired in continous type industrial kiln at 1189 ^{0}C in a 40 min.

Table 1. Chemical analysis of raw materials (wt.%)

Raw Materials	SiO_2	Al_2O_3	Fe_2O_3	TiO_2	CaO	MgO	Na_2O	K_2O	L.I.
Clay	54	31,8	0,67	1,17	0,3	0,45	0,13	2,03	10,05
Kaolen	51	34	0,75	0,25	0,20	0,25	0,15	1,20	12
Na-Feldspar	68,62	19,53	0,016	0,042	0,99	0,10	10,29	0,21	0,14
Quarz	99,35	0,12	0,06	0,01	0,05	0,05	0,05	0,06	0,2

L.I: Loss of ignition

Table 2. Mixture compositions (wt.)

Raw Materials	1	2	3	4
Kaolen	25	25	25	25
Clay	40	40	40	40
Na- Feldspar	30	30	30	30
Quarz	5	5	5	5
Fired scraps of wall tiles	0	2	6	12

wt: weight

3.RESULTS

3.1 Physical properties

Phyiscal properties are considered for industrial products according to standards TS EN 14411. Table 3. shows the slip viscosity, fired loss, fired shrinkage, dry strength and fired strength values of all recipes. As seen in Figure 1, the viscosity increase is observed in the slip with the increase fired scraps of wall tile in floor tile. As seen in the graph in Figure 2, firing shrinkage value decreases to 5.66% of wall tile's scraps and then increases. When the change in the dried and fired strength value with the added fired wall fracture scraps was examined, until the addition value of 5.66%, both of them values is seen to increased then decreased. The reason why dry strength falls after a certain value is that this material is not plastic. Anortite phase is seen in the sample containing 5.66% waste. According to Gdula [8], Ismail and al.[9], Pozutak at al. [10], it is stated that the amount of anorthite in the structure has a strength increasing effect [11]. At the same time, the reduction in the firing shrinkage is thought to be due to the anorthite crystal.

Table 3. Physical features of fired floor tiles samples

	1	2	3	4
Slip viscosity (sn)	33	33	35	37
Loss of ignition (%)	3,49	3,59	3,47	3,39
Fired shrinkage (%)	9.07	8,84	8.96	9.46
Water absorbtion (%)	0,008	0,016	0,016	0,007
Dried strength (kg/cm^2)	16,78	18,35	18.68	16.26
Fired strength (kg/cm^2)	458.45	472.89	488.02	431.49

Figure 1. Viscosity – fired scraps of wall tiles wt. % changes

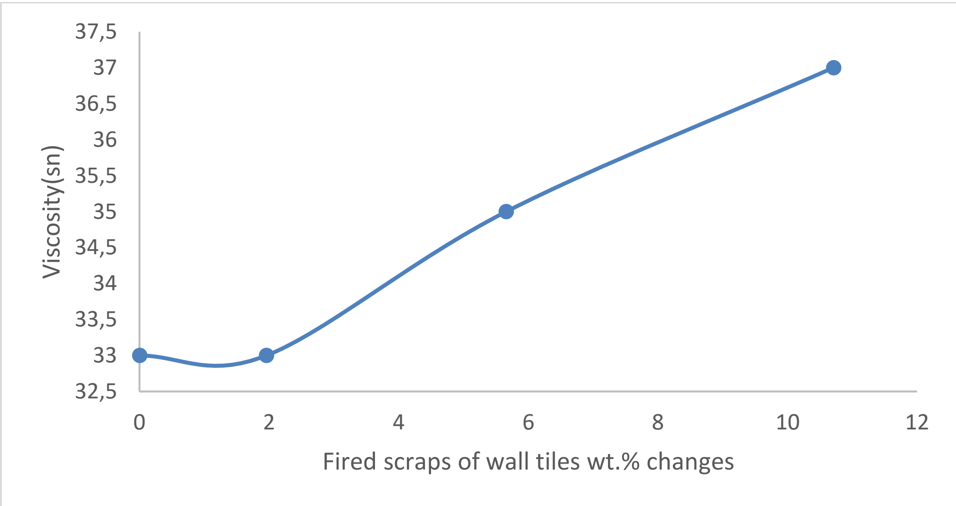

Figure 2. Fired shrinkage - fired scraps of wall tiles wt. % changes

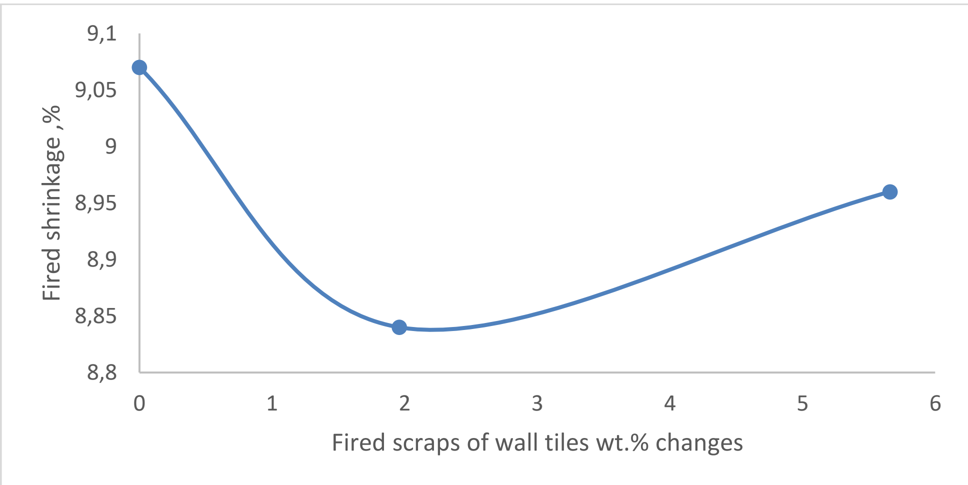

Figure 3. Fired strength- fired scraps of wall tiles wt. % changes

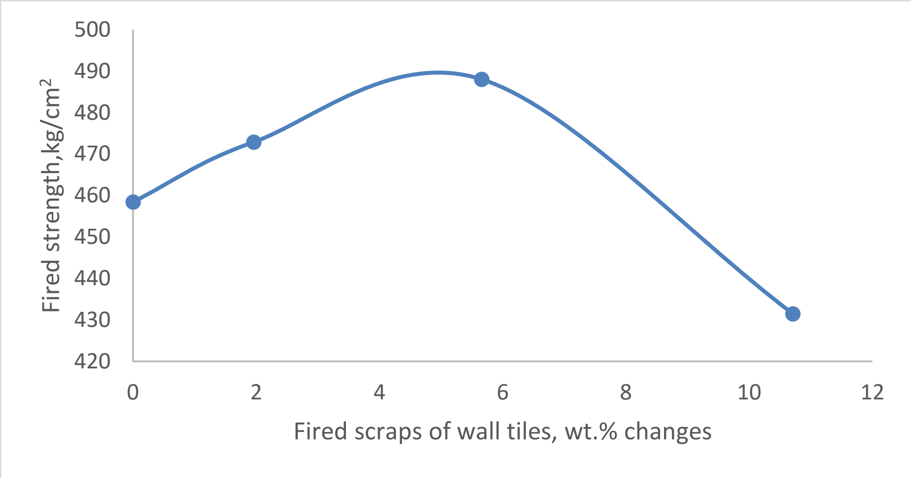

Figure 4. Water absorbtion- fired scraps of wall tiles wt. % changes

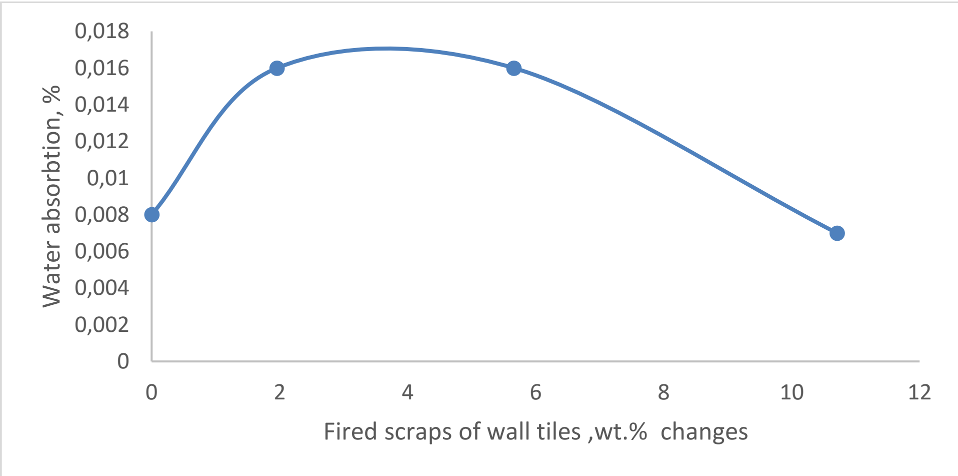

Figure 5. Dried strength- fired scraps of wall tiles wt. % changes

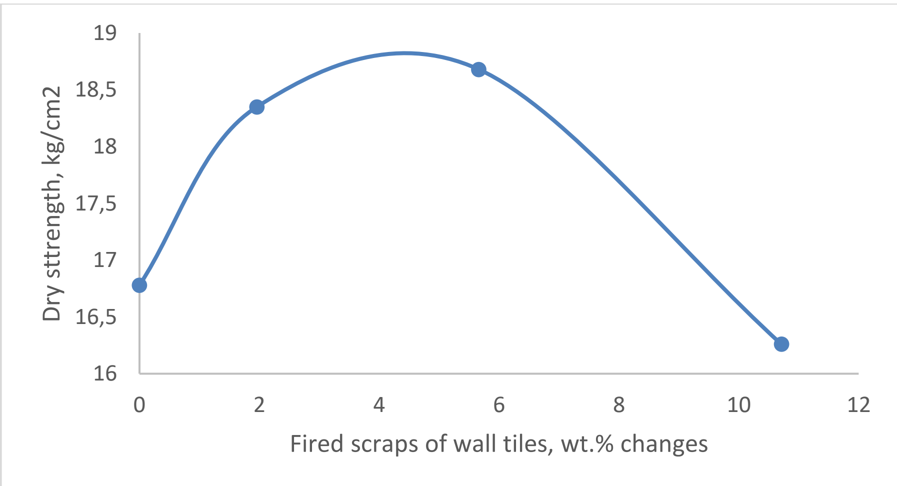

3.2 Microstructure and phase analysis of the body

The phases formed in the samples 1 and 3 were determined from the corresponding XRD patterns are shown in Figure 6. Quartz, mullite, albite and cristobalite were found in standard floor tiles, while quartz, mullite, anorthite and calcium rich albite were found in the floor tile containing 5.66% of fired wall tiles. It is thought that the decrease in the quartz owing to low level of liquid phase viscosity and/or increases of quantity of liquid phase . Although mullite peaks are similar in both structures, anorthite phase is observed in composition number 3. Kara at all.[12] published an article related to floor tiles which was contain XRD graphs include quartz,albite and mullite peaks in fired tile. Floor tile with added fired wall tile scraps contains quartz, mullite, anorthite and albite phase.

Figure 6. XRD patterns of 1 and 3

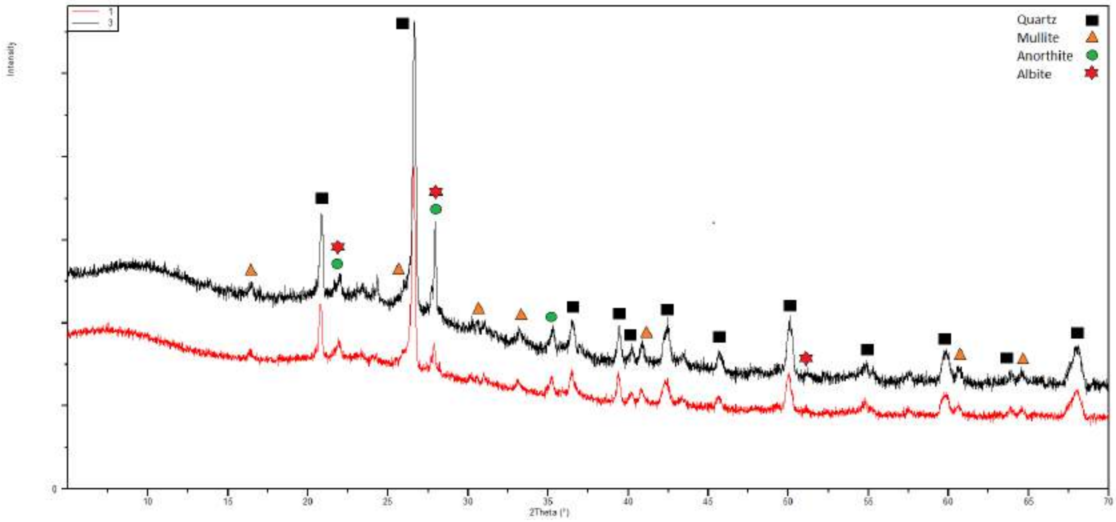

The scanning electron microscope (SEM) images of the standard composition (1) and the highest fired strength sample (3) are shown in Figure 7. Free quartz particle can be seen in 1. At the 1 and 3 composition, it is observed the high sintering with glassy phase. The low homogeneity of mixing process's can lead pore or crack occurence in 1. On the other hand, the composition 3 shows a continuous and much more glassy structure. The increase in sintering provides a decrease in water absorption and an increase in fired strength in the no 3 composition.

Figure 7 **a)** 100 X magnified image of standard (number 1) composition
b) 100 X magnified image of 3 number composition
c) 2000 X magnified image of standard (number 1) composition
d) 2000 X magnified image of 3 number composition

a) 1 no sample

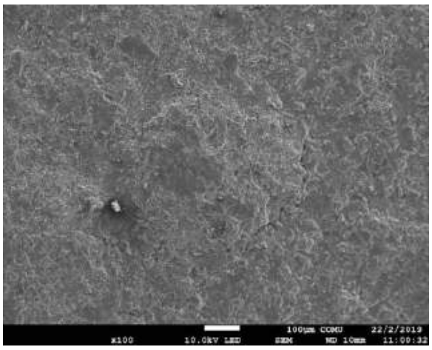

b) 3 no sample

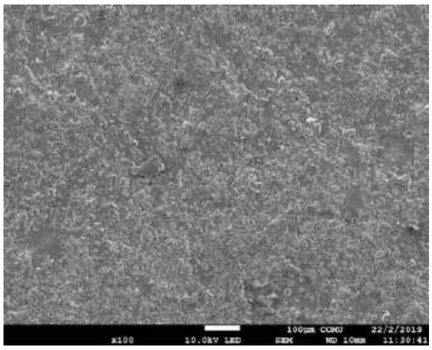

c) 1 no sample

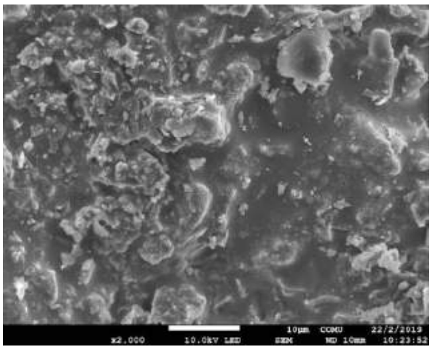

d) 3 no sample

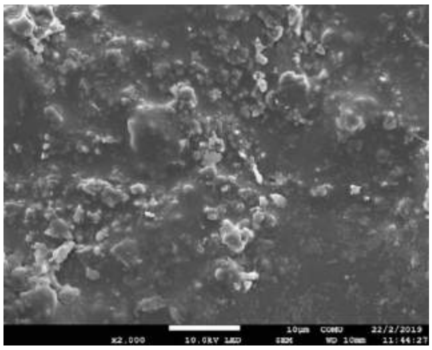

The energy scattering x-ray (EDS) of the recipe 1 and 3 are shown in Figure 8. A high sintering is observed in both structures; The glassy phase is dominant in the ceramic structure. In the composition 3, the amount of Ca is higher than the other, as can be seen from the EDS spectrum. In addition, the reason of other differences of the EDS is nature of raw material and process conditions.

Figure 8. a) EDS analysis of recipe 1
b) EDS analysis of recipe 3

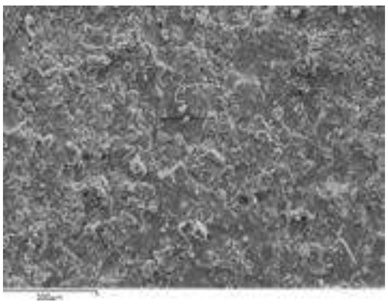

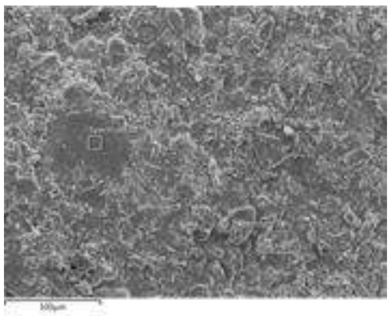

a) 1 no sample

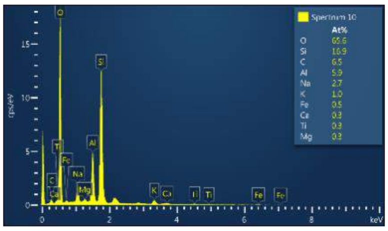

b) 3 no sample

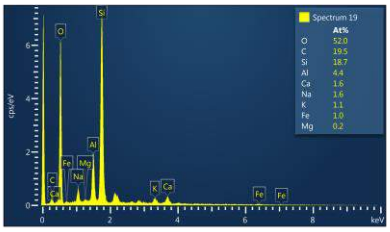

4.CONCLUSIONS

In order to prevent environmental pollution and to reduce the cost of ceramic tiles, it was determined that the wall tile waste could be used up to 5.66 % in the floor tile. Thus, a floor tile structure was obtained in which similar water absorption and fired shrinkage were obtained with high fired strength value. With this amount of adding of scraps, sintering and mechanical properties were improved. In future studies on the subject, the use of fired wall tile waste in floor tiles instead of quartz component can be investigated.

REFERENCES

[1] KARAMANOV, A., KARAMANOVA, E., FERRARI, A.M., FERRANTE, F., PELINO, M.,2006, The Effects of Fired Scrap Addition on The Sintering Behaviour of Hard Porcelain. *Ceramics International*, 32, 727-732.

[2] NODEH, A.A., 2017, Influence of Bone Porcelain Scraps on The Physical Characterictics and Phase Composition of a Hard Porcelain Body. *Ceramica y Vidrio*, 56. 113-118, Spain.

[3] TORRES, P., FERNANDES, H.R., AGATHOPOULOS, S., TULYAGANOV, D.U., FERREİRA J.M.F., 2004, Incorporation of Granite Cutting Sludge in Industrial Porcelain Tile Formulations, *Journal of The European Ceramic Society*, 24. 3177-3185.

[4] JOUNIORA, A.N., HOTZA, D., SOLER, C.V., VILCHES, E.S., 2010, Influence of Composition on Mechanical Behaviour of Porcelain Tile.Part II: Mechanical Properties and Microscopic Residual Stress, *Material Science and Engineering*, A 527, 1736-1743.

[5] MARTINI, E., FORTUNA, D., FORTUNA, A., RUBINO, G., TAGLIAFERRI, V., 2017, Sanitser, an innovative sanitary ware body, formulated with waste glass and recycled materials, *Ceramica*, 63, 542-548

[6] LUZ A.P., RİBİERO S., Use of glass waste as a raw material in porcelain stoneware tile mixtures,2007, Ceramics International 33, 761-765

[7] MATTEUCI, F., DONDI, M., GUARINI, G., 2002, Effects of Soda-Lime Glass on Sintering and Technogical Properties of Porcelain Stoeware Tiles, *Ceramics International*, 28(8) 878-880.

[8] GDULA, R.A., 1971, Anorthite ceramic dielectric. *Am. Ceram. Soc. Bull*., 50(6).555-557.

[9] ISMAİL, M.G.M.U., ARAI, H., 1992, Sol-gel Synthesis of B_2O_3-doped Anorthite and its Characteristics. *J. Ceram. Soc. Jpn.*, 100(12) 1385-1389

[10] POZUTAK, M., SOLVANG, M., DINGWELL, D., 2006, Temperature independent thermal expansivities of calcium aluminosilicates melts between 1150 and 1973 K in the system anorthite- wollastonite-gehlenit: a density model., *Geochim Cosmochim Acta*, 70. 3059-3074.

[11] KURAMA, S., OZEL, E., 2008, The Influence of different CaO source in the Production of Anorthite Ceramics. *Ceramics International*, 35. 827-830.

[12] KARA, A., ÖZER, F., KAYACI, K., ÖZER, P., 2006, Development of a multipurpose tile body: Phase and microstructural development, 26. 3769-3782.

Journal of Scientific Perspectives

Volume **3,** Issue **2,** Year **2019**, pp. **141-158**
E - ISSN: **2587-3008**
URL: http://ratingacademy.com.tr/ojs/index.php/jsp
DOİ: https://doi.org/10.26900/jsp.3.015
Research Article

HADAMARD, SIMPSON AND OSTROWSKI TYPE INEQUALITIES FOR E-CONVEXITY

Musa ÇAKMAK*

** Reyhanlı Vocational School of Social Sciences, Mustafa Kemal University, Hatay 31000, Turkey,*
E-mail: enkucukcakmak@gmail.com
ORCID ID: https://orcid.org/0000-0002-8794-4797

Received: 13 March 2019; Accepted: 29 April 2019

ABSTRACT

In this study, we proposed a new definition to give a different perspec-tive to convex functions. We have introduced the expansion of Hadamard, midpoint Hadamard, trapezoid Hadamard, Simpson and Ostrowski inequalities for the newly defined classes of convex functions.

Keywords: *(a; m; e)-convexity, Hadamard's inequality, Simpson inequality, Ostrowski inequality.*

2010 AMS Subject Classification: *26A33, 26D07, 26D15, 26D60*

1. INTRODUCTION

1.1. **Theorems.** If φ is integrable on $[u_1, u_2]$, then the average value of φ on $[u_1, u_2]$ is

$$(1) \qquad \frac{1}{u_2 - u_1}\int_{u_1}^{u_2} \varphi(z)dz.$$

Let $\varphi : D \subseteq \mathbb{R} \to \mathbb{R}$ be a convex function and $u_1, u_2 \in D$ with $u_1 < u_2$. Then the following double inequality:

$$(2) \qquad \varphi\left(\frac{u_1 + u_2}{2}\right) \leq \frac{1}{u_2 - u_1}\int_{u_1}^{u_2} \varphi(z)dz \leq \frac{\varphi(u_1) + \varphi(u_2)}{2}$$

is known as Hermite-Hadamard inequality for convex mappings. For particular choice of the function φ in (2) yields some classical inequalities of means. Both inequalities in (2) hold in reversed direction if φ is concave. The refinement of the second inequality in (2) is due to Bullen as follows:

$$(3) \quad \frac{1}{u_2 - u_1}\int_{u_1}^{u_2} \varphi(z)dz \leq \frac{1}{2}\left[\varphi\left(\frac{u_1 + u_2}{2}\right) + \frac{\varphi(u_1) + \varphi(u_2)}{2}\right] \leq \frac{\varphi(u_1) + \varphi(u_2)}{2}$$

where φ is as above. This (3) integral inequality is well known in the literature as **Bullen Inequality** [21, Pečarić, Proschan and Tong, 1991]. For some recent results in connection with Hermite-Hadamard inequality and its applications we refer to [[1], [4]-[9], [11]-[25], [27]] where further references are given.

The following inequality is well known in the literature as **Simpson's inequality** [10, Dragomir, Agarwal, and Cerone, 2000];

$$\begin{aligned} (4) \qquad & \int_{u_1}^{u_2} \varphi(z)\,dz - \frac{u_2-u_1}{3}\left[\frac{\varphi(u_1)+\varphi(u_2)}{2} + 2\varphi\left(\frac{u_1+u_2}{2}\right)\right] \\ \leq\ & \frac{1}{1280}\left\|\varphi^{(4)}\right\|_{\infty}(u_2-u_1)^5, \end{aligned}$$

where the mapping $\varphi : [u_1, u_2] \to \mathbb{R}$ is assumed to be four times continuously differentiable on the interval and $\varphi^{(4)}$ to be bounded on (u_1, u_2) , that is,

$$\left\|\varphi^{(4)}\right\|_{\infty} = \sup_{r\in(u_1,u_2)}\left|\varphi^{(4)}(r)\right| < \infty.$$

Let $\varphi : D \subseteq [0, \infty) \to \mathbb{R}$ be a differentiable mapping on D° (the interior of D) such that $\varphi' \in L[u_1.u_2]$, where $u_1, u_2 \in D$ with $u_1 < u_2$. If $|\varphi'| \leq M$, then the following double inequality:

$$(5) \qquad \left|\varphi(z) - \frac{1}{u_2-u_1}\int_{u_1}^{u_2}\varphi(u)du\right| \leq \frac{M}{u_2-u_1}\frac{(z-u_1)^2+(u_2-z)^2}{2}$$

holds. This result is known in the literature as the **Ostrowski inequality** [26].

1.2. **Definitions.** Let $h : J \to \mathbb{R}$ be a nonnegative function, $h \not\equiv 0$. We say that $\varphi : D \to \mathbb{R}$ is an h-convex function, or that φ belongs to the class $SX(h, D)$, if φ is nonnegative and for all $z, \mu \in D$ and $r \in (0, 1)$ we have

$$(6) \qquad \varphi(rz + (1-r)\mu) \leq h(r)\varphi(z) + h(1-r)\varphi(\mu).$$

If inequality (6) is reversed, then φ is said to be h-concave, i.e. $\varphi \in SV(h, D)$. Obviously, if $h(r) = r$, then all nonnegative convex functions belong to $SX(h, D)$ and all nonnegative concave functions belong to $SV(h, D)$; if $h(r) = 1$, then $SX(h, D) \supseteq P(D)$; and if $h(r) = r^s$, where $s \in (0, 1)$, then $SX(h, D) \supseteq K_s^2$, where K_s^2 is $s-$convex in the second sense [26, 27].

The function $\varphi : [0, v] \to \mathbb{R}$ is said to be $(\alpha, m)-$convex, where $(\alpha, m) \in [0, 1]^2$, if for every $z, \mu \in [0, v]$ and $r \in [0, 1]$, we have

$$\varphi(rz + m(1-r)\mu) \leq r^{\alpha}\varphi(z) + m(1-r^{\alpha})\varphi(\mu).$$

Denote by $K_m^\alpha(v)$ the set of the (α, m) −convex functions on $[0, v]$ for which $\varphi(0) \leq 0$. We say that φ is (α, m) −concave if $-\varphi$ is (α, m) −convex. Denote by $K_m^\alpha(v)$ the class of all (α, m) −convex functions on $[0, v]$ for which $\varphi(0) \leq 0$ [24, 25].

1.3. Lemmas.

Lemma 1.1. [14] *Let $\varphi : D \subset \mathbb{R} \to \mathbb{R}$ be a differentiable mapping on D°, $u_1, u_2 \in D^\circ$ with $u_1 < u_2$. If $\varphi' \in L[u_1, u_2]$, then the following equality holds:*

$$\begin{aligned} & \frac{1}{u_2 - u_1} \int_{u_1}^{u_2} \varphi(z)\,dz - \varphi\left(\frac{u_1 + u_2}{2}\right) \\ = & \ (u_2 - u_1) \int_0^{\frac{1}{2}} r\varphi'(ru_1 + (1 - r) u_2)\,dr + \int_{\frac{1}{2}}^1 (r - 1)\,\varphi'(ru_1 + (1 - r) u_2)\,dr. \end{aligned}$$

Lemma 1.2. [1]*Let $\varphi : D \subset \mathbb{R} \to \mathbb{R}$ be a differentiable mapping on D° where $u_1, u_2 \in D$ with $u_1 < u_2$. If $\varphi' \in L[u_1, u_2]$, then the following equality holds:*

$$\begin{aligned} & \frac{\varphi(u_1) + \varphi(u_2)}{2} - \frac{1}{u_2 - u_1} \int_{u_1}^{u_2} \varphi(z)\,dz \\ = & \ \frac{u_2 - u_1}{4} \left[\int_0^1 (-r)\,\varphi'\left(\frac{1 + r}{2} u_1 + \frac{1 - r}{2} u_2\right) dr + \int_0^1 r\varphi'\left(\frac{1 + r}{2} u_2 + \frac{1 - r}{2} u_1\right) dr \right]. \end{aligned}$$

Lemma 1.3. [2]*Let $\varphi : D \subset \mathbb{R} \to \mathbb{R}$ be an absolutely continuous mapping D° where $u_1, u_2 \in D$ with $u_1 < u_2$. If $\varphi' \in L[u_1, u_2]$, then the following equality holds:*

$$\begin{aligned} & \frac{1}{6}\left[\varphi(u_1) + 4\varphi\left(\frac{u_1 + u_2}{2}\right) + \varphi(u_2)\right] - \frac{1}{u_2 - u_1} \int_{u_1}^{u_2} \varphi(z)\,dz \\ = & \ (u_2 - u_1) \int_0^1 p(r)\,\varphi'(ru_2 + (1 - r) u_1)\,dr, \end{aligned}$$

where

$$p(r) = \begin{cases} r - \frac{1}{6}, & r \in \left[0, \frac{1}{2}\right) \\ r - \frac{5}{6}, & r \in \left[\frac{1}{2}, 1\right]. \end{cases}$$

Lemma 1.4. [3]*Let $\varphi : D \subset \mathbb{R} \to \mathbb{R}$ be a differentiable mapping on D°, where $u_1, u_2 \in D$ with $u_1 < u_2$. If $\varphi' \in L[u_1, u_2]$, then the following equality holds:*

$$\varphi(z) - \frac{1}{u_2 - u_1} \int_{u_1}^{u_2} \varphi(u)\,du = (u_2 - u_1) \int_0^1 p(r)\,\varphi'(ru_1 + (1 - r) u_2)\,dr$$

for each $r \in [0, 1]$, where

$$p(r) = \begin{cases} r, & r \in \left[0, \frac{u_2 - z}{u_2 - u_1}\right] \\ r - 1, & r \in \left(\frac{u_2 - z}{u_2 - u_1}, 1\right] \end{cases},$$

for all $z \in [u_1, u_2]$.

The main aim of this paper is to establish refinements inequalities of Hadamard's type, midpoint-Hadamard type, trapezoid-Hadamard type, Simpson's type and Ostrowski's type for $e-$convex functions.

2. MAIN RESULTS

Firstly, Let us define the following special definition on convex functions. Secondly we establish a few different intelligent integral inequalities.

Definition 2.1. *Let* $h : J \subseteq \mathbb{R} \to \mathbb{R}$ *be a nonnegative function. A function* $\varphi : D \subseteq \mathbb{R} \to (0, \infty)$ *is said to be* $(\alpha, m, e^h)-$ *convex function if*

$$\varphi(rz + m(1-r)\mu) \leq e^{h(r^\alpha)}\varphi(z) + me^{h(1-r^\alpha)}\varphi(\mu)$$

for all $z, \mu \in D$ *and* $r \in [0,1]$ *with some fixed* $(\alpha, m) \in (0,1]^2$. *Let us suggest several special cases of new definition;*

(1) If $h(r) = r^s$ for $s \in [0,1]$, then Definition 2.1 reduces to definition of $(\alpha, m, e^s)-$convexity.
(2) If $h(r) = r^{\frac{1}{s}}$ for $s \in [0,1]$, then Definition 2.1 reduces to definition of $(\alpha, m, e^{1/s})-$convexity.
(3) If $h(r) = r^{\frac{1}{\alpha}}$ and $m = 1$, then Definition 2.1 reduces to definition of $e-$convexity.
(4) If $h(r) = r$, then Definition 2.1 reduces to definition of $(\alpha, m, e)-$convexity in the first sense.
(5) If $h(r) = 1$, then Definition 2.1 reduces to definition of $(m, e)-$convexity.
(6) If $h(r) = r^s$ for $s \in [0,1]$,and $\alpha = 1$, then Definition 2.1 reduces to definition of $(\alpha, m, e)-$convexity in the second sense.
(7) If $h(r) = r(1-r)$ and $\alpha = 1$, then Definition 2.1 reduces to definition of $(m, tgs, e)-$convexity.
(8) If $h(r) = \frac{\sqrt{(1-r)}}{2\sqrt{r}}$ and $\alpha = 1$, then Definition 2.1 reduces to definition of $(m, e_{MT})-$convexity.

Now, we prove the following theorems.

Theorem 2.2. *Let* φ *be* $e-$*convex function,* $u_1, u_2 \in D \subset \mathbb{R}$ *with* $u_1 < u_2$, $\varphi \in L[u_1, u_2]$. *Then the following inequalities hold:*

$$\frac{1}{2\sqrt{e}}\varphi\left(\frac{u_1+u_2}{2}\right) \leq \frac{1}{u_2-u_1}\int_{u_1}^{u_2}\varphi(z)\,dz \leq (e-1)(\varphi(u_1)+\varphi(u_2)). \tag{7}$$

Proof. Since φ is $e-$convex, we have

$$\begin{aligned}\varphi\left(\frac{u_1+u_2}{2}\right) &= \varphi\left(\frac{ru_1+(1-r)u_2}{2}+\frac{ru_2+(1-r)u_1}{2}\right)\\ &\leq e^{\frac{1}{2}}\varphi(ru_1+(1-r)u_2)+e^{\frac{1}{2}}\varphi(ru_2+(1-r)u_1)\end{aligned}$$

for all $r\in[0,1]$. By integrating, we get

$$\begin{aligned}\varphi\left(\frac{u_1+u_2}{2}\right) &\leq e^{\frac{1}{2}}\int_0^1\varphi(ru_1+(1-r)u_2)\,dr+e^{\frac{1}{2}}\int_0^1\varphi(ru_2+(1-r)u_1)\,dr\\ &= e^{\frac{1}{2}}\left(\frac{1}{u_2-u_1}\int_{u_1}^{u_2}\varphi(z_1)\,dz_1+\frac{1}{u_2-u_1}\int_{u_1}^{u_2}\varphi(z_2)\,dz_2\right)\\ &= \frac{2e^{\frac{1}{2}}}{u_2-u_1}\int_{u_1}^{u_2}\varphi(z)\,dz.\end{aligned}$$

For the proof of right hand side of (7), we can write

$$\begin{aligned}\frac{1}{u_2-u_1}\int_{u_1}^{u_2}\varphi(z)\,dz &\leq \int_0^1 e^r\varphi(u_1)\,dr+\int_0^1 e^{1-r}\varphi(u_2)\,dr\\ &= \varphi(u_1)\,e^r\big|_0^1-\varphi(u_2)\,e^{1-r}\big|_0^1\\ &= (e-1)(\varphi(u_1)+\varphi(u_2)).\end{aligned}$$

Thus, the theorem is proven. □

Theorem 2.3. *(Midpoint Hadamard) Let $\varphi: D\subset\mathbb{R}\to\mathbb{R}$ be a differentiable mapping on D°, $u_1,u_2\in D$ with $u_1<u_2$ and let $1/r_1+1/r_2=1$ with $r_1>1$. If $|\varphi'|^{r_2}$ is $e-$convex on $[u_1,u_2]$, then the following inequalities hold:*

$$\begin{aligned}&\left|\frac{1}{u_2-u_1}\int_{u_1}^{u_2}\varphi(z)\,dz-\varphi\left(\frac{u_1+u_2}{2}\right)\right|\\ \leq\ &\frac{u_2-u_1}{(r_1+1)\,2^{r_1+1}}\left[\left(\left(\sqrt{e}-1\right)|\varphi'(u_1)|^{r_2}+\left(e-\sqrt{e}\right)|\varphi'(u_2)|^{r_2}\right)^{\frac{1}{r_2}}\right.\\ &\left.+\left(\left(e-\sqrt{e}\right)|\varphi'(u_1)|^{r_2}+\left(\sqrt{e}-1\right)|\varphi'(u_2)|^{r_2}\right)^{\frac{1}{r_2}}\right]\\ \leq\ &\frac{(u_2-u_1)(e-1)}{(r_1+1)\,2^{r_1+1}}\left(|\varphi'(u_1)|+|\varphi'(u_2)|\right).\end{aligned}$$

Proof. From Lemma 1.1 and $e-$convexity of $|\varphi'|^{r_2}$ function on $[u_1, u_2]$ and by using Hölder's integral inequality, we obtain

$$\begin{aligned}
&\left|\frac{1}{u_2-u_1}\int_{u_1}^{u_2}\varphi(z)\,dz-\varphi\left(\frac{u_1+u_2}{2}\right)\right| = (u_2-u_1)\times \\
&\int_0^{\frac{1}{2}} r\left|\varphi'(ru_1+(1-r)u_2)\right|dr+\int_{\frac{1}{2}}^{1}(1-r)\left|\varphi'(ru_1+(1-r)u_2)\right|dr \\
\leq\ & (u_2-u_1)\left[\left(\int_0^{\frac{1}{2}} r^{r_1}dr\right)^{\frac{1}{r_1}}\left(\int_0^{\frac{1}{2}}\left|\varphi'(ru_1+(1-r)u_2)\right|^{r_2}dr\right)^{\frac{1}{r_2}}\right. \\
&\left.+\left(\int_{\frac{1}{2}}^{1}(1-r)^{r_1}dr\right)^{\frac{1}{r_1}}\left(\int_{\frac{1}{2}}^{1}\left|\varphi'(ru_1+(1-r)u_2)\right|^{r_2}dr\right)^{\frac{1}{r_2}}\right] \\
\leq\ & \frac{u_2-u_1}{(r_1+1)\,2^{r_1+1}}\left[\left(\int_0^{\frac{1}{2}}\left(e^r\left|\varphi'(u_1)\right|^{r_2}+e^{1-r}\left|\varphi'(u_2)\right|^{r_2}\right)dr\right)^{\frac{1}{r_2}}\right. \\
&\left.+\left(\int_{\frac{1}{2}}^{1}\left(e^r\left|\varphi'(u_1)\right|^{r_2}+e^{1-r}\left|\varphi'(u_2)\right|^{r_2}\right)dr\right)^{\frac{1}{r_2}}\right] \\
=\ & \frac{u_2-u_1}{(r_1+1)\,2^{r_1+1}}\left[\left(\left(e^{\frac{1}{2}}-1\right)\left|\varphi'(u_1)\right|^{r_2}+\left(e-e^{\frac{1}{2}}\right)\left|\varphi'(u_2)\right|^{r_2}\right)^{\frac{1}{r_2}}\right. \\
&\left.+\left(\left(e-e^{\frac{1}{2}}\right)\left|\varphi'(u_1)\right|^{r_2}+\left(e^{\frac{1}{2}}-1\right)\left|\varphi'(u_2)\right|^{r_2}\right)^{\frac{1}{r_2}}\right].
\end{aligned}$$

For the proof of second inequality, using the fact that

$$\sum_{i=1}^{m}(p_i+q_i)^v\leq\sum_{i=1}^{m}p_i^v+\sum_{i=1}^{m}q_i^v \tag{8}$$

for $(0\leq v<1)$, $u_{11},u_{12},...,u_{1i}\geq 0$, $u_{21},u_{22},...,u_{2i}\geq 0$, we get

$$\begin{aligned}
&\left[\left(\left(e^{\frac{1}{2}}-1\right)\left|\varphi'(u_1)\right|^{r_2}+\left(e-e^{\frac{1}{2}}\right)\left|\varphi'(u_2)\right|^{r_2}\right)^{\frac{1}{r_2}}\right. \\
&\left.+\left(\left(e-e^{\frac{1}{2}}\right)\left|\varphi'(u_1)\right|^{r_2}+\left(e^{\frac{1}{2}}-1\right)\left|\varphi'(u_2)\right|^{r_2}\right)^{\frac{1}{r_2}}\right] \\
\leq\ & (e-1)\left|\varphi'(u_1)\right|+(e-1)\left|\varphi'(u_2)\right|
\end{aligned}$$

Thus, the proof is done. □

Theorem 2.4. *(Trapezoid-Hadamard) Let $\varphi: D\subset\mathbb{R}\to\mathbb{R}$ be a differentiable mapping on D°, $u_1,u_2\in D$ with $u_1<u_2$ and let $1/r_1+1/r_2=1$ with $r_1>1$. If*

$|\varphi'|^{r_2}$ is $e-$convex on $[u_1, u_2]$, then the following inequalities hold:

$$\begin{aligned}
&\left|\frac{\varphi(u_1)+\varphi(u_2)}{2}-\frac{1}{u_2-u_1}\int_{u_1}^{u_2}\varphi(z)\,dz\right| \\
\leq\ & \frac{u_2-u_1}{4(r_1+1)^{1/r_1}}\left[\left((2e-2\sqrt{e})\left|\varphi'(u_1)\right|^{r_2}+(2\sqrt{e}-2)\left|\varphi'(u_2)\right|^{r_2}\right)^{\frac{1}{r_2}}\right. \\
&\left.+\left((2e-2\sqrt{e})\left|\varphi'(u_2)\right|^{r_2}+(2\sqrt{e}-2)\left|\varphi'(u_1)\right|^{r_2}\right)^{\frac{1}{r_2}}\right] \\
\leq\ & \frac{(u_2-u_1)(e-1)}{2(r_1+1)^{1/r_1}}\left(\left|\varphi'(u_1)\right|+\left|\varphi'(u_2)\right|\right).
\end{aligned}$$

Proof. From Lemma 1.2 and $e-$convexity of $|\varphi'|^{r_2}$ function and by using Hölder's integral inequality, we obtain

$$\begin{aligned}
&\left|\frac{\varphi(u_1)+\varphi(u_2)}{2}-\frac{1}{u_2-u_1}\int_{u_1}^{u_2}\varphi(z)\,dz\right| \\
\leq\ & \frac{u_2-u_1}{4}\times \\
&\left[\left(\int_0^1 r^{r_1}dr\right)^{\frac{1}{r_1}}\left(\int_0^1\left|\varphi'\left(\frac{1+r}{2}u_1+\frac{1-r}{2}u_2\right)\right|^{r_2}dr\right)^{\frac{1}{r_2}}\right. \\
&\left.+\left(\int_0^1 r^{r_1}dr\right)^{\frac{1}{r_1}}\left(\int_0^1\left|\varphi'\left(\frac{1+r}{2}u_2+\frac{1-r}{2}u_1\right)\right|^{r_2}dr\right)^{\frac{1}{r_2}}\right] \\
\leq\ & \frac{u_2-u_1}{4(r_1+1)^{1/r_1}}\times \\
&\left[\left(\int_0^1\left(e^{\frac{1+r}{2}}\left|\varphi'(u_1)\right|^{r_2}+e^{\frac{1-r}{2}}\left|\varphi'(u_2)\right|^{r_2}\right)dr\right)^{\frac{1}{r_2}}\right. \\
&\left.+\left(\int_0^1\left(e^{\frac{1+r}{2}}\left|\varphi'(u_2)\right|^{r_2}+e^{\frac{1-r}{2}}\left|\varphi'(u_1)\right|^{r_2}\right)dr\right)^{\frac{1}{r_2}}\right] \\
=\ & \frac{u_2-u_1}{4(r_1+1)^{1/r_1}}\left[\left(\left(2e-2e^{\frac{1}{2}}\right)\left|\varphi'(u_1)\right|^{r_2}+\left(2e^{\frac{1}{2}}-2\right)\left|\varphi'(u_2)\right|^{r_2}\right)^{\frac{1}{r_2}}\right. \\
&\left.+\left(\left(2e-2e^{\frac{1}{2}}\right)\left|\varphi'(u_2)\right|^{r_2}+\left(2e^{\frac{1}{2}}-2\right)\left|\varphi'(u_1)\right|^{r_2}\right)^{\frac{1}{r_2}}\right].
\end{aligned}$$

By using Inequality (8), we get

$$
\begin{aligned}
& \left(\left(2e-2e^{\frac{1}{2}}\right)\left|\varphi'(u_1)\right|^{r_2}+\left(2e^{\frac{1}{2}}-2\right)\left|\varphi'(u_2)\right|^{r_2}\right)^{\frac{1}{r_2}} \\
& +\left(\left(2e-2e^{\frac{1}{2}}\right)\left|\varphi'(u_2)\right|^{r_2}+\left(2e^{\frac{1}{2}}-2\right)\left|\varphi'(u_1)\right|^{r_2}\right)^{\frac{1}{r_2}} \\
\leq\ & (2e-2)\left|\varphi'(u_1)\right|+(2e-2)\left|\varphi'(u_2)\right|,
\end{aligned}
$$

which completes the proof.

Theorem 2.5. *(Trapezoid-Hadamard) Let $\varphi : D \subset \mathbb{R} \to \mathbb{R}$ be a differentiable mapping on D°, $u_1, u_2 \in D$ with $u_1 < u_2$. If $|\varphi'|^{r_2}$ is e−convex on $[u_1, u_2]$, $r_2 \geq 1$, then the following inequalities hold:*

$$
\begin{aligned}
& \left|\frac{\varphi(u_1)+\varphi(u_2)}{2}-\frac{1}{u_2-u_1}\int_{u_1}^{u_2}\varphi(z)\,dz\right| \\
\leq\ & \frac{u_2-u_1}{2^{(3r_2-1)/r_2}}\left[\left((4\sqrt{e}-2e)\left|\varphi'(u_1)\right|^{r_2}+(4\sqrt{e}-6)\left|\varphi'(u_2)\right|^{r_2}\right)^{\frac{1}{r_2}}\right. \\
& \left.+\left((4\sqrt{e}-2e)\left|\varphi'(u_2)\right|^{r_2}+(4\sqrt{e}-6)\left|\varphi'(u_1)\right|^{r_2}\right)^{\frac{1}{r_2}}\right] \\
\leq\ & \frac{u_2-u_1}{2^{(2r_2-1)/r_2}}\left(4\sqrt{e}-e-3\right)\left(\left|\varphi'(u_1)\right|+\left|\varphi'(u_2)\right|\right).
\end{aligned}
$$

Proof. From Lemma 1.2 and $e-$convexity of $|\varphi'|^{r_2}$ function and by using power mean inequality, we establish

$$\begin{aligned}
&\left|\frac{\varphi(u_1)+\varphi(u_2)}{2}-\frac{1}{u_2-u_1}\int_{u_1}^{u_2}\varphi(z)\,dz\right| \\
\leq\ & \frac{u_2-u_1}{4}\times \\
&\left[\left(\int_0^1 rdr\right)^{1-\frac{1}{r_2}}\left(\int_0^1 r\left|\varphi'\left(\frac{1+r}{2}u_1+\frac{1-r}{2}u_2\right)\right|^{r_2}dr\right)^{\frac{1}{r_2}}\right. \\
&\left.+\left(\int_0^1 rdr\right)^{1-\frac{1}{r_2}}\left(\int_0^1 r\left|\varphi'\left(\frac{1+r}{2}u_2+\frac{1-r}{2}u_1\right)\right|^{r_2}dr\right)^{\frac{1}{r_2}}\right] \\
\leq\ & \frac{u_2-u_1}{2^{3-1/r_2}}\times \\
&\left[\left(\int_0^1\left(re^{\frac{1+r}{2}}\left|\varphi'(u_1)\right|^{r_2}+re^{\frac{1-r}{2}}\left|\varphi'(u_2)\right|^{r_2}\right)dr\right)^{\frac{1}{r_2}}\right. \\
&\left.+\left(\int_0^1\left(re^{\frac{1+r}{2}}\left|\varphi'(u_2)\right|^{r_2}+re^{\frac{1-r}{2}}\left|\varphi'(u_1)\right|^{r_2}\right)dr\right)^{\frac{1}{r_2}}\right] \\
=\ & \frac{u_2-u_1}{2^{3-1/r_2}}\left[\left(\left(4e^{\frac{1}{2}}-2e\right)\left|\varphi'(u_1)\right|^{r_2}+\left(4e^{\frac{1}{2}}-6\right)\left|\varphi'(u_2)\right|^{r_2}\right)^{\frac{1}{r_2}}\right. \\
&\left.+\left(\left(4e^{\frac{1}{2}}-2e\right)\left|\varphi'(u_2)\right|^{r_2}+\left(4e^{\frac{1}{2}}-6\right)\left|\varphi'(u_1)\right|^{r_2}\right)^{\frac{1}{r_2}}\right].
\end{aligned}$$

By using Inequality (8), we get

$$\begin{aligned}
&\left(\left(4e^{\frac{1}{2}}-2e\right)\left|\varphi'(u_1)\right|^{r_2}+\left(4e^{\frac{1}{2}}-6\right)\left|\varphi'(u_2)\right|^{r_2}\right)^{\frac{1}{r_2}} \\
&+\left(\left(4e^{\frac{1}{2}}-2e\right)\left|\varphi'(u_2)\right|^{r_2}+\left(4e^{\frac{1}{2}}-6\right)\left|\varphi'(u_1)\right|^{r_2}\right)^{\frac{1}{r_2}} \\
\leq\ & \left(8e^{\frac{1}{2}}-2e-6\right)\left(\left|\varphi'(u_1)\right|+\left|\varphi'(u_2)\right|\right)
\end{aligned}$$

which completes the proof. □

Theorem 2.6. *($Simpson_{r_1,r_2}$) Let $\varphi : D \subset \mathbb{R} \to \mathbb{R}$ be a differentiable mapping on D°, $u_1, u_2 \in D$ with $u_1 < u_2$ and let $1/r_1 + 1/r_2 = 1$ with $r_1 > 1$. If $|\varphi'|^{r_2}$ is* *e−convex on* $[u_1, u_2]$*, then the following inequality holds;*

$$\begin{aligned}
&\left|\frac{1}{6}\left[\varphi(u_1)+4\varphi\left(\frac{u_1+u_2}{2}\right)+\varphi(u_2)\right]-\frac{1}{u_2-u_1}\int_{u_1}^{u_2}\varphi(z)\,dz\right| \\
\leq\ & (u_2-u_1)\left(\frac{1+2^{r_1+1}}{2^{r_1+1}(r_1+1)}\right)^{\frac{1}{r_1}}\left[\left(\left(\sqrt{e}-1\right)|\varphi'(u_2)|^{r_2}+\left(e-\sqrt{e}\right)|\varphi'(u_1)|^{r_2}\right)^{\frac{1}{r_2}}\right. \\
&\left.+\left(\left(e-\sqrt{e}\right)|\varphi'(u_2)|^{r_2}+\left(\sqrt{e}-1\right)|\varphi'(u_1)|^{r_2}\right)^{\frac{1}{r_2}}\right].
\end{aligned}$$

Proof. From Lemma 1.3 and by using Hölder's integral inequality, we can write

$$\begin{aligned}
&\left|\frac{1}{6}\left[\varphi(u_1)+4\varphi\left(\frac{u_1+u_2}{2}\right)+\varphi(u_2)\right]-\frac{1}{u_2-u_1}\int_{u_1}^{u_2}\varphi(z)\,dz\right| \\
\leq\ & (u_2-u_1)\left[\int_0^{\frac{1}{2}}\left|r-\frac{1}{6}\right||\varphi'(ru_2+(1-r)u_1)|\,dr\right. \\
&\left.+\int_{\frac{1}{2}}^{1}\left|r-\frac{5}{6}\right||\varphi'(ru_2+(1-r)u_1)|\,dr\right] \\
\leq\ & (u_2-u_1)\left[\left(\int_0^{\frac{1}{2}}\left|r-\frac{1}{6}\right|^{r_1}dr\right)^{\frac{1}{r_1}}\left(\int_0^{\frac{1}{2}}|\varphi'(ru_2+(1-r)u_1)|^{r_2}dr\right)^{\frac{1}{r_2}}\right. \\
&\left.+\left(\int_{\frac{1}{2}}^{1}\left|r-\frac{5}{6}\right|^{r_1}dr\right)^{\frac{1}{r_1}}\left(\int_{\frac{1}{2}}^{1}|\varphi'(ru_2+(1-r)u_1)|^{r_2}dr\right)^{\frac{1}{r_2}}\right] \\
=\ & (u_2-u_1)\left(\frac{1+2^{r_1+1}}{2^{r_1+1}(r_1+1)}\right)^{\frac{1}{r_1}}\left[\left(\int_0^{\frac{1}{2}}|\varphi'(ru_2+(1-r)u_1)|^{r_2}dr\right)^{\frac{1}{r_2}}\right. \\
&\left.+\left(\int_{\frac{1}{2}}^{1}|\varphi'(ru_2+(1-r)u_1)|^{r_2}dr\right)^{\frac{1}{r_2}}\right].
\end{aligned}$$

Since $|\varphi'|^{r_2}$ is $e-$convex, we get

$$\begin{aligned}
\int_0^{\frac{1}{2}}|\varphi'(ru_2+(1-r)u_1)|^{r_2}dr &= \int_0^{\frac{1}{2}}\left(e^r|\varphi'(u_2)|^{r_2}+e^{1-r}|\varphi'(u_1)|^{r_2}\right)dr \\
&= \left(\sqrt{e}-1\right)|\varphi'(u_2)|^{r_2}+\left(e-\sqrt{e}\right)|\varphi'(u_1)|^{r_2},
\end{aligned}$$

$$\begin{aligned}
\int_{\frac{1}{2}}^{1}|\varphi'(ru_2+(1-r)u_1)|^{r_2}dr &= \int_{\frac{1}{2}}^{1}\left(e^r|\varphi'(u_2)|^{r_2}+e^{1-r}|\varphi'(u_1)|^{r_2}\right)dr \\
&= \left(e-\sqrt{e}\right)|\varphi'(u_2)|^{r_2}+\left(\sqrt{e}-1\right)|\varphi'(u_1)|^{r_2}.
\end{aligned}$$

Thus, we establish

$$\begin{aligned}
&\left|\frac{1}{6}\left[\varphi(u_1)+4\varphi\left(\frac{u_1+u_2}{2}\right)+\varphi(u_2)\right]-\frac{1}{u_2-u_1}\int_{u_1}^{u_2}\varphi(z)\,dz\right| \\
\leq\ &(u_2-u_1)\left(\frac{1+2^{r_1+1}}{2^{r_1+1}(r_1+1)}\right)^{\frac{1}{r_1}}\left[\left((\sqrt{e}-1)\left|\varphi'(u_2)\right|^{r_2}+(e-\sqrt{e})\left|\varphi'(u_1)\right|^{r_2}\right)^{\frac{1}{r_2}}\right. \\
&\left.+\left((e-\sqrt{e})\left|\varphi'(u_2)\right|^{r_2}+(\sqrt{e}-1)\left|\varphi'(u_1)\right|^{r_2}\right)^{\frac{1}{r_2}}\right].
\end{aligned}$$

The proof is done. □

The corresponding version of the midpoint inequality is given in the following result:

Corollary 2.7. *If we take $\varphi(u_1)=4\varphi\left(\frac{u_1+u_2}{2}\right)=\varphi(u_2)$ in Theorem 2.6, then we get*

$$\begin{aligned}
&\left|\varphi\left(\frac{u_1+u_2}{2}\right)-\frac{1}{u_2-u_1}\int_{u_1}^{u_2}\varphi(z)\,dz\right| \\
\leq\ &(u_2-u_1)\left(\frac{1+2^{r_1+1}}{2^{r_1+1}(r_1+1)}\right)^{\frac{1}{r_1}}\left[\left((\sqrt{e}-1)\left|\varphi'(u_2)\right|^{r_2}+(e-\sqrt{e})\left|\varphi'(u_1)\right|^{r_2}\right)^{\frac{1}{r_2}}\right. \\
&\left.+\left((e-\sqrt{e})\left|\varphi'(u_2)\right|^{r_2}+(\sqrt{e}-1)\left|\varphi'(u_1)\right|^{r_2}\right)^{\frac{1}{r_2}}\right].
\end{aligned}$$

151

Theorem 2.8. *(Simpson$_{r_2}$) Let $\varphi : D\subset\mathbb{R}\to\mathbb{R}$ be a differentiable mapping on D°, $u_1,u_2\in D$ with $u_1<u_2$ and let $r_2\geq 1$. If $|\varphi'|^{r_2}$ is $e-$convex on $[u_1,u_2]$, then the following inequality holds;*

$$\begin{aligned}
&\left|\frac{1}{6}\left[\varphi(u_1)+4\varphi\left(\frac{u_1+u_2}{2}\right)+\varphi(u_2)\right]-\frac{1}{u_2-u_1}\int_{u_1}^{u_2}\varphi(z)\,dz\right| \\
\leq\ &(u_2-u_1)\left(\frac{5}{72}\right)^{\frac{r_2-1}{r_2}} \\
&\times\left[\left(\left(2\sqrt[6]{e}-\frac{2}{3}\sqrt{e}-\frac{7}{6}\right)\left|\varphi'(u_2)\right|^{r_2}+\left(2\sqrt[6]{e^5}-\frac{4}{3}\sqrt{e}-\frac{5}{6}e\right)\left|\varphi'(u_1)\right|^{r_2}\right)^{\frac{1}{r_2}}\right. \\
&\left.+\left(\left(2\sqrt[6]{e^5}-\frac{4}{3}\sqrt{e}-\frac{5}{6}e\right)\left|\varphi'(u_2)\right|^{r_2}+\left(2\sqrt[6]{e}-\frac{2}{3}\sqrt{e}-\frac{7}{6}\right)\left|\varphi'(u_1)\right|^{r_2}\right)^{\frac{1}{r_2}}\right].
\end{aligned}$$

Proof. From Lemma 1.3 and by using power mean inequality, we can write

$$
\begin{aligned}
&\left|\frac{1}{6}\left[\varphi(u_1)+4\varphi\left(\frac{u_1+u_2}{2}\right)+\varphi(u_2)\right]-\frac{1}{u_2-u_1}\int_{u_1}^{u_2}\varphi(z)\,dz\right| \\
\leq\ & (u_2-u_1)\left[\int_0^{\frac{1}{2}}\left|r-\frac{1}{6}\right|\left|\varphi'(ru_2+(1-r)u_1)\right|dr\right. \\
&\left.+\int_{\frac{1}{2}}^{1}\left|r-\frac{5}{6}\right|\left|\varphi'(ru_2+(1-r)u_1)\right|dr\right] \\
\leq\ & (u_2-u_1)\left[\left(\int_0^{\frac{1}{2}}\left|r-\frac{1}{6}\right|dr\right)^{1-\frac{1}{r_2}}\left(\int_0^{\frac{1}{2}}\left|r-\frac{1}{6}\right|\left|\varphi'(ru_2+(1-r)u_1)\right|^{r_2}dr\right)^{\frac{1}{r_2}}\right. \\
&\left.+\left(\int_{\frac{1}{2}}^{1}\left|r-\frac{5}{6}\right|dr\right)^{1-\frac{1}{r_2}}\left(\int_{\frac{1}{2}}^{1}\left|r-\frac{5}{6}\right|\left|\varphi'(ru_2+(1-r)u_1)\right|^{r_2}dr\right)^{\frac{1}{r_2}}\right] \\
=\ & (u_2-u_1)\left(\frac{5}{72}\right)^{\frac{r_2-1}{r_2}}\left[\left(\int_0^{\frac{1}{2}}\left|r-\frac{1}{6}\right|\left|\varphi'(ru_2+(1-r)u_1)\right|^{r_2}dr\right)^{\frac{1}{r_2}}\right. \\
&\left.+\left(\int_{\frac{1}{2}}^{1}\left|r-\frac{5}{6}\right|\left|\varphi'(ru_2+(1-r)u_1)\right|^{r_2}dr\right)^{\frac{1}{r_2}}\right].
\end{aligned}
$$

Since $|\varphi'|^{r_2}$ is $e-$convex, we get

$$
\begin{aligned}
&\int_0^{\frac{1}{2}}\left|r-\frac{1}{6}\right|\left|\varphi'(ru_2+(1-r)u_1)\right|^{r_2}dr \\
=\ & \left|\varphi'(u_2)\right|^{r_2}\int_0^{\frac{1}{2}}\left|r-\frac{1}{6}\right|e^{r}dr+\left|\varphi'(u_1)\right|^{r_2}\int_0^{\frac{1}{2}}\left|r-\frac{1}{6}\right|e^{1-r}dr \\
=\ & \left(2\sqrt[6]{e}-\frac{2}{3}\sqrt{e}-\frac{7}{6}\right)\left|\varphi'(u_2)\right|^{r_2}+\left(2\sqrt[6]{e^5}-\frac{4}{3}\sqrt{e}-\frac{5}{6}e\right)\left|\varphi'(u_1)\right|^{r_2},
\end{aligned}
$$

and

$$
\begin{aligned}
&\int_{\frac{1}{2}}^{1}\left|r-\frac{5}{6}\right|\left|\varphi'(ru_2+(1-r)u_1)\right|^{r_2}dr \\
=\ & \left|\varphi'(u_2)\right|^{r_2}\int_{\frac{1}{2}}^{1}\left|r-\frac{5}{6}\right|e^{r}dr+\left|\varphi'(u_1)\right|^{r_2}\int_{\frac{1}{2}}^{1}\left|r-\frac{5}{6}\right|e^{1-r}dr \\
=\ & \left(2\sqrt[6]{e^5}-\frac{4}{3}\sqrt{e}-\frac{5}{6}e\right)\left|\varphi'(u_2)\right|^{r_2}+\left(2\sqrt[6]{e}-\frac{2}{3}\sqrt{e}-\frac{7}{6}\right)\left|\varphi'(u_1)\right|^{r_2}.
\end{aligned}
$$

Thus, by combining all the above terms, we obtain the required result. □

Theorem 2.9. *($Ostrowski_{r_1,r_2}$) Let $\varphi : D \subset \mathbb{R} \to \mathbb{R}$ be a differentiable mapping on D°, $u_1, u_2 \in D$ with $u_1 < u_2$ and let $1/r_1 + 1/r_2 = 1$ with $r_1 > 1$. If $|\varphi'|^{r_2}$ is $e-$convex on $[u_1, u_2]$, then the following inequality holds;*

$$\begin{aligned}
&\left|\varphi(z) - \frac{1}{u_2-u_1}\int_{u_1}^{u_2}\varphi(u)\,du\right| \\
\leq\ & \frac{(u_2-z)^{\frac{r_1+1}{r_1}}}{(u_2-u_1)^{\frac{1}{r_1}}(r_1+1)^{\frac{1}{r_1}}}\left(\left(e^{\frac{u_2-z}{u_2-u_1}}-1\right)|\varphi'(u_1)|^{r_2}+\left(e-e^{\frac{z-u_1}{u_2-u_1}}\right)|\varphi'(u_2)|^{r_2}\right)^{1/r_2} \\
&+\frac{(z-u_1)^{\frac{r_1+1}{r_1}}}{(u_2-u_1)^{\frac{1}{r_1}}(r_1+1)^{\frac{1}{r_1}}}\left(\left(e-e^{\frac{u_2-z}{u_2-u_1}}\right)|\varphi'(u_1)|^{r_2}+\left(e^{\frac{z-u_1}{u_2-u_1}}-1\right)|\varphi'(u_2)|^{r_2}\,dr\right)^{1/r_2}.
\end{aligned}$$

Proof. From Lemma 1.4 and by using the Hölder's integral inequality and since $|\varphi'|^{r_2}$ is $e-$convex, we can write

$$\begin{aligned}
&\left|\varphi(z) - \frac{1}{u_2-u_1}\int_{u_1}^{u_2}\varphi(u)\,du\right| \\
\leq\ & (u_2-u_1)\left[\left(\int_0^{\frac{u_2-z}{u_2-u_1}} r^{r_1}dr\right)^{1/r_1}\left(\int_0^{\frac{u_2-z}{u_2-u_1}}|\varphi'(ru_1+(1-r)u_2)|^{r_2}dr\right)^{1/r_2}\right. \\
&\left.+\left(\int_{\frac{u_2-z}{u_2-u_1}}^1 (1-r)^{r_1}\,dr\right)^{1/r_1}\left(\int_{\frac{u_2-z}{u_2-u_1}}^1|\varphi'(ru_1+(1-r)u_2)|^{r_2}dr\right)^{1/r_2}\right] \\
\leq\ & \frac{(u_2-z)^{\frac{r_1+1}{r_1}}}{(u_2-u_1)^{\frac{1}{r_1}}(r_1+1)^{\frac{1}{r_1}}}\left(\int_0^{\frac{u_2-z}{u_2-u_1}}\left(e^r|\varphi'(u_1)|^{r_2}+e^{1-r}|\varphi'(u_2)|^{r_2}\right)dr\right)^{1/r_2} \\
&+\frac{(z-u_1)^{\frac{r_1+1}{r_1}}}{(u_2-u_1)^{\frac{1}{r_1}}(r_1+1)^{\frac{1}{r_1}}}\left(\int_{\frac{u_2-z}{u_2-u_1}}^1\left(e^r|\varphi'(u_1)|^{r_2}+e^{1-r}|\varphi'(u_2)|^{r_2}\right)dr\right)^{1/r_2} \\
=\ & \frac{(u_2-z)^{\frac{r_1+1}{r_1}}}{(u_2-u_1)^{\frac{1}{r_1}}(r_1+1)^{\frac{1}{r_1}}}\left(\left(e^{\frac{u_2-z}{u_2-u_1}}-1\right)|\varphi'(u_1)|^{r_2}+\left(e-e^{\frac{z-u_1}{u_2-u_1}}\right)|\varphi'(u_2)|^{r_2}\right)^{1/r_2} \\
&+\frac{(z-u_1)^{\frac{r_1+1}{r_1}}}{(u_2-u_1)^{\frac{1}{r_1}}(r_1+1)^{\frac{1}{r_1}}}\left(\left(e-e^{\frac{u_2-z}{u_2-u_1}}\right)|\varphi'(u_1)|^{r_2}+\left(e^{\frac{z-u_1}{u_2-u_1}}-1\right)|\varphi'(u_2)|^{r_2}\,dr\right)^{1/r_2}.
\end{aligned}$$

The proof is completed. □

Corollary 2.10. *If we take $z=\frac{u_1+u_2}{2}$ in Theorem 2.9, then we get*

$$\begin{aligned}
&\left|\varphi\left(\frac{u_1+u_2}{2}\right)-\frac{1}{u_2-u_1}\int_{u_1}^{u_2}\varphi(u)\,du\right| \\
\leq\ & \frac{u_2-u_1}{2^{\frac{r_1+1}{r_1}}(r_1+1)^{\frac{1}{r_1}}}\left[\left(\left(\sqrt{e}-1\right)|\varphi'(u_1)|^{r_2}+\left(e-\sqrt{e}\right)|\varphi'(u_2)|^{r_2}\right)^{1/r_2}\right. \\
&\left.+\left(\left(e-\sqrt{e}\right)|\varphi'(u_1)|^{r_2}+\left(\sqrt{e}-1\right)|\varphi'(u_2)|^{r_2}\,dr\right)^{1/r_2}\right].
\end{aligned}$$

Theorem 2.11. *(Ostrowski$_{r_2}$) Let $\varphi: D\subset\mathbb{R}\to\mathbb{R}$ be a differentiable mapping on D°, $u_1,u_2\in D$ with $u_1<u_2$ and let $r_2\geq 1$. If $|\varphi'|^{r_2}$ is $e-$convex on $[u_1,u_2]$, then the following inequality holds;*

$$\begin{aligned}
&\left|\varphi(z)-\frac{1}{u_2-u_1}\int_{u_1}^{u_2}\varphi(u)\,du\right| \\
=\ & \frac{(u_2-z)^{2\left(1-\frac{1}{r_2}\right)}}{2(u_2-u_1)^{1-\frac{2}{r_2}}} \\
&\times\left(\left(1+\frac{z-u_1}{u_2-u_1}e^{\frac{u_2-z}{u_2-u_1}}\right)|\varphi'(u_1)|^{r_2}+\left(\frac{(u_1-2u_2+z)}{u_2-u_1}e^{\frac{z-u_1}{u_2-u_1}}+e\right)|\varphi'(u_2)|^{r_2}\right)^{1/r_2} \\
&+\frac{(z-u_1)^{2\left(1-\frac{1}{r_2}\right)}}{2(u_2-u_1)^{1-\frac{2}{r_2}}} \\
&\times\left(\left(e^{\frac{u_2-z}{u_2-u_1}}\frac{(2u_1-u_2-z)}{u_2-u_1}+e\right)|\varphi'(u_1)|^{r_2}+\left(1-\frac{e^{\frac{z-u_1}{u_2-u_1}}(u_2-z)}{u_2-u_1}\right)|\varphi'(u_2)|^{r_2}\,dr\right)^{1/r_2}.
\end{aligned}$$

Proof. From Lemma 1.4 and using the power mean integral inequality and since $|\varphi'|^{r_2}$ is $e-$convex , we can write

$$
\begin{aligned}
&\left|\varphi(z)-\frac{1}{u_2-u_1}\int_{u_1}^{u_2}\varphi(u)\,du\right| \\
\leq\ & (u_2-u_1)\left[\left(\int_0^{\frac{u_2-z}{u_2-u_1}} r dr\right)^{1-1/r_2}\left(\int_0^{\frac{u_2-z}{u_2-u_1}} r\left|\varphi'(ru_1+(1-r)u_2)\right|^{r_2}dr\right)^{1/r_2}\right. \\
&\left.+\left(\int_{\frac{u_2-z}{u_2-u_1}}^1(1-r)\,dr\right)^{1-1/r_2}\left(\int_{\frac{u_2-z}{u_2-u_1}}^1(1-r)\left|\varphi'(ru_1+(1-r)u_2)\right|^{r_2}dr\right)^{1/r_2}\right] \\
\leq\ & \frac{(u_2-z)^{2\left(1-\frac{1}{r_2}\right)}}{2(u_2-u_1)^{1-\frac{2}{r_2}}}\left(\int_0^{\frac{u_2-z}{u_2-u_1}}\left(re^r\left|\varphi'(u_1)\right|^{r_2}+re^{1-r}\left|\varphi'(u_2)\right|^{r_2}\right)dr\right)^{1/r_2} \\
&+\frac{(z-u_1)^{2\left(1-\frac{1}{r_2}\right)}}{2(u_2-u_1)^{1-\frac{2}{r_2}}}\left(\int_{\frac{u_2-z}{u_2-u_1}}^1\left((1-r)e^r\left|\varphi'(u_1)\right|^{r_2}+(1-r)e^{1-r}\left|\varphi'(u_2)\right|^{r_2}\right)dr\right)^{1/r_2} \\
=\ & \frac{(u_2-z)^{2\left(1-\frac{1}{r_2}\right)}}{2(u_2-u_1)^{1-\frac{2}{r_2}}} \\
&\times\left(\left(1+\frac{z-u_1}{u_2-u_1}e^{\frac{u_2-z}{u_2-u_1}}\right)\left|\varphi'(u_1)\right|^{r_2}+\left(\frac{(u_1-2u_2+z)}{u_2-u_1}e^{\frac{z-u_1}{u_2-u_1}}+e\right)\left|\varphi'(u_2)\right|^{r_2}\right)^{1/r_2} \\
&+\frac{(z-u_1)^{2\left(1-\frac{1}{r_2}\right)}}{2(u_2-u_1)^{1-\frac{2}{r_2}}} \\
&\times\left(\left(e^{\frac{u_2-z}{u_2-u_1}}\frac{(2u_1-u_2-z)}{u_2-u_1}+e\right)\left|\varphi'(u_1)\right|^{r_2}+\left(1-\frac{e^{\frac{z-u_1}{u_2-u_1}}(u_2-z)}{u_2-u_1}\right)\left|\varphi'(u_2)\right|^{r_2}dr\right)^{1/r_2}
\end{aligned}
$$

The proof is completed. □

Corollary 2.12. *If we take $z=\frac{u_1+u_2}{2}$ in Theorem 2.11, then we get*

$$
\begin{aligned}
&\left|\varphi\left(\frac{u_1+u_2}{2}\right)-\frac{1}{u_2-u_1}\int_{u_1}^{u_2}\varphi(u)\,du\right| \\
\leq\ & \frac{u_2-u_1}{2^{3-\frac{2}{r_2}}}\left[\left(\left(1+\frac{1}{2}\sqrt{e}\right)\left|\varphi'(u_1)\right|^{r_2}+\left(\frac{3}{2}\sqrt{e}+e\right)\left|\varphi'(u_2)\right|^{r_2}\right)^{1/r_2}\right. \\
&\left.+\left(\left(e-\frac{3}{2}\sqrt{e}\right)\left|\varphi'(u_1)\right|^{r_2}+\left(1-\frac{1}{2}\sqrt{e}\right)\left|\varphi'(u_2)\right|^{r_2}dr\right)^{1/r_2}\right] \\
\leq\ & \frac{u_2-u_1}{2^{3-\frac{2}{r_2}}}\left(\left(1+e-\sqrt{e}\right)\left|\varphi'(u_1)\right|+\left(1+e+\sqrt{e}\right)\left|\varphi'(u_2)\right|\right).
\end{aligned}
$$

REFERENCES

[1] ALOMARİ M., DARUS M., KIRMACIU.S., Refinements of Hadamard-type inequalities for quasi-convex functions with applications to trapezoidal formula and to special means, Comp. and Math. with Appl., V.59, 2010, pp. 225-232.

[2] ALOMARİ M., DARUS M., DRAGOMİR S.S., New inequalities of Simpson's type for s-convex functions with applications, RGMIA Research Report Collection Volume 12 (4), 2010.

[3] ALOMARİ M., DARUS M., Some Ostrowski type inequalities for quasi-convex functions with applications to special means, RGMIA Research Report Collection Volume 13, article 2, 2010.

[4] BESSENYEİ M., The Hermite-Hadamard inequality on simplices, Amer. Math. Monthly 115 (2008), no. 4, 339-345. MR 2009b:52023

[5] BESSENYEİ M., Hermite-Hadamard-type inequalities for generalized convex functions, J. Inequal. Pure Appl. Math. 9 (2008), no. 3, Article 63, pp. 51 (electronic).

[6] BESSENYEİ M., The Hermite-Hadamard inequality in Beckenbach's setting, J. Math. Anal. Appl. 364 (2010), no. 2, 366-383. MR MR2576189

[7] BESSENYEİ M. and PÁLES Zs., Higher-order generalizations of Hadamard's inequality, Publ. Math. Debrecen 61 (2002), no. 3-4, 623-643. MR 2003k:26021

[8] BESSENYEİ M. and PÁLES Zs., Characterizations of convexity via Hadamard's inequality, Math. Inequal. Appl. 9 (2006), no. 1, 53-62. MR 2007a:26010

[9] BOMBARDELLİ M. and VAROŠANEC S., Properties of h -convex functions related to the Hermite-Hadamard-Fejér inequalities, Comput. Math. Appl. 58 (2009) 1869-1877.

[10] DRAGOMİR S. S., AGARWAL R. P., and CERONE P., On Simpson's inequality and applications, J. Inequal. Appl. 5 (2000), no. 6, 533{579; Available online at http://dx.doi.org/10.1155/S102558340000031X.

[11] DRAGOMİR S. S., PEČARİĆ J. and PERSSON L.E., Some inequalities of Hadamard type, Soochow J.Math., 21, 335-241, 1995.

[12] GÖZPİNAR A., SET E., DRAGOMİR S. S., some generalized Hermite-Hadamard type inequalities involving fractional integral operator for functions whose second derivatives in absolute value are s-convex, Acta Math. Univ. Comenianae, in press

[13] HUDZİK H. and MALİGRANDA L., Some remarks on s-convex functions, Aequationes Math., 48, 100-111, 1994.

[14] KIRMACI U.S., Inequalities for differentiable mappings and applications to special means of real numbers to midpoint formula, Appl.Math.Comput. 147 (1), 137-146 (2004).

[15] MAKÓ J. and PÁLES Zs., Approximate Hermite-Hadamard type inequalities for approximately convex functions, Math. Inequal. Appl., 16 (2), 507-526, (2013).

[16] MAKÓ J. and PÁLES Zs., Implications between approximate convexity properties and approximate Hermite-Hadamard inequalities, Cent. Eur. J. Math. 10 (2012), no. 3, 1017-1041.

[17] MİTRİNOVİĆ D. S., PEČARİĆ J. , and FİNK A.M., Classical and new inequalities in analysis, KluwerAcademic, Dordrecht, 1993.

[18] ÖZDEMİR M.E., GÜRBÜZ M. and AKDEMİR A.O., Inequalities for h-Convex Functions via Further Properties, RGMIA Research Report Collection Volume 14, article 22, 2011.

[19] SARIKAYA M.Z., SAĞLAM A. and YILDIRIM H., some Hadamard-type inequalities for h-convex functions, J. Math. Inequal. 2 (3) (2008) 335-341.

[20] NOOR M.A., NOOR K.I., IFTİKHAR S. On Integral Inequalities of Hermite-Hadamard Type for Harmonic (h,s)-Convex Functions, International Journal of Analysis and Applications 11(1) (2016), 61-69.

[21] SARIKAYA M.Z., SET E. and ÖZDEMİR M.E., On some new inequalities of Hadamard-type involving h-convex functions, Acta Math. Univ. Comenian LXXIX (2) (2010) 265-272.

[22] PACHPATTE B. G., Mathematical Inequalities, North-Holland Mathematical Library, Elsevier Science B.V. Amsterdam, 2005.

[23] PEČARİĆ J.E., PROSCHAN F., TONG Y.L., Convex Functions, Partial Orderings and Statistical Applications, Academic Press, 1991.

[24] TOADER G.H., ON a generalisation of the convexity, Mathematica, 30 (53) (1988), 83-87.

[25] TOADER G.H., Some generalisations of the convexity, Proc. Colloq. Approx. Optim, Cluj-Napoca (Romania), 1984, 329-338.

[26] TUNÇ M. , Ostrowski-type inequalities via h-convex functions with applications to special means, Jour. Ineq. and Appl. 2013 (1), 326, 2013.

[27] VAROŠANEC S., On h-convexity, J. Math. Anal. Appl., Volume 326, Issue 1 (2007), 303-311.

JSP

Journal of Scientific Perspectives

Volume **3,** Issue **2,** Year **2019**, pp. **159-164**
E - ISSN: **2587-3008**
URL: http://ratingacademy.com.tr/ojs/index.php/jsp
DOİ: https://doi.org/10.26900/jsp.3.016
Review Article

THE IMPORTANCE OF THE MEDICINAL PLANT NASTURTIUM OFFICINALE L. IN THE ANTICANCER ACTIVITY RESEARCH

Erkan YALÇINKAYA * & Serdar ÖZGÜÇ ** & Yusuf Orçun TÖRER *** & Ulvi ZEYBEK ****

** Talaytepe Aile Sağlığı Merkezi, Diyarbakır, TURKEY, E-mail: erkanyalcinkaya@gmail.com*
ORCID ID: https://orcid.org/0000-0003-3458-6073

*** İzmir Tabip Odası, İzmir, TURKEY, E-mail: serdarozguc@gmail.com*
ORCID ID: https://orcid.org/0000-0001-9904-9098

**** Üzümlü Aile Sağlığı Merkezi, Antalya, TURKEY, E-mail: yusuforcun@gmail.com*
ORCID ID: https://orcid.org/0000-0003-3434-2132

***** Ege Üniversitesi, Eczacılık Fakültesi, Farmasötik Botanik Anabilim Dalı, Bornova, İzmir, TURKEY, E-mail: zeybeku@hotmail.com*
ORCID ID: https://orcid.org/0000-0003-1053-8771

Received: 2 December 2018; Accepted: 27 March 2019

ABSTRACT

Cancer is known as one of the main cause of death worldwide. It is difficult to discover novel agents that selectively kill tumor cells or inhibit their proliferation without toxicity. Searching for more active and selective compounds with less toxicity is the main target of cancer researches. Nasturtium officinale L. has been used for a long time as a food and medicinal plant. Main therapeutic effects of this plant are due to rich essential nutrients as well as health-promoting plant secondary metabolites such as phenolics and glucosinolates. The plant was repoted to have antiviral, antiinflammatory, diuretic, expectorant, antidiabetic, hepatoprotective, antihyperlipidemic and anticancer properties. The aim of this study is to make review about the previous reports on secondary metabolites of Nasturtium officinale L. in terms of or their effects against various cancer cell lines.

Keywords: *Antiviral, anti-inflammatory, anticancer, Nasturtium officinale*

1. INTRODUCTION

Cancer, as a complex disease is still one of the most important causes of deaths today in the modern world. Over a century, the extensive research about the etiopathogenesis of cancer and the studies on developing new drugs, led the scientists to search for new candiates of new anticancer compounds. Unfortunately, because of severe side effects and targeting of single pathways instead of addressing the many factors that enable cancer to develop, the classical chemotherapetics could not reach to aimed success rates. Therefore, recent studies are focused on plant secondary metabolites and their semi-synthetic analogues which have multi-targeted effects on cellular signal pathways [1].

2. MATERIAL AND METHODS

In the present review, information about medicinal properties and biochemical properties of *Nasturtium officinale* L., was gathered by searching scientific databases such as Elsevier, Google Scholar, PubMed, Springer, related book chapters and original research articles.

3. AIM OF THE PRESENT REVIEW

In the present review, pharmacological properties of *Nasturtium officinale* L. were discussed and evaluated for future cancer treatments.

4. MEDICINAL PROPERTIES

4.1 Ethnomedicinal Properties

Nasturtium officinale L., a perennial plant from Brassicaceae family, is traditionally used as raw and cooked form for culinary and for medicinal purposes such as respiratory system diseases, diabetes, oxidative stress, asthma, and immune deficiency [2-12].

4.2 Therapeutical Properties

The major active compounds of *Nasturtium officinale* are found to be phenolic compounds and glucosinolates. Main phenolic compounds were reported to be chlorogenic acid and isorhamnetin. Gluconasturtiin, a precursor of 2-phenylethyl isothiocyanate is reported as a glucosinolate compound with anticarcinogenic and antimicrobial activity. In addition to these secondary metabolites, having high amounts of minerals and with high antioxidant activity, it is worth for searching *Nasturtium officinale* for cancer protective effects [13-15].

N. officinale L. with high content of polyphenolic substances and glucosinolates, may help for anti-inflammatory response and increase antioxidant capacity in cancer patients or patients at high risk group [10,16-22]. Main flavonoids of *N. officinale* L. are found to be quercetin, kaempferol, isorhamnetin, chlorogenic acid, quercetin-3-O-rutinoside, cafeoiltartaric acid and caftaric acid [10,23-24].

Phenylethyl isothiocyanate was found to have an activity to inhibit the migration and invasion of human colorectal carcinoma cells and stop the proliferation of cancer cells. In the cell lines of human breast cancer, phenylethyl isothiocyanate was shown to decrease matrix-metalloprotease-9 and ALDH1 marker and also inhibit tumor invasion [25-27].

N. officinale has an angiogenesis inhibitory activity by decreasing the translation regulator 4E protein 1 (4E-BP1) phosphorylation, by decreasing the effect of hypoxia induction factor (HIF) one of the angiogenesis regulators, and by nuclear factor kB (NF-kB), activator protein (AP1) and tubulin. [28]. It was proven to be cancer protective by decreasing DNA damage and regulation of micro RNA's [23, 29-30].

7-methylsulfinylheptyl, 8-methylsulfinyloctyl and sitosterol 3-O-glucopyranoside isolated from *N. officinale*, specifically inhibit p-450 enzymes and activates phase 2 enzymatic reactions [31]. After consumption of *Nasturtium officinale*, the tobacco smoke specific lung cancer markers 4-(methylnitrosamino)-1-(3-pyridyl)-1-butanol (NNAL) and [4-methylnitrosamino)-1-(3-pyridyl) but-1-yl]-beta-omega-D-glucosiduronic acid (NNAL- Gluc) was found to be increased in urine samples at 24 hours and therefore this effect was attributed for anticancer potential of the plant on tobacco-related and other types of lung cancer [32,33].

Some synergistic activities were also shown between *Juglans regia,* broccoli and *Nasturtium officinale* L. extracts [34].

5. CONCLUSION

Nasturtium officinale L. can easily be considered as safe because of its traditional culinary use and wide therapeutic range for cancer cell-specific effects that inhibit the cancer cell proliferation.

As a traditional culinary plant with vitamins, minerals and phytonutrients such as isothiosionates and gluconasturtiin, *Nasturtium officinale* L. may be considered as potential source for anticancer compounds of natural origin. Further *in vitro* and *in vivo* studies and clinical researches are needed to be conducted on *Nasturtium officinale* L.

REFERENCES

[1] GIORDANO, S., PETRELLI, A., 2008, From Single- to Multi-Target Drugs in Cancer Therapy: When Aspecificity Becomes an Advantage, *Current Medicinal Chemistry*, 15, 422.

[2] BARKER, D.J., 2009, Pacific Northwest Aquatic Invasive Species Profile: Nasturtium officinale (Watercress). https://depts.washington.edu/oldenlab/wordpress/wpcontent/uploads/2013/03/Nasturtium-officinale_Barker.pdf

[3] DOLATKHAHI, M., DOLATKHAHI, A., & NEJAD, J.B., 2014, Ethnobotanical study of medicinal plants used in Arjan- Parishan protected area in Fars Province of Iran. *Avicenna journal of phytomedicine*, 4(6), 402-12.

[4] ANDRADE, J. M., LUCERO MOSQUERA, H., & ARMIJOS, C., 2017. Ethnobotany of Indigenous Saraguros: Medicinal Plants Used by Community Healers "Hampiyachakkuna" in the San Lucas Parish, Southern Ecuador. *BioMed research international*, 9343724.

[5] ABBASI, A.M., KHAN, M.A., SHAH, M.H., SHAH, M.M., PERVEZ, A., AHMAD, M., 2013, Ethnobotanical appraisal and cultural values of medicinally important wild edible vegetables of Lesser Himalayas-Pakistan, J. Ethnobiol. Ethnomed., 9(1), 66.

[6] S. AL-QURA`N.,2006. Ethnobotany of Folk Medicinal Potentiality of Aquatic Plants in Jordan. Research Journal of Botany, 1, 75-84.

[7] FLAVIA, L. P., JOSE, M. F., JOAO, P. V. L., 2012. Ethnopharmacological survey: a selection strategy to identify medicinal plants for a local phytotherapy program. Brazilian Journal of Pharmaceutical Sciences, 48, (2).299-313.

[8] FAWZI MAHOMOODALLY, M., PRIYAMKA SREEKEESOON D., 2017, A Quantitative Ethnopharmacological Documentation of Natural Pharmacological Agents Used by Pediatric Patients in Mauritius, *BioMed Research International*, 1-14.

[9] AIRES, A., CARVALHO, R., ROSA, E.A.S., SAAVEDRA M. J., 2013, Phytochemical characterization and antioxidant properties of baby-leaf watercress produced under organic production system, CyTA, *Journal of Food*, 11:4, 343-351.

[10] ZEB, A., 2015, Phenolic profile and antioxidant potential of wild watercress (*Nasturtium officinale* L.). *SpringerPlus*, 4, 714.

[11] HARO, G., IKSEN, I., RUMANTİ, R.M., MARBUN, N., SARİ, R.P., GULTON, R.P.J., 2018, Evoluation of Antioxidant activity and Minerals Value From Watercress (Nasturtium officinale R.Br.), 11 (1), 232-237.

[12] PAHWA, R., JIALAL, I., 2018, Chronic Inflammation. StatPearls Publishing LLC, Treasure Island (FL).

[13] BALISTRERI, C.R., CARUSO, C., CANDORE, G., 2010, The role of adipose tissue and adipokines in obesity-related inflammatory diseases. *Mediat Inflamm*, 802078.

[14] LIBRA, M., NICOLETTI, F., 2017, Diet, inflammation and cancer: a journey from prevention to treatment. In: Accardi G, Caruso C, editors. Updates in pathobiology: causality and chance in ageing, age-related diseases and longevity. Palermo, *University Press*, 145–162.

[15] ACCARDI, G., CARUSO, C., 2018, Immune-inflammatory responses in the elderly: an update. *Immun Ageing*, 15, 1-11.

[16] SANTOS J, OLIVEIRA MBPP, IBÁÑEZ E, HERRERO M. 2014, Phenolic profile evolution of different ready-to-eat baby-leaf vegetables during storage. *J Chromatogr A*.1327:118–31.

[17] AIRES, A., CARVALHO, R., ROSA, EAS, SAAVEDRA, M.J. 2013, Phytochemical characterization and antioxidant properties of baby-leaf watercress produced under organic production system. *CyTA- J Food*., 11, 343–51.

[18] MARTÍNEZ-SÁNCHEZ, A., GIL-IZQUIERDO, A., GIL, M.I., FERRERES F., 2008, A comparative study of flavonoid compounds, vitamin C, and antioxidant properties of baby leaf Brassicaceae species. *J Agric Food Chem*., 56, 2330–2340.

[19] DI NOIA, J., 2014, Defining powerhouse fruits and vegetables: a nutrient density approach. *Preventing chronic disease*, 11, 1-5.

[20] HEBATOLLAH, S., MOSTAFAZADEH, M., SADEGHI, H., MNADERİAN, MEHRZAD JAFARİ BARMAK, MOHAMMAD SHARİF TALEBİANPOOR & FOUAD MEHRABAN (2014) In vivo anti-inflammatory properties of aerial parts of *Nasturtium officinale*, *Pharmaceutical Biology*, 52(2), 169-174.

[21] SHAHANI, S., BEHZADFAR, F., JAHANI, D., GHASEMI, M., SHAKI, F., 2017, Antioxidant and anti-inflammatory effects of *Nasturtium officinale* involved in attenuation of gentamicin-induced nephrotoxicity, *Toxicology Mechanisms and Methods*, 27(2), 107-114.

[22] GILL, C.I., HALDAR, S., BOYD, L.A., BENNETT, R., WHITEFORD, J., BUTLER, M., PEARSON, J.R., BRADBURY, I., ROWLAND, I.R., 2007. Watercress supplementation in diet reduces lymphocyte DNA damage and alters blood antioxidant status in healthy adults. *Am J Clin Nutr.* 85, 504–510.

[23] LAI K.C., HSU, S.C., KUO, C.L., IP, S.W., YANG, J.S., HSU, Y.M., HUANG H.Y., WU S.H., CHUNG, J.G., 2010, Phenethyl Isothiocyanate Inhibited Tumor Migration and Invasion via Suppressing Multiple Signal Transduction Pathways in Human Colon Cancer HT29 Cells, *Journal of Agricultural and Food Chemistry,* 58 (20), 11148-11155.

[24] PEREIRA LUCÍLIA, P., SILVA P., DUARTE, M., RODRIGUES, L., DUARTE C. M. M, ALBUQUERQUE, C., TERESA SERRA, A., 2017, Targeting Colorectal Cancer Proliferation, Stemness and Metastatic Potential Using Brassicaceae Extracts Enriched in Isothiocyanates: A 3D Cell Model-Based Study, *Nutrients*, 9(4), 368.

[25] ROSE, P., HUANG, Q., ONG, C.N., WHITEMAN, M., 2005, Broccoli and watercress suppress matrix metalloproteinase-9 activity and invasiveness of human MDA-MB-231 breast cancer cells. *Toxicol Appl Pharmacol*. 209 (2), 105-113.

[26] SYED ALWI, S. S., CAVELL, B. E., TELANG, U., MORRIS, M. E., PARRY, B. M., PACKHAM, G., 2010, In vivo modulation of 4E binding protein 1 (4E-BP1) phosphorylation by watercress: a pilot study. *The British journal of nutrition*, 104 (9), 1288-96.

[27] CAVELL, B.E., SYED ALWI S.S., DONLEVY, A., PACKHAM, G., 2011, Anti-angiogenic effects of dietary isothiocyanates: mechanisms of action and implications for human health, *Biochem Pharmacol*. 81 (3), 327-36.

[28] PAN, J H., ABERNATHY, B., KIM, Y. J., LEE J. H., KIM, J. H., SHIN, E. C., KIM J. K., 2018, Cruciferous vegetables and colorectal cancer prevention through microRNA regulation: A review, *Critical Reviews in Food Science and Nutrition*, 58 (12), 2026-2038.

[29] FOGARTY, M.C., HUGHES, C.M., BURKE, G., BROWN, J.C., DAVISON, G.W., 2013, Acute and chronic watercress supplementation attenuates exercise-induced peripheral mononuclear cell DNA damage and lipid peroxidation, *Br J Nutr*. 109 (2), 293-301.

[30] ROSE, P., FAULKNER, K., WILLIAMSON, G., MITHEN, R., 2000, 7-Methylsulfinylheptyl and 8-methylsulfinyloctyl isothiocyanates from watercress are potent inducers of phase II enzymes, *Carcinogenesis*, 21 (11), 1983–1988.

[31] YAZDANPARAST, R., BAHRAMIKIA, S., ARDESTANI, A., 2008, Nasturtium officinale reduces oxidative stress and enhances antioxidant capacity in hypercholesterolaemic rats, *Chem Biol Interact*., 172 (3):176-84

[32] HECHT, S.S., CHUNG, F.L, RICHIE, JR J.P., AKERKAR, S. A., BORUKHOVA, A, SKOWRONSKI, L., CARMELLA, S. G., 1995, Effects of watercress consumption on metabolism of a tobacco-specific lung carcinogen in smokers, *Cancer Epidemiol Biomarkers Prev.,* 4 (8), 877-884.

[33] HOSSEINI S. A., MOHAMMADI, J., DELAVIZ H., SHARIATI, M., Effect of Juglansregia and Nasturtum officinalis on biochemical parameters following toxicity of kidney by CCl4 in Wistar rats, *Electron J Gen Med.,* 15(3), 1-7.

[34] GINTING, H., DALIMUNTHE, A., REWENY, J., 2017, Acute Toxicity Effect of The Ethanolic Extract of Watercress Herb (Nasturtium officinale R. Br.) in Mice, *Indonesian J. of Cancer Chemoprevention*, 7, 9-16.